`

RHODES UNIVERSITY
Where leaders learn

Development and optimisation of a qPCR assay for the enumeration of Cryptophlebia leucotreta granulovirus (CrleGV) used for commercial applications

A thesis submitted in fulfilment of the
requirements for the degree of

Master of Science

In

Microbiology

of

RHODES UNIVERSITY

By

Thuthula Mela

March 2022

Declaration

I, Thuthula Mela (g16m2932) hereby declare that the thesis submitted is my own work. It is being submitted for the degree of Master of Science at Rhodes University. It has not been previously submitted for assessment of any degree at any other university or other body, organisation outside of the university.

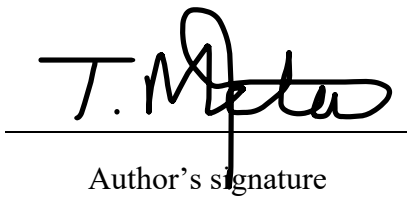

Author's signature

25 March 2022

Date

Abstract

The citrus industry contributes significantly to the South African agricultural sector. *Thaumatotibia leucotreta* (Meyrick) (Lepidoptera: Tortricidae) is highly important to the South African citrus industry as it is classified as a phytosanitary pest by most international markets. *Thaumatotibia leucotreta* has caused an estimated annual loss of up to R100 million to the industry. In order to control *T. leucotreta* in South Africa, an integrated pest management (IPM) programme has been used. One of the components of this programme is Cryptophlebia leucotreta granulovirus (CrleGV), which has been formulated to a registered biopesticide namely Cryptogran and has been successfully applied in the field for over 15 years. To use CrleGV as biopesticides, quantification of the viral particles is required to perform bioassays for field trials and formulation, among other applications. Darkfield microscopy is a traditional method used for the quantification of CrleGV; however, the method is characterised as being subjective, tedious, labour intensive, and time-consuming. This study aims to develop and optimise a qPCR technique to accurately quantify CrleGV-SA OBs using plasmid DNA for downstream applications.

Firstly, *lef-8*, *lef-9*, and *granulin* conserved genes from CrleGV-SA and CrleGV-CV3 genome sequences were analysed by performing multiple alignments to evaluate the degree of identity between these genes. This was done to design two sets of oligonucleotides (internal and external) from regions with the highest identity. Subsequently, *in silico* testing was done to evaluate the designed oligonucleotides to determine whether they specifically bind to the selected target regions.

Secondly, three sets of DNA plasmids (pJET1.2-Gran, pJET1.2-lef-9, and pJET1.2-lef-8) were constructed, each containing a target region for either *granulin*, *lef-9*, and *lef-8* genes for use as standards in a downstream qPCR assay. This was achieved by first extracting gDNA from CrleGV-SA OBs and using the gDNA as a template to PCR amplify the target regions of the selected gene regions with the designed oligonucleotides. Subsequently, the PCR amplified regions were then directly ligated into the pJET1.2/blunt vector, and the plasmids were confirmed by colony PCR, restriction enzyme digestion, and Sanger sequencing.

Thirdly, two different methods of CrleGV-SA gDNA extraction were compared to determine which method has the best yields in terms of concentration. The extraction methods compared were the Quick-DNA Miniprep Plus kit according to manufacturer's instructions (Method 1a),

pre-treatment with Na_2CO_3 prior to using the Quick-DNA Miniprep Plus kit (Method 1b), pre-treatment with Na_2CO_3, and neutralisation with Tris-HCl prior to gDNA extraction using the Quick-DNA Miniprep Plus kit (Method 1c) and the CTAB method (Method 2). The gDNA concentration and purity for all samples were determined using a Nanodrop spectrophotometer. Method 1c (Na_2CO_3 and Tris-HCl pre-treated plus Quick-DNA Miniprep Plus kit) was the most efficient at extracting genomic DNA compared with the other methods, resulting in the highest DNA concentration in short processing time.

Fourthly, plasmid standards were evaluated for use in the qPCR assay. This was done as it was important to consider the efficacy of the oligonucleotides; including the ability of the oligonucleotides to anneal to the appropriate segment of DNA without extensive formation of oligonucleotides dimers, non-specific annealing, or formation of secondary structure. In addition, it was done to ensure that highly accurate standard curves were generated. The standard curves were to be utilised in the downstream qPCR assay to determine the quantity of test samples by interpolation, reading from the values within the standard curve.

Lastly, darkfield microscopy and qPCR methods of enumeration were compared to verify their accuracy and determine the most consistent and comparable method. This was achieved by quantifying the purified, crude-purified, and viral formulated CrleGV-SA suspensions using these methods. Subsequently, a statistical analysis was conducted to compare the results produced by the two enumeration methods. The obtained results showed that the *granulin*, *lef-8* and *lef-9* qPCR values did not significantly differ from the darkfield microscopy results. The findings of this study revealed that the two assays, *lef-8* qPCR and *lef-9* qPCR, were more robust, sensitive, and efficient for the quantification of CrleGV-SA. Thus, this study has successfully developed a qPCR assay that is comparable with the traditional darkfield microscopy counting technique. This is the first study to use the qPCR technique to enumerate CrleGV-SA using plasmid standards. The developed qPCR assay is reliable, rapid, and cost-effective and has a great potential to be used as an alternative method to darkfield microscopy in the laboratory and commercial settings.

Table of Contents

List of Abbreviations

% - Percentage

°C - Degrees Celsius

µl - Microliter

AGE - Agarose gel electrophoresis

Amp^R - Ampicillin Resistance

ANOVA - Analysis of variance

BLAST - Basic Local Alignment Search Tool

bp - Base pair

BV - Budded virion

CTAB - hexadecyltrimethylammonium bromide

Cq - Quantification cycle

dNTPs - deoxyribonucleotide triphosphates

ddH_2O - Double distilled water DNA

DNA - Deoxyribonucleic acid

dsDNA - DNA Double-Stranded

eco47IR - Escherichia coli Type-2 restriction enzyme

EDTA - Ethylenediaminetetraacetic acid

ELISA - enzyme-linked immunosorbent assays

EPF - Entomopathogenic fungi

EPN - Entomopathogenic nematodes

EPV - Entomopathogenic viruses

Ext - External

FCM - False codling moth

FC - flow cytometry

gDNA - Genomic deoxyribonucleic acid

Gran - Granulin

GVP - gross value of production

HPLC - high-performance liquid chromatography

Int – Internal

IPM - Integrated pest management

Lef - Late expression factor

M - Molar

MCS - Multiple cloning site

mg - Milligram

mL - Millilitre

mM - Millimolar

NCBI - National Center for Biotechnology Information

NPV - Nucleopolyhedrovirus

NTC - No template control

OB - Occlusion Body

ODV - Occlusion derived virion

PCR - Polymerase chain reaction

qPCR - Quantitative polymerase chain reaction

SA - South Africa

SEM - Scanning electron microscope

SYBR - Synergy Brands

TAE - Tris base, acetic acid and EDTA

T_m - Melting Temperature

UV - Ultraviolet

Viruses:

AgipNPV - Agrotis ipsilon nucleopolyhedrovirus

AgseNPV - Agrotis segetum nucleopolyhedrovirus

CpGV - Cydia pomonella granulovirus

CrleGV - Cryptophlebia leucotreta granulovirus

CuniNPV - Culex nigripalpus nucleopolyhedrovirus

NeseNPV - Neodiprion sertifer nucleopolyhedrovirus

SpexNPV - Spodoptera exempta nucleopolyhedrovirus

List of figures

List of tables

Acknowledgments

I would like to acknowledge the following people for supporting and assisting me towards the successful completion of this work:

- My supervisor Professor Caroline Knox for advising and assisting me; if it were not for her guidance, none of this would have been possible.
- My other supervisor Dr Michael David Jukes for all his assistance, guidance, and support throughout the research, he played a huge role, and I am very grateful.
- My co-supervisors, Prof Martin Hill, and Prof Sean Moore, for all the advice, assistance, and encouragement.
- Centre for Biological Control, Rhodes University, and Citrus Research International for financial and resource support.
- Tahnee Bennett, for all the support and encouragement.
- Lastly, I would like to thank all my friends and family for always being there for me.

Chapter 1

Literature review

1.1 Introduction

In South Africa, agriculture is one of the most critical sectors, as it plays a vital role in the local economy. The citrus industry contributes significantly to the South African agricultural sector (Newton, 1989). In terms of gross value, the citrus industry is the third-largest industry after deciduous fruit and vegetables. The citrus industry continues to be one of the critical industries that creates 160 000 direct jobs and contributes approximately R20 billion from exports only (DALRRD, 2020). South Africa exports two million tons of citrus annually, making it the 2nd largest global exporter. Over the past years, the gross value of production (GVP) for citrus has increased. This increase was mainly due to increased exports and the weakening of the Rand against the major currencies of South Africa's trading partners (DALRRD, 2020). However, there are constant significant threats to the industry resulting in fruit loss, including plant diseases and damage caused by insect pests (Moore *et al*., 2004). With citrus representing a large proportion of agricultural production in South Africa, developing novel methods in order to protect crops from potentially devastating pests is important.

1.1.1 Pests in the South African citrus industry

Citrus in South Africa is affected by a number of pests such as thrips, red mite, bollworm, and fruit fly (Hattingh, 1994). Of primary interest to this research is the lepidopteran pest *Thaumatotibia leucotreta* (Meyrick) (Lepidoptera: Tortricidae), commonly known as false codling moth (FCM). *Thaumatotibia leucotreta* occurs naturally in sub-Sahara Africa and is an important pest in the South African citrus industry (Moore *et al*., 2004). The female moths lay eggs directly on the fruit surface, and the larvae bore their way into the fruit and feed internally, resulting in fruit dropping (Mkiga *et al*., 2019). *Thaumatotibia leucotreta* causes an estimated annual direct loss of up to R100 million to the southern African citrus industry (Moore *et al*., 2004). However, the moth threatens citrus exports due to quarantine restrictions imposed by importing countries; the detection of a single larva could result in the rejection of the entire consignment (Moore, 2002; Moore, 2017). However, these losses can be due to improved *T. leucotreta* management systems, but as a result, the cost of *T. leucotreta* management has increased dramatically (Hattingh *et al*., 2020).

1.1.2 Taxonomy and distribution of *T. leucotreta*

Thaumatotibia leucotreta was first recorded as the Natal codling moth due to its discovery in the Natal Province by Fuller in 1901 (Newton, 1989). The pest was later found in the northern areas of South Africa and was referred to as orange codling moth (Newton, 1989). The insect was first taxonomically described by Meyrick (1912) as *Argyroploce leucotreta* (Eucosmidae, Olethreutidae). Later in 1955, Clarke revised to Cryptophlebia leucotreta, then 41 years later, Komai placed it into the genus where it is currently grouped, *Thaumatotibia* (Venette *et al*., 2003). Since then, the classification of this species is as shown in (Table 1.1).

Table 1.1: Taxonomic classification of *T. leucotreta* (Komai *et al*., 1999).

Kingdom	**Animalia**
Phylum	Arthropoda
Class	Insecta
Order	Lepidoptera
Family	Tortricidae
Genus	*Thaumatotibia*
Species	*leucotreta*
Binomial name	*Thaumatotibia leucotreta* (Meyrick, 1912)
Common name	False codling moth

Thaumatotibia leucotreta is endemic and indigenous to Africa. Its distribution is primarily within sub-Sahara Africa (Stibick, 2007) (Figure 1.1).

Figure 1.1: Geographic distribution of *T. leucotreta*. The red bullets indicate the presence of insect pests (Stibick, 2007).

Thaumatotibia leucotreta is widely distributed in South Africa and is found in all eight citrus-producing regions, Limpopo, Eastern Cape, Western Cape, Mpumalanga, KwaZulu-Natal, Northern Cape, and Northwest provinces (CGA, 2019). The pest impact varies under different climatic conditions; in drier areas of the north of the country, the pest is much less common (Moore *et al*., 2017; Newton, 1989). Importantly, *T. leucotreta* has not been established in Europe, North America, and Israel. However, in 2017, there were three occurrences of *T. leucotreta* in Europe, the United Kingdom, and Belgium (Brunel *et al*., 2013). Although the identification of individual moths does not necessarily confirm the establishment of *T. leucotreta* in the continent, it is of concern that the pest can become a significant risk to the agricultural industries of these regions (Brunel *et al*., 2013).

1.1.3 Host range and its economic importance

Thaumatotibia leucotreta has a broad host range with over 80 different plant species recorded, including commercially produced crops such as stone fruit, pome fruit, macadamias, litchis, cotton, citrus, and avocados (Van den Berg, 1995) (Table 1.2).

Table 1.2: Agriculturally important host plants of *T. leucotreta* (EPPO, 2019).

Scientific Name	Common Name
Capsicum spp.	Pepper
Citrus spp.	Orange
Gossypium spp.	Cotton
Litchi chinensis	Litchi
Macadamia spp.	Macadamia
Mangifera indica	Mango
Persea americana	Avocado
Prunus spp.	Apricot/Peach
Psidium guajava	Guava
Punica granatum	Pomegranate
Solanum melongena	Eggplant
Vitis spp.	Grape
Zea mays	Corn

Kirkman and Moore, (2007) conducted a survey of *T. leucotreta* occurrence on host plants from South Africa; approximately 24 were cultivated, and 50 were wild plant species. In South Africa, citrus is the preferred host for *T. leucotreta*, especially the highly susceptible Navel oranges (Newton, 1989). The broad host range of *T. leucotreta* causes problems as it enables the persistence of population numbers even after the citrus fruit has been harvested (Van den Berg, 1995). However, Kirkman and Moore, (2007) conducted a study whereby they reported a low occurrence of alternative hosts near citrus orchards. Additionally, *T. leucotreta* is a poor disperser (Newton, 1989); therefore, alternative hosts are considered problematic if they occur next to citrus orchards at high densities.

As previously mentioned, *T. leucotreta* affects a wide range of cultivated plants and can have a significant economic impact due to the damage it causes. The population densities of a pest insect can be determined through the use of monitoring systems. The insect larvae damage the fruit by burrowing into the fruit and feed internally (Figure 1.2). The larval penetration holes cause postharvest losses due to secondary infection by bacteria and fungi, which then cause fruit decay (Kirkman and Moore, 2007). In addition to direct crop losses, the interception of

exported fruit which is contaminated with restricted organisms that pose a phytosanitary risk is a significant risk to the South African citrus export industry to target export regions; Europe, the Middle East, Asia, the Russian Federation and North America (PPECB, 2017). Detection of any live *T. leucotreta* larvae results in rejection of the entire consignment, resulting in significant financial losses (Moore, 2017; Moore and Hattingh, 2017). The strict fruit monitoring systems are always in place; however, larval penetration marks on fruit are typically only visible a few days after penetration. The above stated could result in infested fruit, which has been harvested shortly after infestation being packed for the export market (Moore, 2002).

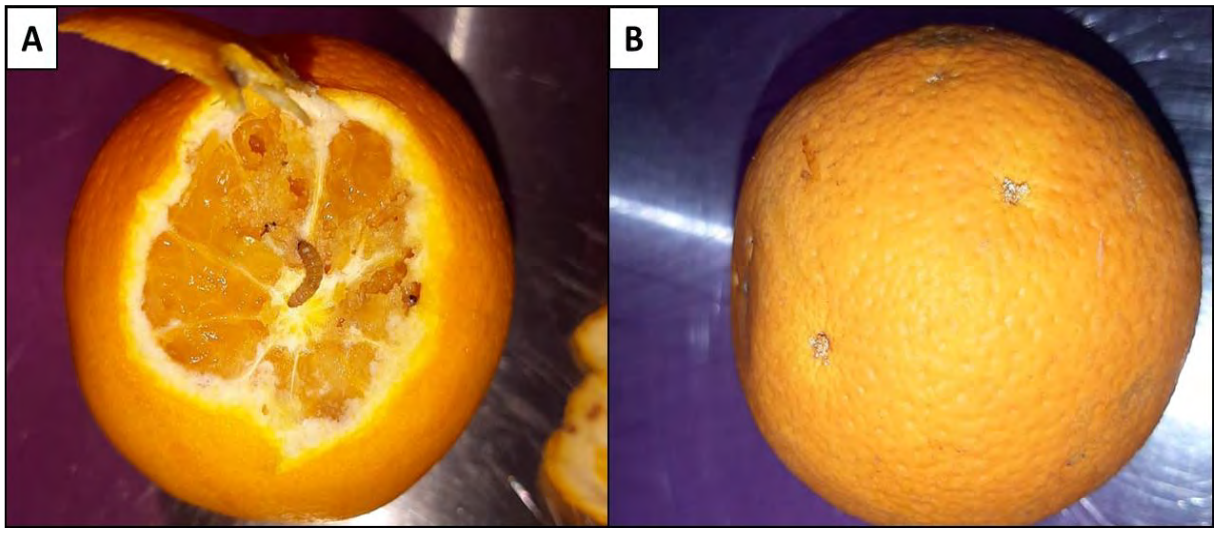

Figure 1.2: Damage to citrus fruit caused by the larvae of *T. leucotreta*, with A) showing the damage within the fruit and B) damage on the surface of the fruit (Images: Tahnee Bennett).

1.1.4 The life cycle of *T. leucotreta*

The life cycle of *T. leucotreta* may take between 30–174 days to complete, dependent on the prevailing conditions. The life cycle initiates with the laying of eggs by a gravid female moth on the surface of the host plant, citrus. After a few days, when the eggs fully develop, the neonate larva emerges and begins to penetrate and feed upon the host plant's fruit (Stibick, 2007). The time from egg hatch to successful entry into the fruit is a critically important period in the field biology of *T. leucotreta,* because newly hatched larvae enter the fruit through the rind. Fully developed larvae drop and burrow into the upper layer of the surrounding soil and begin to pupate. The adult moth eclose from these pupae (Stibick, 2007). The cycle starts again when the subsequent mating of male and female takes place (Figure 1.3). The life cycle stages are explained in greater detail below.

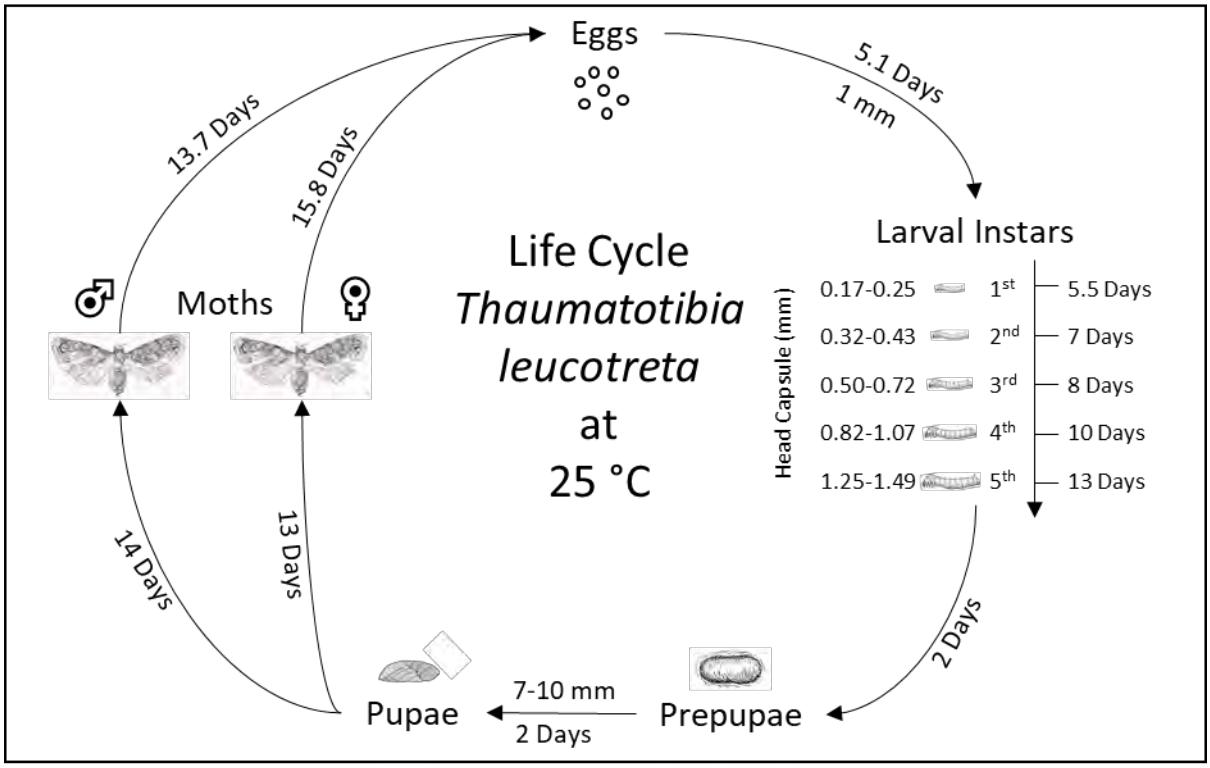

Figure 1.3: The life cycle of *T. leucotreta* showing egg, larval, pupal and adult stages. The eggs are flat with an oval-shape and have a length of 0.77 ± <0.001 mm and a width of 0.6 ± <0.001 mm. The eggs hatch and develop into a larva that later drops to the ground, burrow into the soil, spins a cocoon, and then pupates. The final stage of development for *T. leucotreta* is the adult moth (Jukes, 2018 and Daiber, 1980, 1979a, 1979b, 1979c).

At an optimum temperature of 25ºC, fertile females lay 100 to 250 eggs. However, there is usually only one egg per fruit, and only a few often survive due to lack of food and cannibalism when more than one egg is laid per fruit (Stibick, 2007). Eggs are susceptible to cold temperatures and an extended period of low humidity. The developmental times vary depending on environmental temperature and humidity (Daiber, 1979a). Higher humidity increases the percentage of eggs that hatch. Temperature and nutrition availability can also affect the development of the egg; larvae can take between 5 and 13 days to develop in temperature ranges of between 15 and 25 °C, respectively (Daiber, 1979a, 1979b, 1979c). Fully developed eggs hatch into neonate *T. leucotreta* larvae and begin to feed. Depending on how conducive the temperatures and nutrition availability are, larvae can take between 56 and 13 days to develop in temperature ranges of between 15 and 25 °C, respectively (Daiber, 1979c). Instars are determined by measuring the head capsule width, typically *T. leucotreta* undergoes five instars (Hofmeyr *et al*., 2016). Fully developed *T. leucotreta* larvae exit the infested host fruit and fall to the ground, burrowing into the surrounding soil to spin cocoons and pupate. The final stage of development for *T. leucotreta*, which is the adult moth, has a life span that is also temperature dependent. The time scale for the development decreases from 24.5 and 34.5 days at 10 °C to 13.7 and 15.8 days at 25 °C for male and female moths, respectively (Daiber, 1980).

1.1.5 Control of *T. leucotreta*

Since 1926, various products have been tested and applied for the control of *T. leucotreta* (Coombes *et al*., 2015). Due to the increasing regulatory and market pressures implemented by the western market on the southern African citrus industry, innovative and effective control methods need to be established in order to contain this pest (Hattingh *et al.,* 2019). An integrated pest management (IPM) programme is used in South Africa to control *T. leucotreta.* The programme components include insecticides, mating disruption, sterile insect technique, and biopesticides (Moore and Hattingh, 2017). The IPM programme was defined as a system that advises the selection of pest control tactics, either individually or in a coordinated approach (Bajwa and Kogan, 2002). It involves the application of a combination of various environmentally safe control methods with chemical control, based on the state of the environment, to reduce insect pest survival and the risk of resistance occurring (Moore and Hattingh, 2017). Additionally, IPM aims to protect crops at low cost and at low risks to humans and the environment. Joint control methods have been shown to promote the population growth of beneficial organisms in fruit orchards (Charleston *et al.,* 2003). South Africa uses an IPM

strategy that includes chemical insecticides in combination with alternative methods such as pheromone traps, cultural practices, sterile insect release, and the use of natural enemies and microbes, such as viruses, to control *T. leucotreta* (Charleston *et al*., 2003). Several registered chemical products have been used to control *T. leucotreta* in the agricultural industry. Since the late 1970s, the South African legislature has resulted in the reduction in the number of chemical insecticides, thereby amplifying the necessity for safer alternatives for pest control (Hattingh *et al.,* 2019). Relevant to this study is biological control, which involves the use of natural enemies such as predators, parasitoids, and entomopathogens to suppress pests and maintain populations of beneficial organisms (Bale *et al.,* 2008; Hoddle and Van Driesche, 2009). Biological control options used to control *T. leucotreta* include entomopathogenic nematodes (EPN), entomopathogenic fungi (EPF), entomopathogenic viruses (EPV), and parasitoids. These options have been tested and shown to be effective in the field (Malan *et al*., 2011; Moore and Hatting, 2012; Malan, *et al*., 2018). A major component of the IPM programme, and significantly relevant to this project, is the use of viruses in the control of *T. leucotreta* in South Africa, baculoviruses.

1.2 Baculoviruses and their role as biological control agents

1.2.1 Baculovirus classification and structure

Highly virulent baculoviruses in the family *Baculoviridae* have been successfully used for the control of a wide variety of different insect pests worldwide (Knox *et al.,* 2015). Since the discovery of baculoviruses, scientists have attempted to isolate and characterise new isolates to improve the understanding of their biology and taxonomy. The first major taxonomic division was recognised within the *Baculoviridae*, resulting in two genera, the nucleopolyhedroviruses (NPVs), and the granuloviruses (GVs). This division was primarily based on their morphological characteristics and has since undergone a further revision to incorporate genetic data. The classification of *Baculoviridae* has been updated based on evolutionary distances and phylogenetic analysis using alignments of concatenated *lef*-8, *lef*-9, and *polh* nucleotide sequences of members in the family, and the family is now divided into four genera (Jehle *et al*., 2006). The genera are *Betabaculovirus*, *Alphabaculovirus*, *Deltabaculovirus*, and *Gammabaculovirus*, with the *Betabaculovirus* and *Alphabaculovirus* used for biocontrol (Jehle *et al*., 2006). The genus *Alphabaculovirus* includes all lepidopteran specific nucleopolyhedroviruses that have a single nucleocapsid (SNPV) or multiple nucleocapsids (MNPV). The genus *Betabaculovirus* consists of lepidopteran specific

granuloviruses. The *Gammabaculovirus* includes hymenopteran-specific baculoviruses, and finally, *Deltabaculovirus,* which, to date, comprises only CuniNPV and possibly the still undescribed dipteran-specific baculoviruses (Jehle *et al*., 2006). The granuloviruses have a similar life cycle to that of alphabaculoviruses, while not much is known about the remaining two genera (Rohrmann, 2019).

Baculoviruses are occluded viruses with genomes consisting of circular double-stranded DNA (dsDNA) with sizes varying between 80 and 180 kb (Herniou *et al*., 2003). There are two main morphological structures associated with baculovirus virions; the occlusion derived virion (ODV) and the budded virion (BV). Both the ODV and BV consist of cylindrical nucleocapsids surrounded by a lipid envelope. The BV envelope surrounds a single nucleocapsid and has several embedded proteins, which assist in cell recognition. Occlusion derived virions are surrounded by a large proteinaceous structure and are referred to as occlusion bodies (OBs) containing either one or multiple ODVs. The NPVs have large OBs consisting of numerous rod-shaped ODVs. The second group, granuloviruses, consists of small granular occlusion bodies (OB) that contain a single ODV (Figure 1.4) (Okano *et al*., 2006). The primary protein involved in the OB structure differs between these groups, with *granulin* found in the GV OBs and *polyhedrin* (*polh*) found in NPV OBs. These viruses infect the insect orders Lepidoptera, Hymenoptera, and Diptera and naturally control insect populations (Okano *et al.*, 2006).

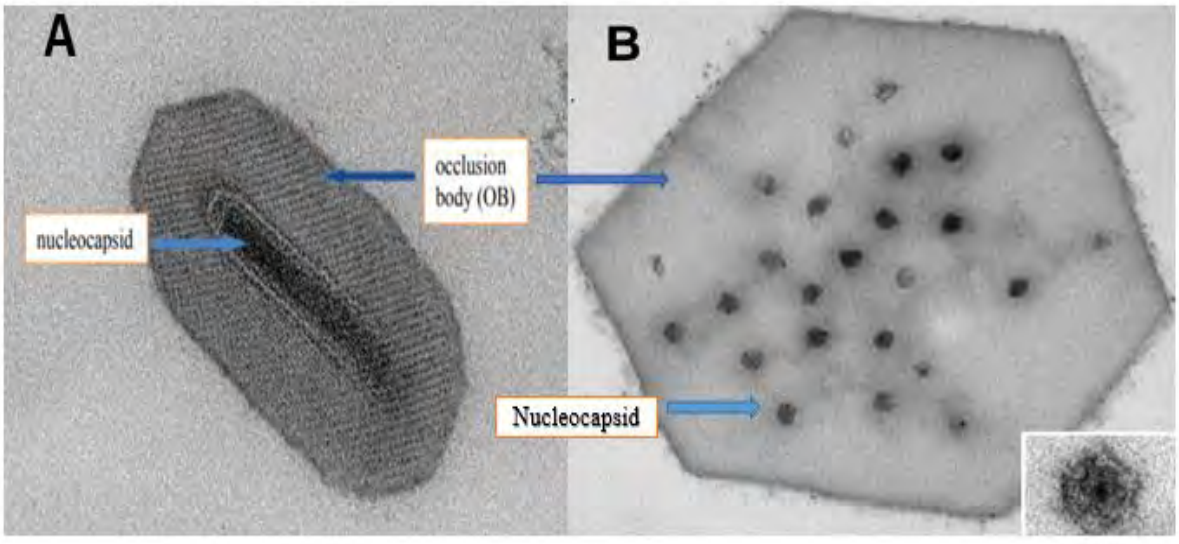

Figure 1.4: Baculoviruses have been divided into two groups based on OB morphology. A) granuloviruses have a single virion in granule form. B) NPVs have multiple virions in polyhedral form OBs (Dhladhla *et al*., 2018; Harrison *et al*., 2017).

1.2.2 Genome characteristics

The baculovirus genome consists of a circularised dsDNA molecule with sizes varying from about 80 to over 180 kb, which encode between 90 and 180 genes (Friesen, 2007). The comparison of known genome sequences of all baculoviruses provided a platform for identifying the standard sets of genes, the baculovirus core genes (Miele *et al*., 2011). These core genes seem to be the crucial factors for some of the main biological functions of the virus during infection. They are involved in viral processes such as DNA replication, transcription, virion structure, and impairing cellular metabolism (Garavaglia *et al*., 2012).

1.2.3 Core genes

To date, *Baculoviridae* has a set of 38 genes that are recognised as encoding sequences shared by members of this family (Rohrmann, 2019). Rohrmann, 2019 presented core genes in all baculovirus genomes by functional groupings such as transcription (*Late expression factor 4*, *Late expression factor 5*, *Late expression factor 8*, *Late expression factor 9*, *P47*, *Very late factor 1*), replication (*Alkaline nuclease*, *DNA helicase*, *DNA polymerase*, *Late expression factor 1*, *Late expression factor 2*), and unknown function (*Ac78*, *Ac81*, *Ac93*, *Ac101,* and *Ac103*). Relevant to this study are the *late expression factor 8/9* (*lef-9* and *lef-8*) core genes that encode for viral RNA polymerase subunits, which are responsible for the regulation of the transcription of late and very late viral genes (Clem and Passarelli, 2013; Guarino *et al.*, 1998). The *granulin* gene encodes *granulin* in granuloviruses and is one of the most conserved genes in lepidopteran-specific betabaculoviruses (Rohrmann, 1986). The *lef-8*, *lef-9* and *granulin* genes are selected for this study because they have been identified in all completely sequenced *betabaculovirus* genomes and have previously been shown to be suitable for studying baculovirus phylogeny (Herniou *et al.*, 2001; Herniou *et al.*, 2003; Lange *et al.*, 2004; Wennmann *et al*., 2018).

1.2.4 The life cycle of baculoviruses

The infection of an insect takes place by the ingestion of plant material contaminated with baculovirus OBs by larvae susceptible to the virus. Thereafter, the outer protein matrix is dissolved in the insect's midgut by the alkaline fluid present (Figure 1.5) (Rohrmann, 2019). The released enveloped virions called occlusion-derived viruses (ODVs) attach and fuse to the midgut epithelial cells of the insect, initiating primary infection (Figure 1.5). The budded virus is formed in the nucleus of the epithelial cells; after that, the budded virus leaves the midgut epithelium by a budding process to the hemocoel, where secondary infection occurs (Figure 1.5) (Rohrmann, 2019). During the late stages of infection, OBs begin to accumulate in the

infected cells. Once the infection has progressed, the virus liquefies the insect cells, and the OBs are released to the environment when the insect dies and disintegrates (Figure 1.5) (Rohrmann, 2019).

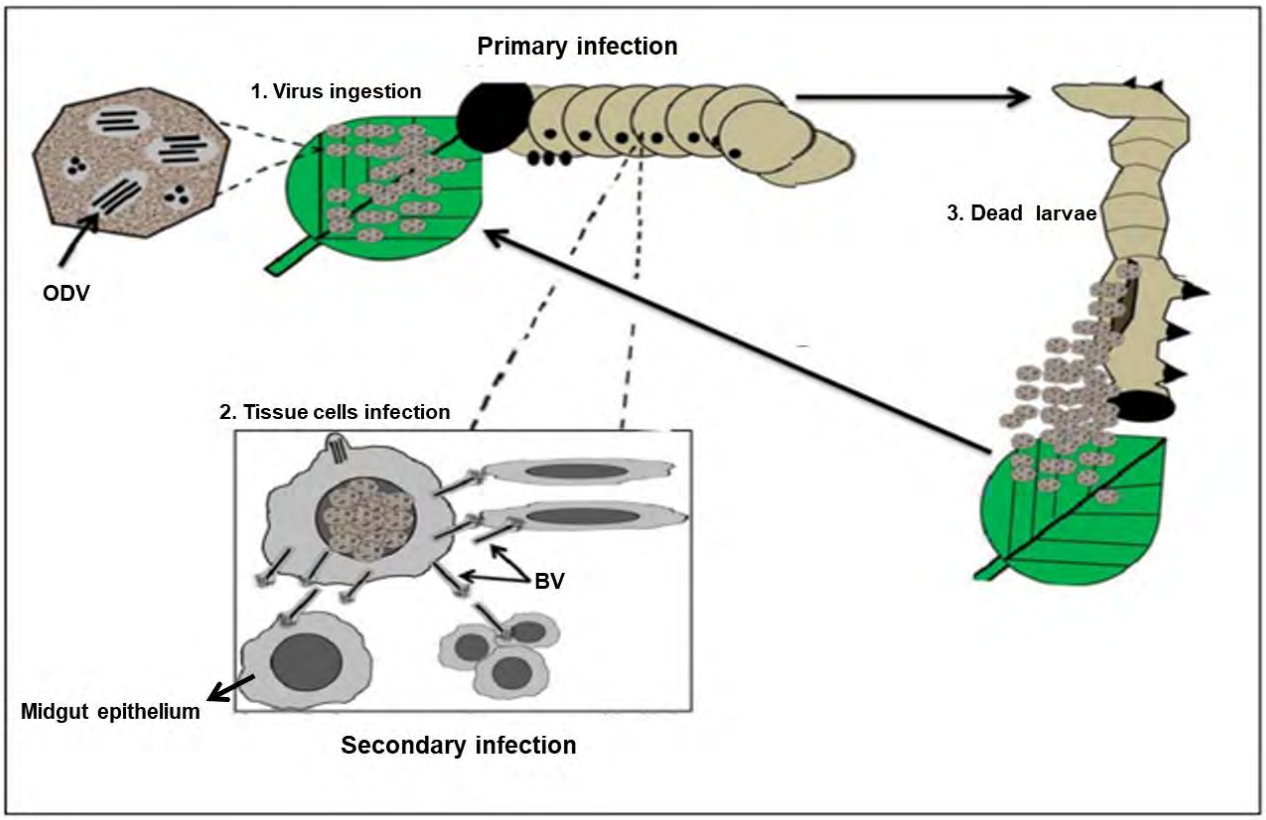

Figure 1.5: The life cycle of a baculovirus causing systemic infection. 1. The insect feeds on the OB; after ingestion, the OBs dissolve in the midgut and then release ODVs, which infect the midgut epithelial cells. 2. The virions leave the epithelial cell in the form of budded viruses and start the systemic infection. Early in systemic infection, more BVs are produced and infect other insect cells. 3. OBs accumulate, and the cell then dies, releasing the OBs back into the environment (Modified from Kroemer, *et al*., 2015).

1.2.5 Baculoviruses as biocontrol agents

Baculoviruses have been developed into biopesticides and have been used for more than 60 years in the agricultural industry worldwide (Moscardi, 1999; Ahmad *et al.*, 2011; Hattingh *et al.,* 2019). These viruses generally have a very narrow host range, limited to a few closely related species or often even to a single species, with high virulence and therefore are unlikely to cause harm to non-target organisms in the environment, enabling baculoviruses to be highly selective pest control agents (Moscardi, 1999; Szewczyk *et al.*, 2006; Ahmad *et al.*, 2011; Moore *et al*., 2020). Over the years, studies on baculoviruses as a control method have proven it to be safe for humans to work with (Rodriguez *et al.*, 2012). Baculoviruses can be applied

along with other pesticides (Moore *et al.*, 2004). Baculoviruses are popular components for integrated pest management (IPM) programs for controlling crop pests in the field (Moscardi, 1999; Knox *et al.,* 2015; Hatting *et al.,* 2019). Several NPVs and granuloviruses have been formulated into commercial products, while many others are used without a brand name. Successful applications of baculoviruses for protection of citrus crops against *T. leucotreta* is demonstrated by the three biopesticides that are currently registered in South Africa, namely Cryptogran® (River Bioscience, South Africa), Cryptex®, and Gratham® (both Andermatt-Biocontrol AG, Switzerland) (Hatting *et al.,* 2018, Moore, 2019; 2021). The products consist of Cryptophlebia leucotreta granulovirus (CrleGV-SA) as their active component (Moore *et al*., 2011).

1.2.6 Cryptophlebia leucotreta granulovirus

Cryptophlebia leucotreta granulovirus (CrleGV) was first described by (Angelini *et al*., 1965), with the virus isolated from infected *T. leucotreta* larvae collected from the Ivory Coast. Using restriction endonuclease analysis with DNA extracted from the virus demonstrated that the virus was novel, as its virus DNA profile was not previously documented (Moore *et al.*, 2004). After the first discovery, other isolates were discovered from infected larvae on the Cape Verde Islands and laboratory-reared insects collected in South Africa and housed at the Hoechst Corporation in Germany (Knox *et al.,* 2015). The name of the virus arose from the earlier name of *T. leucotreta*, which was Cryptophlebia leucotreta. In the late 1990s, the host name was changed to *Thaumatotibia leucotreta* (Komai *et al.*, 1999). Cryptophlebia leucotreta granulovirus (CrleGV) belongs to the Baculoviridae family, and many viruses in this family have been developed and registered as insecticides (Federici, 1997). Cryptophlebia leucotreta granulovirus South Africa (CrleGV-SA) is a previously genetically characterised South African isolate (Singh *et al.*, 2003). After developing a virus production system and large-scale field trials, the virus was formulated to a registered biopesticide, namely Cryptogran, and has been successfully used in the field for over 15 years (Moore *et al.*, 2015). Recently, the complete genome of CrleGV-SA has been sequenced and is available in the NCBI's GenBank (Accession number MF974563.1). A study examining the CrleGV-SA over several years of commercial use found that the CrleGV genome is genetically stable (Van Der Merwe *et al.*, 2017).

1.2.7 Challenges encountered in the development of baculovirus biopesticides

Baculoviruses have several advantages as biopesticides, including a narrow host range that allows targeted control of pests and the ability to spread through pest populations after

application by horizontal transmission. Additionally, these viruses also cause reduced environmental damage compared to other control options (Moscardi, 1999; Erlandson., 2008; Szewczyk *et al*., 2008). Biopesticides offer a potential solution to the increasing concern over the use of chemical pesticides in the agricultural industry while maintaining a more environmentally friendly approach.

Although many baculoviruses have been successfully developed into commercial biopesticides, there remain several challenges and limitations which require further research and development. These disadvantages include the speed of kill, virulence, ultraviolet (UV) susceptibility, development of resistance in targeted hosts, and cost of production (Fritsch *et al*., 2007; Jehle *et al*., 2006; Jehle, 2008). The virulence and speed of kill against a specific host have the most significant influence on the efficacy of commercial products. For example, exposure of UV susceptible baculovirus to UV radiation results in rapid inactivation of virions (Arthurs *et al*., 2008). Another challenge is the potential of becoming resistant to baculoviruses; currently, one example of resistance development has been observed. Resistance was observed in European populations of *Cydia pomonella*, which showed decreased susceptibility towards a commercially formulated baculovirus CpGV that was isolated in Mexico (CpGV-M) (Asser-Kaiser *et al*., 2007). Since then, additional types of resistance to CpGV have been identified in *C. pomonella* (Jehle *et al*., 2017).

Quantifying or counting the baculoviruses is fortunately relatively straightforward; however, OBs of GV are more challenging, as they are smaller ovoids 0.2×0.5μm and are demanding to count under dark field microscopy (Grzywacz and Moore, 2017). This technique is tedious and somewhat inaccurate, as it requires significant sample preparation prior to use that can have an impact on what is visualised. It is not able to distinguish viral particles that are positioned within the different focal planes of the counting chamber and so high concentrations of particles can "run together" to create the appearance of larger particle. Additionally, the technique is time-consuming and can yield inconsistent results (Grzywacz and Moore, 2017). This step is essential as it is crucial to ensure that a baculovirus product is efficacious (apart from the manner in which it is applied) that the registered concentration to be applied is adequate to achieve an acceptable level of pest control.

These limitations show the importance of the need to developing innovative solutions to overcome both these and novel obstacles that may be encountered. In order to use granuloviruses for commercial purposes, quantification of the viral particles is required to perform bioassays for field trials and formulation, among other applications.

1.2.8 Quantification of baculoviruses

Various techniques have been used for the quantification of baculoviruses particles, namely, spectrophotometry (Singh *et al*., 2003), microscopy, flow cytometry, and quantitative PCR (qPCR) (Dhladhla *et al.*, 2018). The type of microscopy technique used to quantify baculoviruses is dark field microscopy. Microscopy is the traditional method used and provides an essential platform for virus enumeration and has been used extensively in medical and biological sciences to study the morphology of biological systems, including insect viruses (Dhladhla *et al.*, 2018). Although the technique is cheap and not technical, it requires specialised skills; it is not very sensitive or species-specific. Other microscopic limitations include being tedious, labour intensive and causes eye strain during the counting of GVs. It can only be used to count viruses in samples with relatively high viral loads, such as infected larvae (Graham *et at*., 2015). Additionally, the microscopic enumeration technique does not allow for enumeration and differentiation between different viruses (Jukes, 2018).

Another technique is flow cytometry, which involves the direct count of virus particles obtained from cell cultures stained with SYBR Green dye (the dye used in qPCR), using a flow cytometer (Shen *et al.*, 2002). Virus samples need to be prepared from cell cultures, and the virus particles are then fixed using paraformaldehyde, freeze-thawed, and heated to optimise staining by SYBR Green. The limitations of this technique are that it is costly, requires specialised skills, and not all particles identified as viruses by the flow cytometric measurement are, in fact, viruses. Although SYBR Green dye is used, specific baculovirus concentrations cannot be calculated in a mixed infection. This is due to the unspecific nature of this technique, thus cannot distinguish between different viruses (Dhladhla *et al.*, 2018). A low fraction of particles has been found to be interferants that were not registered as viruses by microscopic scoring (Nüsse *et al.*, 1992).

Quantitative PCR (qPCR) is another method used to quantify viruses and is a highly sensitive method based on amplifying a specific DNA gene of interest. When used at the whole genome level, this approach can be used to identify species and has been used to differentiate between variants on a given gene or gene fragments (Krejmer-Rabalska *et al.,* 2019). This method is highly sensitive; however, there are constraints such as having to design oligonucleotides, construct plasmids, and it has high equipment costs (Hitchman *et al*., 2007).

Other studies have utilised this qPCR for the quantification of baculoviruses. Graham *et al.*, (2015) used this technique to quantify the dynamics of covert baculovirus infections within the

lepidopteran host, *Spodoptera exempta*. Krokene *et al*., (2013) also conducted a qPCR assay that accurately estimated the total number of NeseNPV genomes extracted from a sample. However, qPCR could not determine the exact amount of virus occlusion bodies present because the number of viral particles or genomes varies significantly between individual occlusion bodies of NPVs. In a recent paper by Krejmer-Rabalska *et al.,* (2019), several granuloviruses were discriminated by qPCR based on the amplification of three conserved genes, *lef-8*, *lef-9*, and *granulin*. Their approach, however, was not meant to quantify the viruses but instead developed a method for discriminating between the representative groups of betabaculoviruses. Dhladhla *et al.*, (2018) attempted to develop alternative methods, including qPCR for CrleGV quantification, and compare their accuracy, effectiveness, and efficiency. The viral gDNA standard curves with 100% efficiency, indicated by the slope of the line, were generated, indicating that qPCR can be used as an alternative enumeration method for any baculovirus. However, the reliability of standards for qPCR is a crucial issue as the standards used in this study were of CrleGV gDNA. Genomic DNA was extracted using the traditional CTAB (hexadecyltrimethylammonium bromide) method, and the concentration was determined using the Qubit fluorometer. Lately, sample preparation for qPCR has turned towards the use of DNA extraction kits because traditional methods such as phenol/chloroform extraction have been reported to yield inconsistent DNA recovery from baculovirus samples (Lo and Chao, 2004). Additionally, gDNA standards kept for prolonged periods at -20 ˚C or repeated freeze/thaw cycles result in poor amplification efficiency as they become susceptible to degradation (Burns *et al*., 2006). Once made, standards are typically used for extended periods, and stability of standards is thus critical; this shows the importance of choosing the appropriate standards.

Plasmid DNA containing the target sequence has been commonly used as the standard in qPCR due to its high stability (i.e., little degradation during storage) and ease in preparation (Wong and Medrano, 2005). Although plasmid construction may be time-consuming, using plasmids as qPCR standards has many advantages compared with other strategies. Plasmids are highly stable molecules even after prolonged storage times at room temperature; they generate extremely reproducible standard curves with reliable efficacy and sensitivity (Formisano-Tréziny *et al*., 2012). Additionally, unlike viral gDNA standards, plasmid standards are easier and cheaper to sequence, and due to their stability, plasmid molecules are easy to distribute around the world (Burns *et al*., 2006). George *et al*., (2012) compared the qPCR efficiency when using gDNA and plasmids as standards; the results showed that the use of gDNA as

standards could result in primer dimerisation due to the difficulty encountered by the PCR components to access the baculovirus genome.

1.3 Motivation

Baculoviruses have been formulated and registered as biopesticides to control several pests such as *T. leucotreta* in South Africa and many other countries. CrleGV-SA has been used for many years as a biopesticide for the control of *T. leucotreta*. In order to use it as a biopesticide, OBs have to be quantified to perform bioassays for field trials and formulation, among other applications. The traditional method used for counting CrleGV-SA is dark field microscopy; however, this method is not reliable due to its limitations. It is characterised as being tedious, subjective, time-consuming, and has the disadvantage of being contaminated by non-biological debris or biological material. Several studies have successfully applied the qPCR technique to quantify certain baculoviruses as an alternative to dark field microscopy. However, there is still a knowledge gap, as there is only one study by Dhladhla *et al.*, (2018), whereby there was an attempt to develop a qPCR method to quantify CrleGV. In their research, they compared methods of enumeration of CrleGV-SA. Quantitative polymerase chain reaction (qPCR) was one of the methods described and was concluded to be the technique that offered the most significant potential as an enumeration method for GVs for routine experiments in the production of GVs biopesticides. The CrleGV gDNA was used to create the standards, targeting the *granulin* gene in the qPCR assay. However, using gDNA as standards in qPCR comes with limitations as the gDNA becomes unstable over time, and traditional extraction methods like CTAB can yield inconsistent DNA recovery. Thus, gDNA standard design, production, concentration determination, and stability over long time storage can be highly problematic. Plasmids carrying DNA target sequences are the most widely used type of template in qPCR methods; determination of plasmid concentration is based on simple theoretical calculation. There are commercially available plasmid extraction kits that yield pure plasmid DNA. The cost, time, and efforts in preparing plasmid DNA are worth it if one considers the stability of plasmid DNA, sensitivity, and reproducibility of the standard curves.

1.4 Overall aim and objective

This study aims to develop and optimise a qPCR technique to accurately quantify CrleGV-SA OBs using plasmid DNA for downstream applications. Furthermore, the qPCR technique will be compared to dark field microscopy.

The specific objectives are:

1) To conduct a sequence analysis of betabaculoviruses, align the selected genes to identify conserved regions and to design two sets of external and internal oligonucleotides for PCR amplification of selected conserved regions of the CrleGV-SA genome
2) To test the two sets of oligonucleotides by conventional PCR on CrleGV-SA genomic DNA and construct plasmids for use as a standard in the qPCR assay by cloning of the amplified outer regions
3) To compare two methods of DNA extraction from purified CrleGV-SA OBs for optimum genomic DNA yield
4) To develop and optimise a quantitative PCR (qPCR) assay for the quantification of CrleGV-SA OBs
5) To compare the qPCR method of enumeration with the current method, microscopy, to verify its accuracy and determine the most consistent and comparable method using unknown samples

Overview of chapters

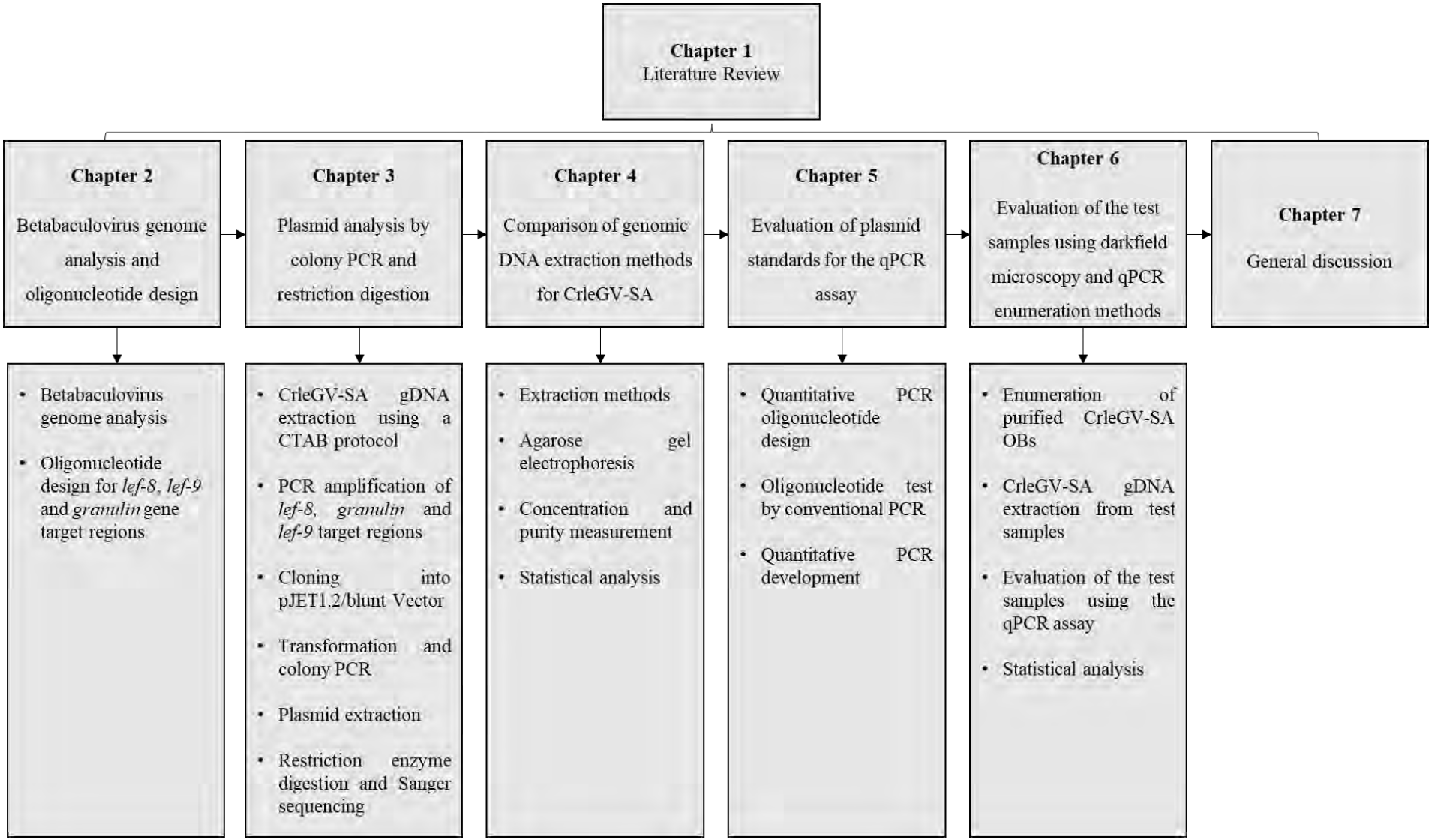

Chapter 2

Betabaculovirus genome analysis and oligonucleotide design

2.1 Introduction

To date, 90 baculovirus reference genomes are available in the National Centre for Biotechnology Information (NCBl) database, including 50 from alphabaculoviruses and only 26 from betabaculoviruses (Rohrmann, 2019). This information generated by sequencing of baculovirus genomes has enabled the identification of conserved genes, variation in genomes and provided the data necessary to compare novel isolates. Different baculoviruses have diverse gene content present in their genomes. Despite this, a set of 38 genes present in all sequenced baculovirus genomes has been identified (Rohrmann, 2019). About half of the conserved genes are virion-associated proteins involved in capsid structure, the occlusion-derived virus envelope, and larval infectivity. The others are related to DNA replication or processing and late or very late transcription (Garavaglia *et al*., 2012; Rohrmann, 2019). As mentioned in the previous chapter, the *lef-8*, *lef-9* and *granulin* genes are selected for this study as they have been identified in all fully sequenced *betabaculovirus* genomes and have previously been shown to be suitable for studying baculovirus phylogeny (Herniou *et al.*, 2001; Herniou *et al.*, 2003; Lange *et al.*, 2004). The target genes are present as a single copy in GV genomes. The *lef-8* and *lef-9* genes encode for subunits of the baculovirus RNA polymerase, which initiates transcription from late and very late promoters (Guarino *et al.,* 1998). The *granulin* gene encodes *granulin*, a major matrix protein of the occlusion bodies (OBs) in granuloviruses, and is one of the most conserved genes in lepidopteran-specific baculovirus (Rohrmann, 2019).

The baculoviruses of interest in this chapter are CrleGV-SA and CrleGV-CV3. The sequencing of baculovirus genomes is an important aspect of baculovirology, enabling identification, phylogenetic analysis, and it allows gene composition to be studied (Rohrmann, 2019). These viruses were selected based on a study by Jehle *et al*., 2006, which analysed gene fragments of 37 granuloviruses from nine different families. These baculovirus genomes have been sequenced and are present on GenBank (NCBI, USA). As discussed in the previous chapter, CrleGV was first isolated from infected larvae in the Ivory Coast (Angelini *et al*., 1965).

Another CrleGV isolate was recovered from the Cape Verde Islands (CrleGV-CV), and another CrleGV isolate was reported in a laboratory culture of FCM (FCM material collected from South Africa) held by the Hoechst Corporation in Germany (Knox *et al.,* 2015). CrleGV-SA has been successfully utilised to control *T. leucotreta* for over 10 years and has been shown to remain genetically and biologically stable across this duration (Moore *et al*., 2015; van der Merwe *et al*., 2017).

As mentioned in the previous chapter, using plasmid DNA as a standard in qPCR assays for virus enumeration is advantageous in terms of easy, cost-efficient production, distribution, and long-term stability. Construction of plasmid standards for the qPCR assay involves cloning the target sequence into the plasmid of interest. Typically, target regions are identified, and oligonucleotides must be designed for amplification. This chapter describes the analysis of the three conserved genes from CrleGV-SA and CrleGV-CV3 genome sequences. First, a comparison of *lef-8*, *lef-9*, and *granulin* genes from the two viruses was performed by multiple alignments to evaluate the degree of identity between these genes. Secondly, two sets of oligonucleotides were designed to meet specific criteria from regions with the highest identity. Lastly, *in silico* testing was conducted to evaluate the designed oligonucleotides to determine whether they specifically bind to the selected target regions.

2.2 Materials and methods

2.2.1 Betabaculovirus genome analysis

Genomic DNA sequences available on GenBank of closely related baculoviruses, namely CrleGV-SA and CrleGV-CV3 were analysed to validate the similarity between the *lef-8*, *lef-9*, and *granulin* genes. Table 2.1 shows the only full genome sequences available in GenBank (NCBI) and are the betabaculoviruses selected for the alignment.

Table 2.1: The genome sequences of the betabaculoviruses CrleGV used in this study and the corresponding GenBank (NCBI) accession numbers.

Granuloviruses	Virus abbreviation	Accession number	Publication
Cryptophlebia leucotreta granulovirus South Africa	CrleGV-SA	MF974563.1	van der Merwe *et al*., 2017
Cryptophlebia leucotreta granulovirus Cape Verde	CrleGV-CV3	AY229987.1	Jehle And Baekhaus 1994

2.2.2 Oligonucleotide design for *lef-8*, *lef-9* and *granulin* gene target regions

Genomic DNA sequences for the baculoviruses mentioned in section 2.2.1 were downloaded from GenBank. The target genes (Table 2.2) were extracted from the complete genome sequences and aligned using the Geneious R11 software. This enabled the identification of conserved regions within each target gene among the two viruses to which primers could be designed. For each selected gene from the complete CrleGV-SA genome sequence, two sets of oligonucleotides were designed and tested using the Primer3 (v4.0.0) online tool. The first set was the external oligonucleotides; this set was designed to produce amplicons that will be cloned into a vector of interest in downstream experiments and encompassed an inner region which would be targeted during qPCR analysis. The external oligonucleotides were designed from regions that do not form oligonucleotide-dimers while also having an optimal melting temperature of 59 °C, producing partial amplicons of 500-1000 bp. The second set is the internal oligonucleotides; these were designed for use in downstream qPCR assays. These were designed to meet specific criteria, such that the length is 20 bp, the amplicon size is 150-200 bp, a melting temperature (T_m) of 57 °C - 62 °C, one GC clamp, and a GC percentage ranging between 30 and 70, enabling them to be further utilised in the qPCR analysis. The designed oligonucleotides were synthesised by Inqaba Biotech (Pretoria, South Africa). Figure 2.1 below shows a general schematic diagram of the above-described gene alignments and the design of external and internal oligonucleotides.

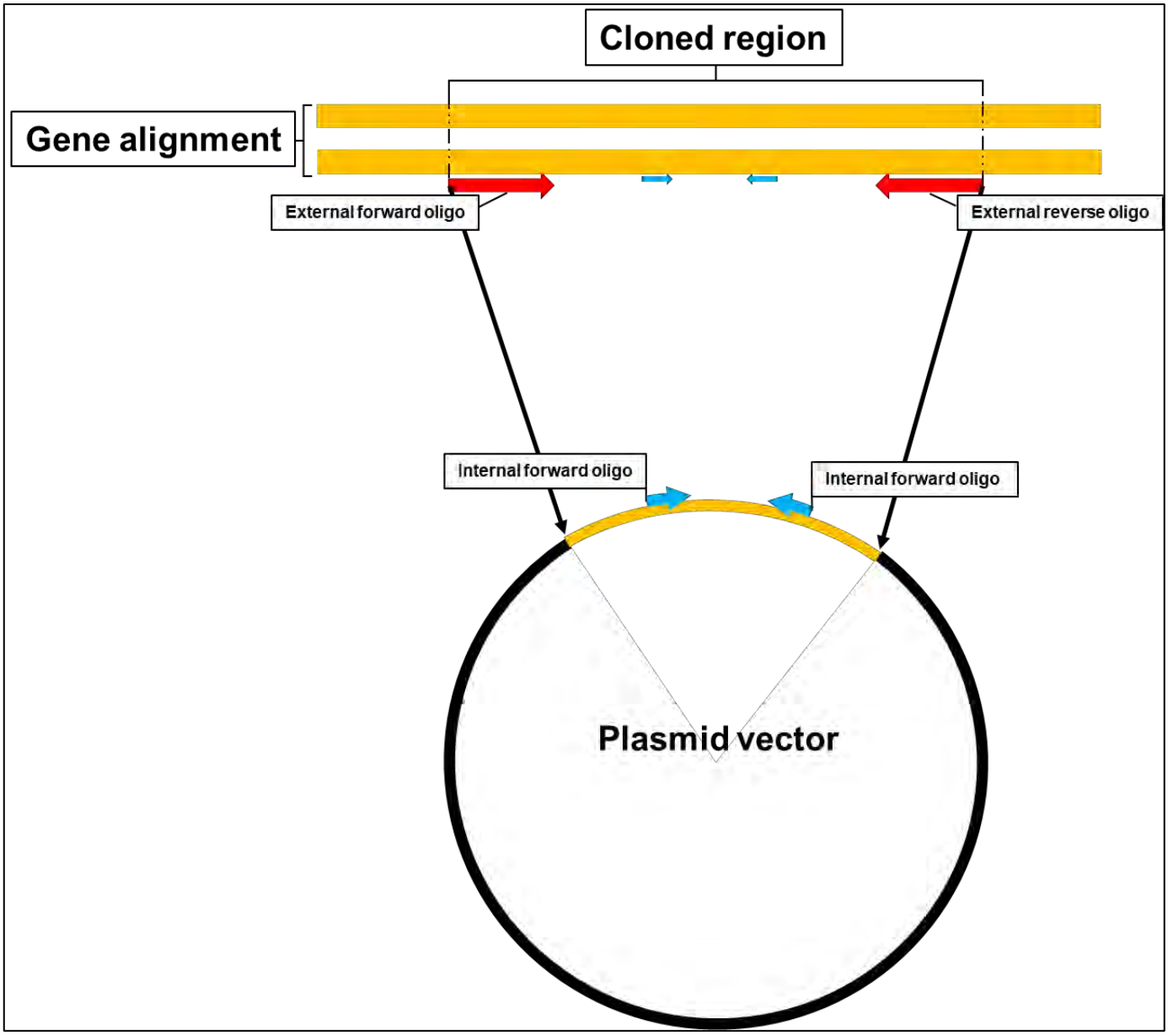

Figure 2.1: Schematic diagram showing the alignment of the selected genes, the general binding regions of external and internal oligonucleotides, and the cloned region. The yellow bars indicate the general gene alignment with the red arrows showing the forward and reverse external oligonucleotide binding regions. The blue arrows show the forward and reverse internal oligonucleotide binding regions.

Table 2.2 below shows the genes selected for this study, accession number, gene position in the genome, and the gene sizes.

Table 2.2: The genes selected for alignment to identify conserved regions.

Granuloviruses	Selected Genes	Accession number	Position in genome	Size (bp)
Cryptophlebia leucotreta granulovirus-South Africa	*Granulin*	MF974563.1	1-747	747
	Lef-8		101902-104499	2596
	Lef-9		91581-93350	1498
Cryptophlebia leucotreta granulovirus-Cape Verde	*Granulin*	AY229987.1	1-747	747
	Lef-8		101473-104070	2597
	Lef-9		91475-92974	1499

2.3 Results

2.3.1 Gene alignment and primer binding

An alignment between CrleGV-SA and CrleGV-CV3 was performed in Geneious R11 to identify highly conserved regions from the three selected genes.

2.3.1.1 *Granulin* gene alignment and oligonucleotide binding

The *granulin* gene sequences were aligned, and the external oligonucleotides bind from the region spanning from 33 to 641 in the alignment shown in Figure 2.2. Meanwhile, the internal oligonucleotides bind from the region spanning from 243 to 399 on the gene.

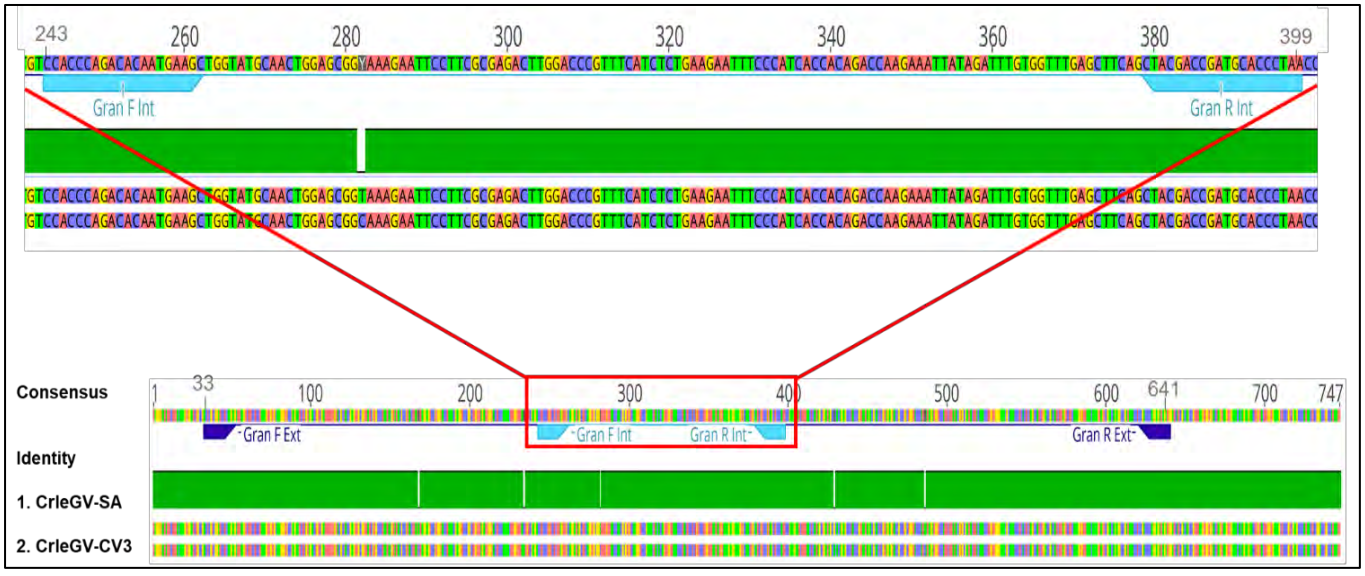

Figure 2.2: Nucleotide alignment of the *granulin* from CrleGV-SA and CrleGV-CV3. The green bars show alignment identity. The internal forward and reverse oligonucleotide binding

regions are annotated as light blue bars, and the external forward and reverse oligonucleotide binding regions are the purple bars.

2.3.1.2 *Lef-9* gene alignment and oligonucleotide binding

The *lef-9* gene sequences were aligned, and the external oligonucleotides bind from the region spanning from 365 to 1027 in the alignment shown in Figure 2.3. The internal oligonucleotides bind from the region spanning from 696 to 878 on the gene.

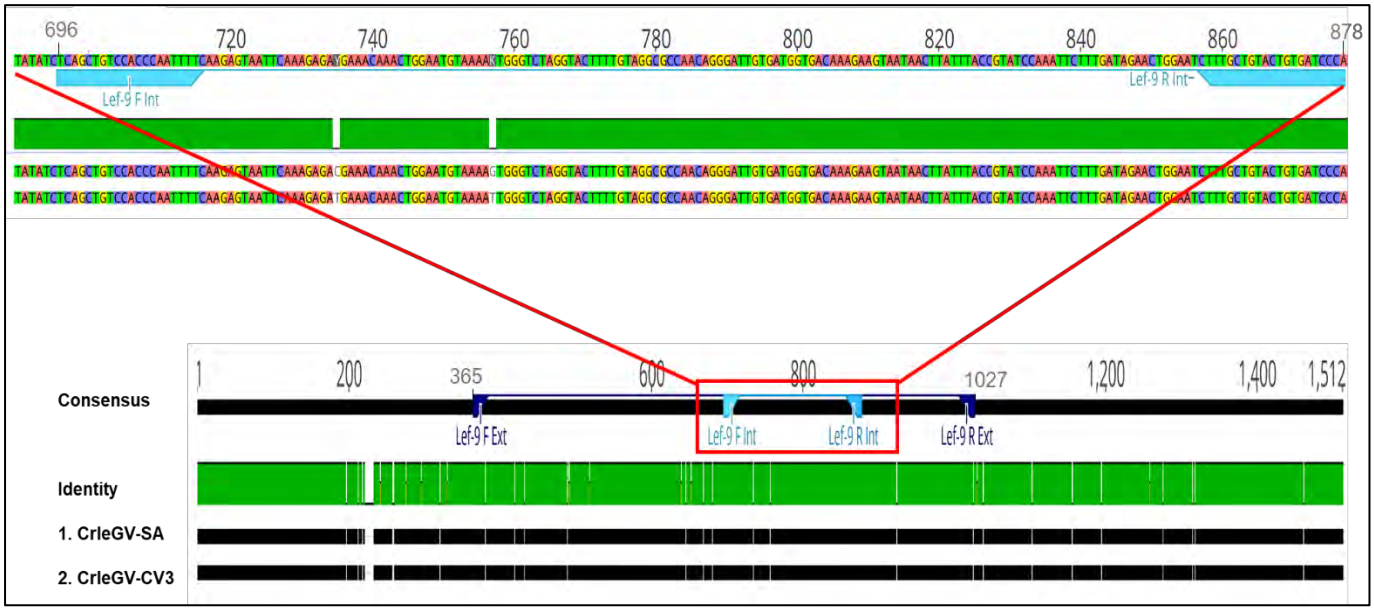

Figure 2.3: Nucleotide alignment of the *lef-9* from CrleGV-SA and CrleGV-CV3. The green bars show alignment identity. The internal forward and reverse oligonucleotide binding regions are annotated as light blue bars, and the external forward and reverse oligonucleotide binding regions are the purple bars.

2.3.1.3 *Lef-8* gene alignment and oligonucleotide binding

The *lef-8* gene sequences were aligned, and the external oligonucleotides bind from the region spanning from 153 to 834, alignment shown in Figure 2.4. The internal oligonucleotides bind from the region spanning from 398 to 548 on the gene.

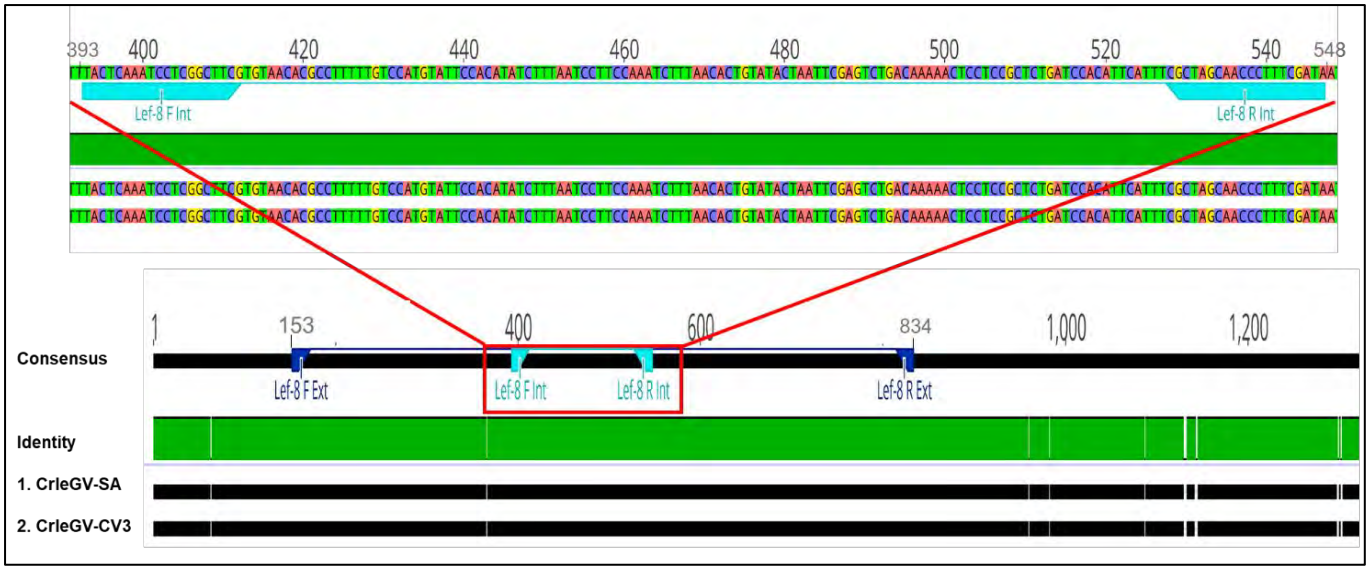

Figure 2.4: Nucleotide alignment of the *lef-8* from CrleGV-SA and CrleGV-CV3. The green bars show alignment identity. The internal forward and reverse oligonucleotide binding regions are annotated as light blue bars, and the external forward and reverse oligonucleotide binding regions are the purple bars.

Oligonucleotides were designed and tested using the Primer3 (v4.0.0) online tool and Geneious R11 software based on the target regions of CrleGV-SA *granulin*, *lef-9*, and *lef-8* genes. Primer3 (v4.0.0) automatically selected regions that did not form hairpin/secondary structures and primer dimers while having an optimal melting temperature of 59 °C (Table 2.3).

Table 2.3: Oligonucleotide design against CrleGV –SA *granulin*, *lef-9*, and *lef-8* genes.

	Primer name	Oligonucleotide sequence (5' – 3')	Melting temperature °C	Length bp	Hairpin	GC %	PCR product size bp
External oligonucleotides	Gran-ext R	CTACATACACCAGGGGACGG	59	20	0	60	608
	Gran-ext F	TCACGACGGTACCACTTGTG	60	20	0	55	
	Lef-8-ext R	ACATACCCCACACGCAATTG	59	20	0	50	681
	Lef-8-ext F	CGAGCCTAGTACCCTCCAAC	59	20	0	55	
	Lef-9-ext R	ACTCTGGGCATCTTGAAGTTG	59	21	0	55	662
	Lef-9-ext F	TGCCTAACTTCAACTTGTGGG	59	21	0	55	
Internal oligonucleotides	Gran-int R	TTAGGGTGCATCGGTCGTAG	59	20	0	55	156
	Gran-int F	CCACCCAGACACAATGAAGC	59	20	0	55	
	Lef-8-int R	ACACAAAATCCATGTCCGGC	59	20	0	50	155
	Lef-8-int F	GGAAACTACGACGATGACAAAAC	58	20	0	44	
	Lef-9-int R	TGGGATCACAGTACAGCAAAG	58	21	0	48	182
	Lef-9-int F	TCAGCTGTCCACCCAATTTTC	59	21	0	48	

2.4 Discussion

This chapter aimed to determine the degree of nucleotide conservation of the CrleGV-SA and CrleGV-CV3 *granulin*, *lef-9*, and *lef-8* gene sequences available on GenBank prior to oligonucleotide design. This analysis involved the alignment of the three gene sequences from the viruses respectively to determine regions with the highest degree of identity where oligonucleotides could be designed. Following this was an oligonucleotide design from the CrleGV-SA sequence for each selected gene. The last objective was to conduct *in silico* testing to check whether the designed oligonucleotides properly bind to the target regions prior to Sanger sequencing.

The first objective for this chapter was to analyse the *granulin*, *lef-9*, and *lef-8* genes of CrleGV-SA and CrleGV-CV3 by aligning the genes, respectively. These alignments enabled the selection of gene regions that are highly identical between the two baculoviruses. For each gene, two sets of oligonucleotides were designed, with the first set being the external oligonucleotides, namely Gran-ext F, Gran-ext R, Lef-9-ext F, Lef-9-ext R, Lef-8-ext F and Lef-8-ext R. These were designed from regions that do not form primer-dimers while also having an optimal melting temperature of 59 °C. The external oligonucleotides were successfully designed for all three genes. These were to be utilised to amplify the CrleGV-SA gDNA target regions in preparation for cloning into plasmids with the qPCR target regions found within the cloned regions. The Gran-ext oligonucleotides were designed to produce amplicons with a size of 608 bp, meanwhile, the Lef-9-ext oligonucleotides produced amplicons with a size of 662 bp, and the Lef-8-ext oligonucleotides produced amplicons with a size of 681 bp. Subsequently, the second set of oligonucleotides designed were the internal oligonucleotides, namely Gran-int F, Gran-int R, Lef-9-int F, Lef-9-int R, Lef-8-int F, and Lef-8-int R. They were designed to meet specific criteria, such as the length and melting temperature, enabling them to be further utilised directly in the qPCR analysis. The Gran-int oligonucleotides were designed to produce amplicons with a size of 156 bp, the Lef-9-int oligonucleotides produced amplicons with a size of 182 bp, and the Lef-8-int oligonucleotides produced amplicons with a size of 155 bp. Each pair of the internal oligonucleotides was designed to produce an amplicon size suitable for a qPCR analysis, meeting the recommended for ideal qPCR cycling conditions in which amplicon sizes ranging between 100 and 200 bp (Bustin and Huggett, 2017). Reliable qPCR demands good oligonucleotides; thus Table 2.3 shows the absence of hairpin structures or cross-dimerisation potential and GC % content.

In conclusion, two sets of oligonucleotides were designed and tested *in silico* for the amplification of selected regions on the CrleGV genome in preparation for plasmid construction. The next chapter (Chapter 3) involves testing the synthesised oligonucleotides on CrleGV gDNA by conventional PCR followed by the construction of recombinant plasmids via ligation of the external regions generated by PCR into the cloning vector pJET1.2 blunt.

Chapter 3

Plasmid analysis by colony PCR and restriction digestion

3.1 Introduction

In the previous chapter, sets of external and internal oligonucleotides targeting regions of the CrleGV *granulin*, *lef-9* and *lef-8* gene sequences were designed and tested *in silico*. The objective for this chapter was to construct plasmids containing the *granulin*, *lef-9*, and *lef-8* gene target regions for use as standards in a qPCR assay. In several studies , qPCR has been used as a method of enumeration for baculoviruses as the technique is well known for being a simple and rapid method (Hitchman *et al*., 2007; Krokene *et al*., 2013; Graham *et al*., 2015; Dhladhla *et al*., 2018; Jukes, 2018; Kaletta *et al*., 2020). The qPCR technique permits the accurate quantification of samples based on the rate at which a target region amplifies relative to a known set of standards. Typically, a standard curve is constructed using standards generated by gDNA extracted from purified OBs by CTAB DNA extraction or other alternative extraction methods. These standards usually produce a linear standard curve, from which the quantity of gDNA of unknown samples is estimated for the virus concentration (Dhladhla *et al*., 2018; Jukes, 2018). As mentioned in the previous chapters, the use of gDNA standards is associated with poor PCR amplification efficiencies due to potential stability issues of gDNA standards. The traditional extraction methods such as phenol/chloroform extraction have also been reported to yield inconsistent DNA recovery from baculovirus samples (Lo and Chao, 2004; George *et al*., 2012).

Plasmid DNA standards are often used to overcome these challenges. Plasmid constructs are advantageous because these preparations generate high-quality, pure, and concentrated standards that can be independently quantified and converted to the number of copies of target DNA (Sivaganesan *et al*., 2008). For absolute quantification approaches, an assumption must be made that plasmid standards and unknown gDNA samples amplify with the same efficiency; even though factors such as secondary structure, and presence of non-target DNA could alter amplification performance in the unknown gDNA samples (Lo and Chao, 2004). Using plasmid standards in qPCR is a valid and accurate method for determining baculovirus concentrations; thus, several studies have used plasmid standards to estimate unknown viral

DNA concentrations. George *et al*., (2012) developed a protocol that could be used to quantify baculoviruses using qPCR without the need to purify the baculovirus genome. For their study, plasmid standards were generated and quantified by NanoDrop for the qPCR assay. Another study where plasmid standards were used was by Lo and Chao (2004). They reported on a rapid and straightforward method for titre determination of baculovirus using qPCR. Zwart *et al*., (2008) also used plasmid constructs to create standard curves. In their study, the plasmid DNA was quantified with a NanoDrop spectrophotometer and verified by gel electrophoresis; the number of plasmid copies was calculated based on the DNA concentration. In their study, mixtures of quantified baculoviruses were made and used to validate SYBR Green I-base qPCR to determine genotype frequencies in mixed genotype populations. In each of the studies mentioned above, the results demonstrated that the method is suitable for creating highly accurate standard curves with plasmids, as they are extremely reproducible with reliable efficacy and sensitivity.

As previously mentioned, only one study has described qPCR as a method for CrleGV-SA quantification (Dhladhla *et al*., 2018). However, plasmid standards were not utilised in their research. Therefore, the overall aim of this chapter was to construct three plasmids, each containing a target region for either *granulin*, *lef-9*, and *lef-8* genes for use as standards in a downstream qPCR assay. The first objective was to extract gDNA from CrleGV-SA OBs using a modified CTAB extraction method. Secondly, the extracted gDNA was used as a template to PCR amplify the target regions of the selected gene regions using the oligonucleotides designed in Chapter 2. Finally, the PCR amplified regions were then directly ligated into the pJET1.2/blunt vector, and the plasmids were verified using colony PCR, restriction enzyme digestion, and Sanger Sequencing.

3.2 Materials and methods

3.2.1 CrleGV-SA gDNA extraction using a CTAB protocol

A 200 µl CrleGV OB sample extracted from infected *T. leucotreta* larvae was mixed with 90 µl of 1 M Na_2CO_3 and incubated at 37 °C for 30 minutes. The sample was then treated with 120 µl of 1M Tris-HCl with pH of 6.8, 90 µl of 10% SDS and 20 µl of Proteinase K (25 mg/ml), and further incubated at 37 °C for 30 minutes. A 10 µl volume of RNase A (10 mg/ml) was added to the sample, following was a final incubation at 37 °C for 30 minutes. Samples were centrifuged at a speed of 12,100× g for 3 min, the supernatants were collected, and 400 µl of preheated (70 °C) CTAB buffer (54 mM CTAB, 0.1 M Tris-HCl pH 8, 20 mM Na_2EDTA, 1.4 M NaCl) was added prior to incubation at 70 °C for 45 minutes. A volume of 400 µl of

chloroform that was pre-cooled to 4 °C was added to the CTAB mixture and inverted several times before centrifugation at 6700× g for 10 minutes. The upper aqueous phase was collected, and 400 µl of ice-cold isopropanol was added to the samples in order to precipitate the DNA overnight at −20 °C. The DNA was centrifuged at 12,100× g for 20 minutes and washed with ice-cold ethanol (70% v/v, −20 °C) before the final centrifugation at 12,100× g for 5 minutes. The pellet was dried, thoroughly removing the ethanol, before re-suspending the samples in 20 µl of ddH_2O and storing them at −20 °C until use.

Genomic DNA concentration and purity (A260/280 and A260/230) was measured in triplicate using a Nanodrop 2000 spectrophotometer (Thermo Scientific, USA). A 5 µl volume of the gDNA was visualised by 1 % agarose gel electrophoresis (AGE) stained with ethidium bromide and separated at 80 V for 30 minutes in 1 × TAE buffer (40 mM Tris-acetate, 20 mM acetic acid, 1 mM EDTA). Additionally, a GeneRuler 1 kb DNA Ladder (Thermo Scientific, USA) was used as a molecular weight marker, and the bands were visualised using a ChemiDoc™ XRS+ (Bio-Rad, USA).

3.2.2 PCR amplification of *lef-8*, *granulin* and *lef-9* target regions

The target regions of the *lef-8*, *granulin,* and *lef-9* genes were PCR amplified using the external and internal oligonucleotides designed and the extracted CrleGV-SA gDNA as template. The PCR reactions were assembled according to the manufacturer's protocol for the *Taq* DNA Polymerase (Ampliqon, Denmark).

Each 25 µl PCR reaction contained 12.5 µl 2× *Taq* DNA Polymerase, 2 µl of 10 µM forward oligonucleotide, 2 µl of 10 µM reverse oligonucleotide, 4 µl of 114.9 ng/µl template DNA and 4.5 µl of distilled water. The control reactions were set up the same as described above for each reaction but with no template DNA. The PCR master mix reactions were transferred to individual PCR tubes, and the individual reactions were mixed by brief centrifugation.

The PCR cycle parameters had an initial denaturation step of 95 °C for 1 minute and 30 cycles of 95 °C for 30 seconds, 55 °C for 30 seconds, 72 °C for 30 seconds, and a final extension step 72 °C for 2 minutes. Amplicons were visualised alongside Quick-Load 50 bp DNA Ladder by 3% AGE stained with ethidium bromide and separated at 80 V for 30 minutes in 1 × TAE buffer (40 mM Tris-acetate, 20 mM acetic acid, 1 mM EDTA). The concentration (ng/µl) of the amplicons was determined in triplicate using a NanoDrop® 2000 Spectrophotometer (NanoDrop products, Wilmington, DE, USA).

3.2.3 Cloning into pJET1.2/blunt Vector

The amplified target region products were cloned into pJET1.2/blunt using the CloneJET PCR Cloning Kit (Thermo Fisher Scientific, Difco Laboratories).

Three ligation reactions were set up in a total volume of 18 µl. Each reaction contained 10 µl of 2× Reaction Buffer, 1 µl of PCR product (*granulin*, *lef-9* or *lef-8),* 6 µl of water, and 1 µl DNA blunting enzyme. Ligations were incubated at 70°C for 5 min to activate the DNA blunting enzyme. Into the mixture, 1 µl of pJET1.2/blunt Cloning Vector (50n g/µl) and 1 µl of T4 DNA Ligase were added, the mixture was vortexed and centrifuged for 3-5 seconds, followed by incubation at room temperature (22 °C) for 5 minutes.

3.2.4 Transformation and colony PCR

Escherichia coli Top 10 cells were transformed by mixing 100 µl of competent cells with ligation mixtures and chilled on ice for 15 minutes. The cells were heat-shocked by incubation at 42°C for no more than 45 seconds and placed back on the ice for 2 minutes. Luria broth (600 µl) was added to the cells and incubated at 37 °C for 30 minutes. After that, transformants were plated on an agar plate containing 100 µg/ml ampicillin and incubated at 37°C overnight. Successfully transformed bacteria were screened by colony PCR using the internal oligonucleotide and the pJET1.2/blunt oligonucleotides.

Each 25 µl PCR reaction contained 12.5 µl 2× *Taq* DNA Polymerase, 0.5 µl of 10 µM forward oligonucleotide, 0.5 µl of 10 µM reverse oligonucleotide, and 11.5 µl of distilled water. The control reactions were set up the same as described above for each reaction. The PCR master mix reactions were transferred to individual PCR tubes, a colony was resuspended into each PCR tube, and individual reactions were mixed by brief centrifugation.

The PCR cycle parameters had an initial denaturation step of 95 °C for 1 minute and 30 cycles of 95 °C for 30 seconds, 55-60 °C for 30 seconds, 72 °C for 30 seconds, and a final extension step 72 °C for 2 minutes. A volume of 2 µl of each amplicon and Quick-Load 50 bp DNA Ladder were visualised by 3% AGE with ethidium bromide and separated at 80 V for 30 minutes in 1 × TAE buffer (40 mM Tris-acetate, 20 mM acetic acid, 1 mM EDTA).

3.2.5 Plasmid extraction

Two colonies positive via colony PCR were inoculated into 5 ml of Luria broth containing ampicillin (100µg/ml) and incubated overnight at 37°C with shaking to bulk up the plasmids. The plasmids of interest were extracted from the cultures using the GeneJET™ Plasmid Miniprep Kit (Thermo Scientific, USA) according to manufacturer's protocol. DNA concentration (ng/µl) of the plasmids was determined in triplicate using a NanoDrop® 2000 Spectrophotometer (NanoDrop products, Wilmington, DE, USA).

3.2.6 Restriction enzyme digestion and Sanger sequencing

After the plasmid extraction, restriction digestion was performed to validate the insert's presence or absence, respectively, using the FastDigest *Xho*I and *Xba*I restriction enzymes (Thermo Fisher Scientific, USA).

Restriction digest reactions contained 1 µl of *Xho*I, 1 µl of *Xba*I, 3 µl of 10 × restriction enzyme buffer, 13 µl ddH_2O, and 2 µl template plasmid DNA were prepared. Reactions were incubated at 37 °C in a water bath for 10 minutes. Samples were visualised by 1% AGE with ethidium bromide and resolved at 80 V for 30 minutes, alongside with GeneRuler 1kb DNA Ladder. Gels were visualised using the ChemiDoc™ XRS+ (Bio-Rad, USA) with image captured and band sizes estimated in the Image Lab™ (Bio-Rad, USA) software.

Plasmids were sequenced using the pJET1.2/blunt forward by the Inqaba Biotechnical Industries (Pty) Ltd., Pretoria, South Africa. Sequences were subjected to ABI Base Recall software to auto-correct ambiguities (Elyazghi *et al*., 2017). Regions of poor sequence quality at the beginning and end of fragments were identified and trimmed automatically by ABI Base Recall , the lengths of the regions to remove were calculated based on the cumulative histogram of Phred Quality Scores. After the internal quality control checks the sequences were exported automatically as FASTA-formatted files and further analysed by NCBI (BLAST) analysis to identify the sequences.

3.3 Results

3.3.1 Cryptophlebia leucotreta granulovirus gDNA extraction

Purified CrleGV OBs were provided and gDNA extracted using the CTAB method described in section 3.2.1. Figure 3.1 below shows a bright band in lane 1 running above the 10000 bp ladder band. There are limitations in gel resolution; thus, the precise size of the DNA could not be determined due to its large size. The concentration of DNA extracted from purified OBs was approximately 114.9 ng/µl.

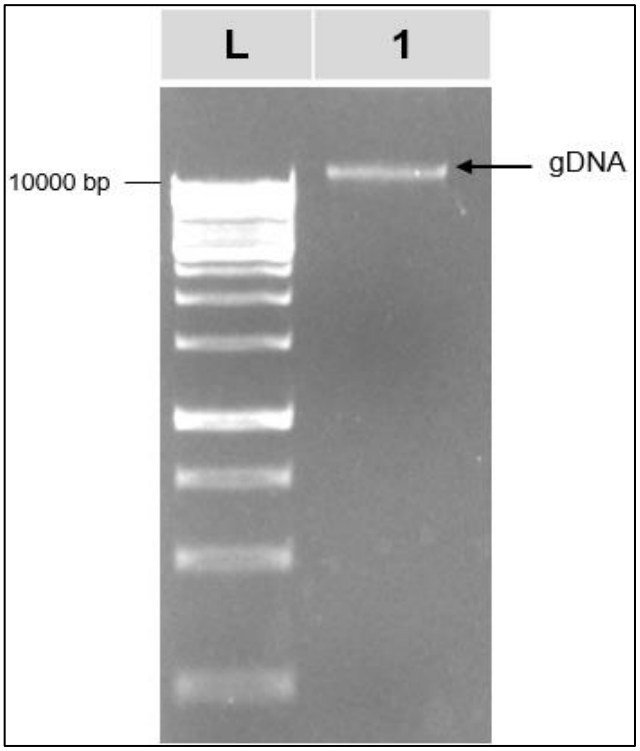

Figure 3.1: Agarose gel electrophoresis of CrleGV gDNA. Lane 1 – GeneRuler 1kb DNA Ladder; Lane 2- CrleGV-SA gDNA. Electrophoresis was carried out at 80V for 30 minutes.

3.3.2 PCR amplification of *granulin*, *lef-9* and *lef-8*

The *granulin*, *lef-9,* and *lef-8* target regions were successfully amplified using DNA extracted from purified OBs. Figure 3.2 below shows the amplicons obtained using the external and internal oligonucleotides designed for each gene region. The *granulin* PCR amplicons are shown in Figure 3.2 A. In lanes 1 and 3, single bands with the expected sizes of approximately 150 bp (internal oligonucleotides) and 610 bp (external oligonucleotides) are visible, respectively. Similarly, Figure 3.2 B are the amplicons obtained using the external and internal oligonucleotides designed for *lef-9*. Lanes 1 and 3 have single bands with the expected sizes of approximately 180 bp (internal oligonucleotides) and 660 bp (external oligonucleotides), respectively. Figure 3.2 C shows the amplicons obtained using the external and internal oligonucleotides designed for the lef-8 target regions; lanes 1 and 3 are single bands with the expected sizes of approximately 150 bp (internal oligonucleotides) and 680 bp (external oligonucleotides), respectively. For all three target regions, no bands are visible in lanes 2 and

4, which represent the negative controls as no gDNA template was added to these PCR reactions.

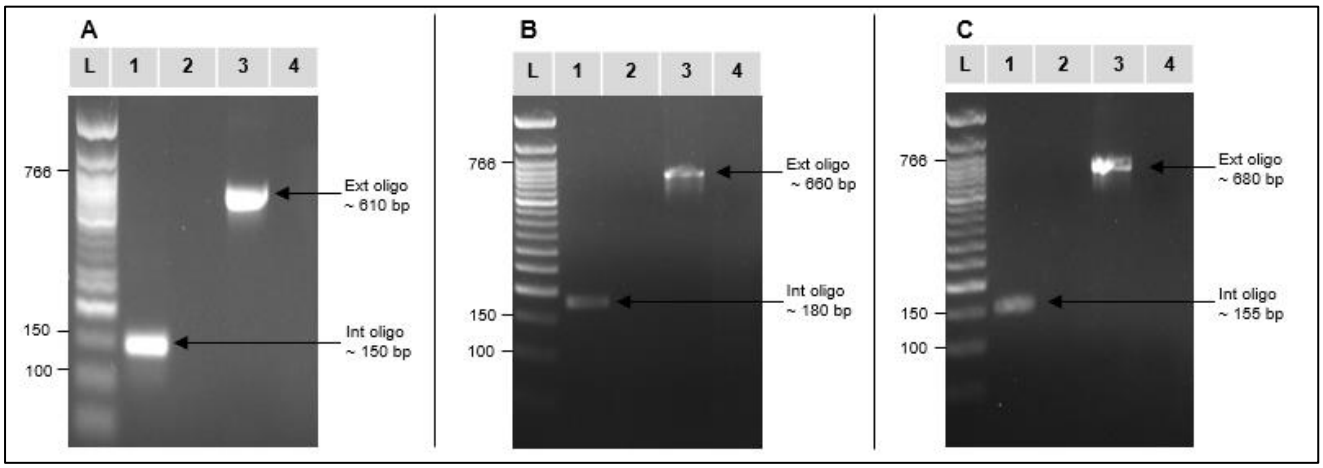

Figure 3.2: PCR amplification of CrleGV *granulin*, *lef-9* and *lef-8* from DNA extracted from OBs. A - *gran*, B - *lef-9*, and C - *lef-8*: L– Quick-Load 50 bp DNA Ladder, 1 - Internal oligonucleotide PCR product, 2 - Internal oligonucleotide no template control, 3 - External oligonucleotide PCR product, 4 - External oligonucleotide no template control.

The amplicons in Figure 3.2 A, B and C lanes 1 and 3 match the expected size of the *granulin*, *lef-9*, and *lef-8* amplicons. The concentrations of the *granulin*, *lef-9*, and *lef-8* amplicons produced by the external oligonucleotides were 345.8 ng/µl, 322.7 ng/µl, and 232.6 ng/µl.

3.3.3 Ligation and restriction digestion

The *granulin*, *lef-9*, and *lef-8* target region amplicons were ligated into the pJET1.2/blunt vector with ligations transformed into *Escherichia coli* Top 10 cells. Colonies were screened by colony PCR using the internal and the pJET1.2 oligonucleotides to confirm whether the transformation was successful or not (Figure 3.3 A, B, and C). Plasmids were extracted from two positive colonies from each plate and digested with *Xho*I and *Xba*I to validate the presence of the insert. The plasmids and digestions were analysed on a 1% agarose gel, shown in Figure 3.3 D, E, and F.

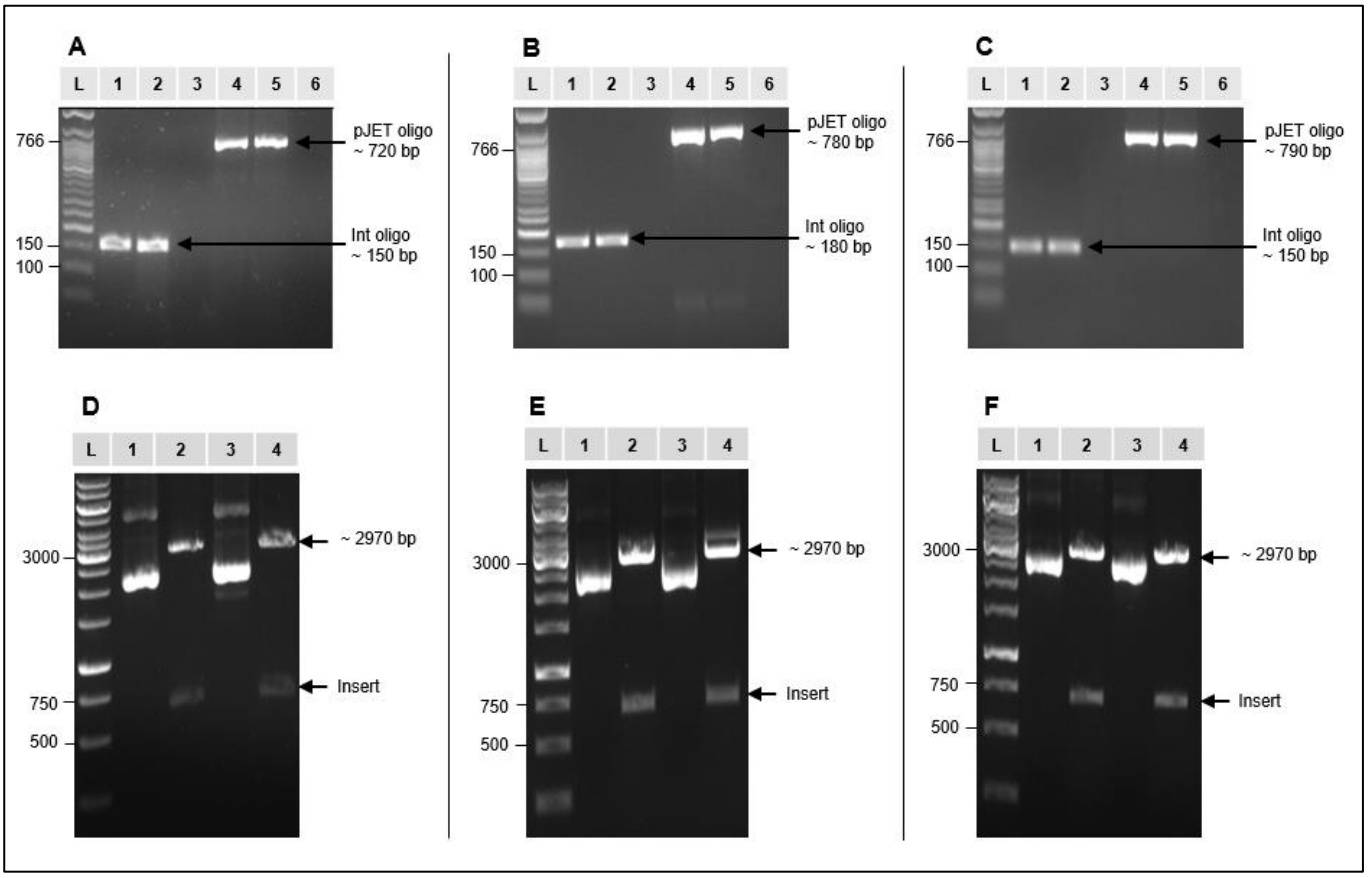

Figure 3.3: Agarose gel electrophoresis showing the colony PCR amplicons (A, B, and C) and the extracted and digested (*Xho*I and *Xba*I) plasmids (D, E, and F). A is the *granulin*, B - *lef-9*, and C - *lef-8* colony PCR amplicons. For each gel with amplified target gene regions: Lane L - Quick-Load 50 bp DNA Ladder; Lanes 1 & 2 - Amplicons amplified with the internal oligonucleotides; Lane 3 - No template control (Internal oligonucleotide); Lanes 4 & 5 - Amplicons amplified with the pJET1/2 oligonucleotides; Lane 6 - No template control (pJET1/2 oligonucleotides). D is the *granulin*, B - *lef-9*, and C - *lef-8* plasmid. For each plasmid: Lane L - GeneRuler 1 kb DNA Ladder; Lane 1 - Plasmid extracted from colony 1; Lane 2 - Plasmid extracted from colony 1 (digested); Lane 3 - Plasmid extracted from colony 2; Lane 4 - Plasmid extracted from colony 2 (digested).

Figure 3.3 A shows the amplicons of the *granulin* target regions obtained; lanes 1 and 2 are single bands with the correct size of approximately 150 bp, and lanes 4 and 5 are also single bands with the expected size of approximately 720 bp. Similarly, in Figure 3.3 B, amplicons of the *lef-9* target regions are shown, and in lanes 1 and 2 single bands with the correct size of approximately 180 bp were obtained. In lanes 4 and 5, single bands with the expected size of

approximately 780 bp are also shown. The AGE gel image in Figure 3.3 C shows the *lef-8* amplicons obtained: lanes 1 and 2 show single bands with the expected size of approximately 150 bp and lanes 4 and 5 show individual bands with a correct size of approximately 790 bp. As anticipated, in all three gels, no bands were visible in lanes 3 and 6, which represent the no template controls as no gDNA template was added to these PCR reactions.

Figure 3.3 D shows undigested *granulin* plasmids in lanes 1 and 3, and two conformations are visible, with one being the supercoiled. Following digestion with *Xho*I and *Xba*I, two bands are visible in lanes 2 and 4. The top band of approximately 2970 bp represents the vector backbone. The bottom band aligning with the 750 bp ladder mark represents the cloned insert. Figure 3.3 E are the undigested *Lef-9* plasmids; lanes 1 and 3 also have two conformations visible, including the supercoiled conformations. After digestion with *Xho*I and *Xba*I, two bands are visible in lanes 2 and 4, with the top band of approximately 2970 bp representing the vector backbone and the 690 bp bottom band aligning with the 750bp ladder mark representing the cloned insert.

Similarly, Figure 3.3 F shows undigested *Lef-8* plasmids in lanes 1 and 3 with two conformations again visible. Following digestion with *Xho*I and *Xba*I, two bands are visible in lanes 2 and 4. The vector backbone is represented by the upper band of approximately 2970 bp, while the lower band of approximately 710 bp aligns with the 750bp ladder mark representing the digested *lef-8* insert.

The *granulin*, *lef-9* and *lef-8* plasmids from the colony of interest were named pJET1.2-gran, pJET1.2-lef-9, and pJET1.2-lef-8. Figure 3.4 shows a generalised map of the recombinant pJET1.2/blunt cloning vector containing an Ampicillin resistance (Amp^R) gene (red), a lethal gene (eco47IR) (light grey), and an origin of replication (pMB1) (black). This vector also has a multiple cloning site (MSC) (yellow) with the position of the *Xho*I and *Xba*I sites (flanking the gene) shown in the figure below. The gene insert position is shown in the figure (green), which represents each of the three targeted regions shown below.

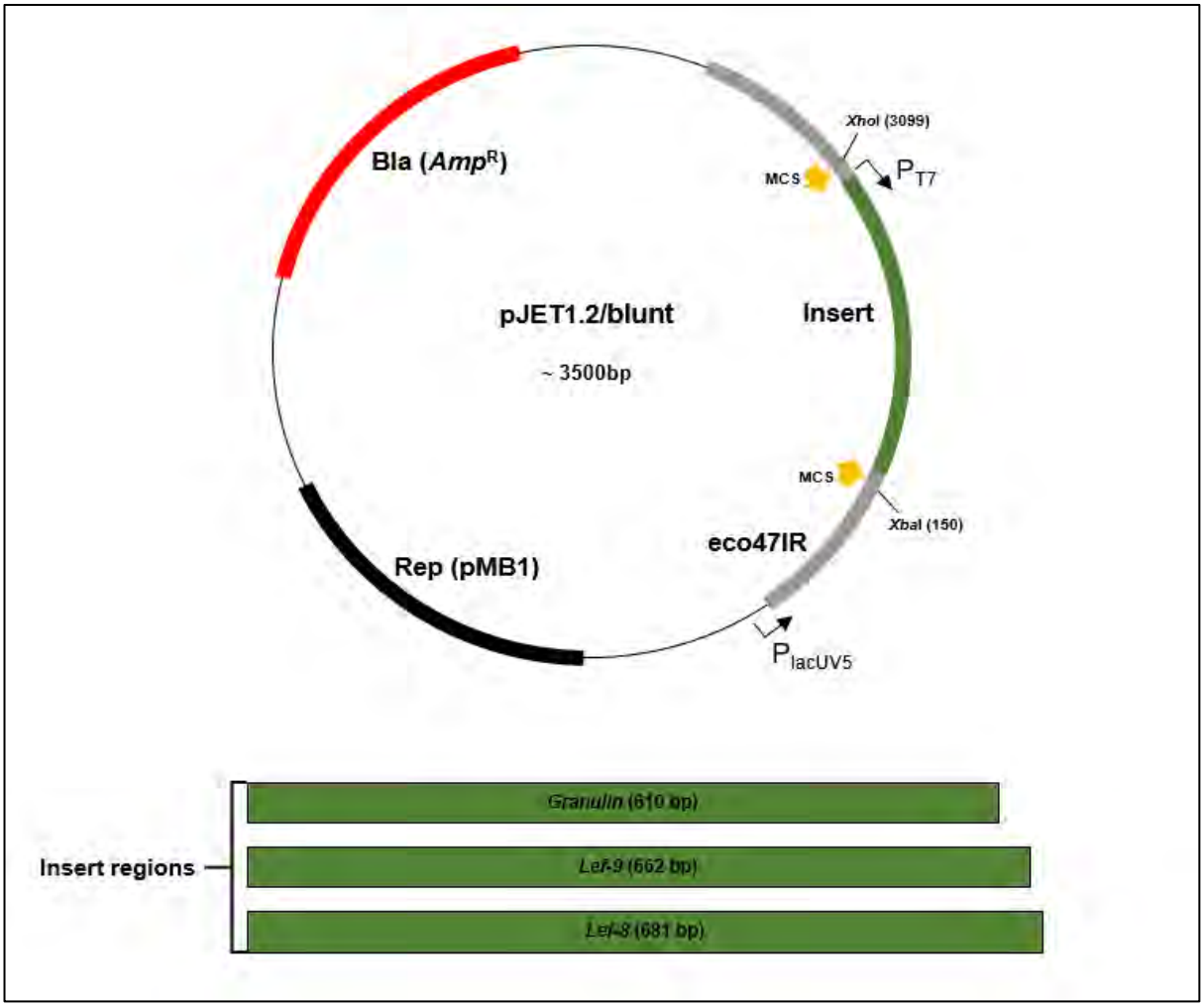

Figure 3.4: Generalised map of the recombinant pJET1.2/blunt vector with the cloned inserts. Features: *Amp*^{R} in red, the eco47IR lethal gene in light grey, pMB1 origin of replication (Rep) in black, the multiple cloning site (MCS) in yellow, and target insert in green. The three target inserts are depicted below, with the respective sizes given.

3.3.4 Plasmid sequence analysis

All three plasmids were Sanger sequenced in the forward direction only. The chromatograms obtained showed minimal background noise and strong signal quality. Each plasmid sequence FASTA file exported from ABI Base Recall was analysed by BLAST analysis. The pJET1.2-lef-9 insert sequence top hit was to that of the CrleGV-SA isolate, against the region spanning from 92203 to 92863 in the reference genome (accession: MF974563.1). Percentage identity of 100 % was determined, with an E-value of 0.0 and a query coverage of 92 %. Similarly, the BLAST analysis results of the pJET1.2-lef-8 also produced a percentage identity of 100 % when compared against the region spanning from 102076 to 102736 of the reference isolate,

CrleGV-SA isolate. The determined E-value was 0.0 and a query coverage of also 92 %. With these results, the alignment analysis was unnecessary as there were no gaps or mismatches to identify. However, the *granulin* insert analysis had a top hit that was similar to that of the CrleGV-SA isolate, compared to the region spanning from 33 to 639 in the reference genome. The identity percentage was determined to be 99.96 %, with an E-value of 0 and a query coverage of 61 %. This slight difference in percentage identity resulted in an alignment analysis to determine the possible gaps or mismatches present. The pJET1.2-Gran insert sequence was aligned with the *granulin* target reference sequence (cloned into the pJET1.2 vector map) on Geneious R11 software. The slight percentage identity difference was due to two mismatches observed in the alignment of the sequence against the reference isolate sequence. The analysis of the pJET1.2-gran and reference isolate alignment revealed a total of two mismatches at nucleotides 91C→T and 407G→C (Figure 3.5). The mismatches do not affect the *granulin* internal oligonucleotides sequences as they fall outside the internal target region.

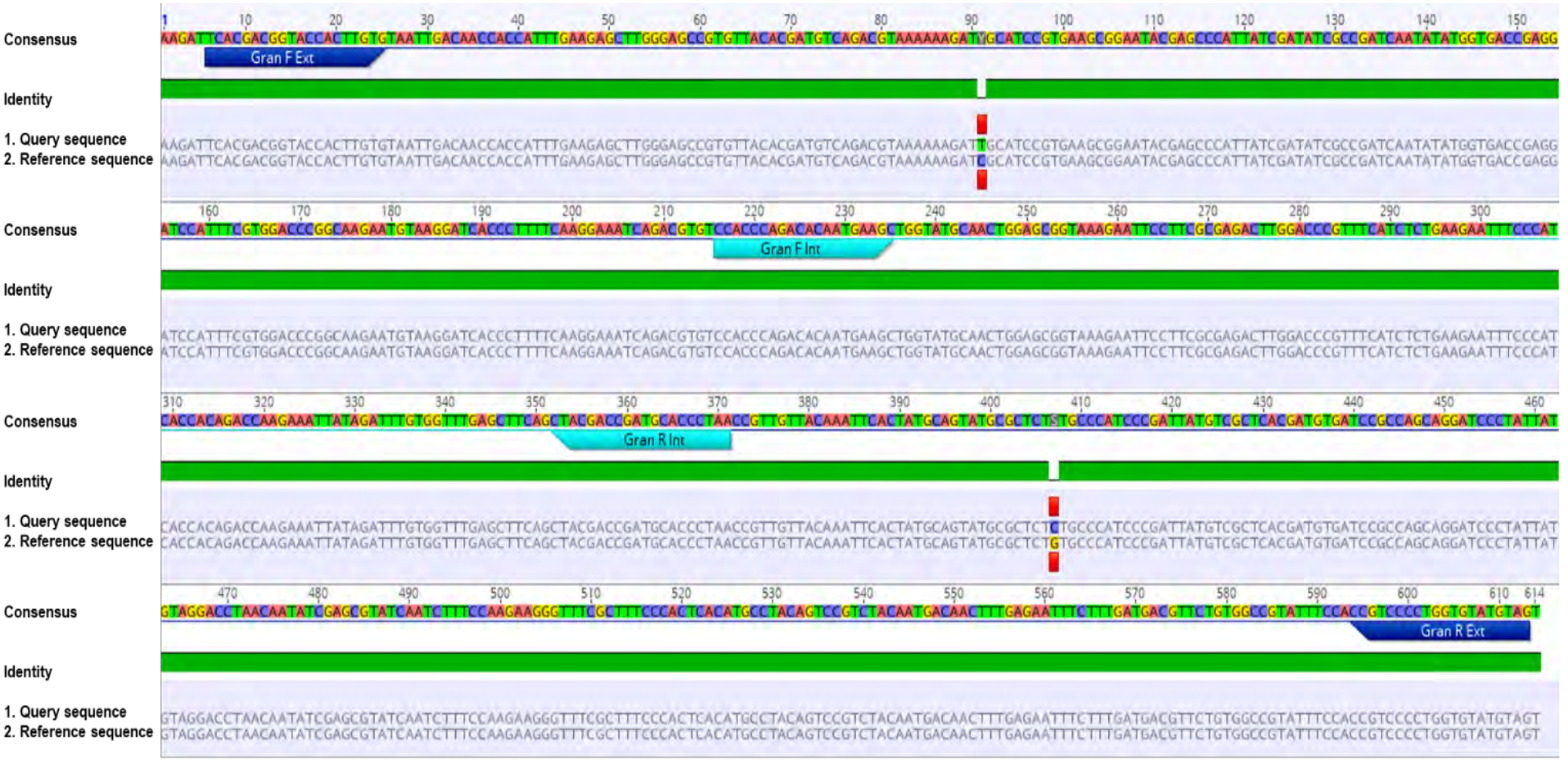

Figure 3.5: Alignment analysis of the *granulin* target region sequence against the *granulin* plasmid sequence. The positions of the mismatched nucleotides are annotated in red. The internal forward and reverse oligonucleotide binding regions are annotated as light blue bars, and the external forward and reverse oligonucleotide binding regions are the purple bars.

3.4 Discussion

The overall aim of this chapter was to construct three plasmids that will be utilised as standards in a qPCR assay for the quantification of CrleGV OBs. Firstly, gDNA was extracted from CrleGV-SA OBs. Subsequently, the targeted regions, the *granulin*, *lef-9*, and *lef-8* genes, were PCR amplified using the designed external oligonucleotides, respectively. The PCR amplicons were then directly ligated into pJET1.2/blunt, and *E. coli* Top 10 cells were transformed with these ligations. Plasmids that were positively screened by colony PCR were extracted, and restriction digestion was conducted to determine whether the inserts were present and were of the correct size or not. These plasmids underwent further confirmation by Sanger sequencing by Inqaba Biotech (South Africa).

The first objective was to extract CrleGV-SA gDNA from purified OBs using the CTAB DNA extraction protocol. The gDNA extraction was successful and a single band was visible on the gel, running above the 10,000 bp band of the DNA ladder. The precise size of the DNA could not be determined due to its large size, similar to what has been observed in other studies following gDNA extraction from baculoviruses (Van der Merwe *et al*., 2017; Jukes, 2018). The extracted gDNA was used as a template to PCR amplify the *granulin*, *lef-9*, and *lef-8* target regions using the respective external oligonucleotides. As mentioned in the previous chapter, the external oligonucleotides were designed to produce amplicons that will be cloned into a vector of interest, while the internal oligonucleotides were designed for use in downstream qPCR assays. When complementary gDNA was present, the external oligonucleotides targeted regions in the *granulin* and *lef-9*, *lef-8* genes producing amplicons of 610 bp, 662 bp and 681 bp, respectively. The internal oligonucleotides produced *granulin* and *lef-9*, *lef-8* amplicons of expected sizes of 158 bp, 182 bp, and 155 bp.

The next objective was to ligate the external PCR amplicons generated using the external oligonucleotides of the *granulin* and *lef-9*, *lef-8* target regions into pJET1.2/blunt to create three recombinant plasmids. The pJET1.2/blunt vector is a blunt-end vector that was used for this project due to its ease in cloning (Thieme *et al*., 2011). Following ligation, Top 10 *E. coli* cells were transformed and cultured. A feature of the pJET1.2/blunt vector system is the presence of the lethal gene (eco47IR). When the vector re-circularises with no insert present, the eco47IR gene is restored, enabling expression of a lethal protein which kills the host bacteria, serving as a positive selection and preventing the formation of non-recombinant colonies (Hoseini & Sauer, 2015). Thus, the transformation was successful as there were colonies observed on the LA plates containing ampicillin. These were further analysed by screening the colonies for

plasmids with inserts using colony PCR with the pJET1.2/blunt forward and reverse oligonucleotides. To determine the expected sizes of the colony PCR amplicons, a plasmid map with the various inserts was generated in the Geneious R11 software (Biomatters, New Zealand). The colony PCR results revealed that the target region insert was present in all the constructed plasmids as the amplicons produced were the correct size.

The plasmids of interest (pJET1.2-Gran, pJET1.2-lef-9, and pJET1.2-lef-8) were further analysed for insert presence by performing restriction digestion on the plasmids. *Xho*I and *Xba*I was utilised to digest the plasmids as their recognition sites flank the insert (Figure 3.4). For each digested plasmid, insert DNA bands were visible in the agarose gel image and were the expected size.

Final confirmation of the recombinant plasmids involved all three plasmids being sent for Sanger Sequencing. A BLAST analysis was conducted to search for similar sequences available in NCBI's GenBank database. The E-values obtained for these sequences were zero, with a coverage ranging from 61 % to 92 %. The percentage identities ranged between 99.96 % - 100 % against the CrleGV-SA isolate, indicating that the correct inserts had been successfully amplified and cloned into the pJET1.2/blunt vectors. The pJET1.2-lef-9 and pJET1.2-lef-8 had a percentage identity of 100 %; however, pJET1.2-Gran was 99.96 % identical to the CrleGV-SA reference isolate. Given that inserted gene regions were PCR amplified from CrleGV-SA gDNA isolate, a 100 % identity was the expected outcome for all these sequences. The mismatches detected in the alignment of the pJET1.2-Gran insert were synonymous and may be due to the fact that baculoviruses are comprised of mixed genotypes (Van der Merwe *et al*., 2017; Motsoeneng *et al*., 2019), and perhaps a different CrleGV genotype to the one present on the database was sequenced this time. Another explanation for these mismatches could be the introduction of the incorrect nucleotides by the *Taq* polymerase used to amplify the target regions of these genes. However, this is unlikely since the enzyme system has an error rate of approximately 1 error per 2.2×10^5 nucleotides incorporated. The third possible reason that could have been responsible for these mismatches might be the sequencing software used to sequence this target region of the *granulin* gene. This is also similarly unlikely, given the high read qualities achieved in each of the sequencing runs, and the high degree of identity to the remaining sequences.

In conclusion, plasmids containing the target sequences of *granulin, lef-9*, and *lef-8* were successfully constructed and validated by colony PCR, restriction digest analysis, and Sanger

sequencing. These plasmids will be used as standards in qPCR assays. The next chapter, Chapter 4, describes the comparison of gDNA extraction methods as it is crucial to extract unknown gDNA samples with methods that yield optimum DNA quantity. This study must use a method that yields maximum DNA from unknown samples for the reliability of the qPCR assay.

Chapter 4

Comparison of genomic DNA extraction methods for CrleGV-SA

4.1 Introduction

In the previous chapter, three plasmids were constructed, each containing a target region for either *granulin*, *lef-9*, or *lef-8* genes for use as standards in developing a qPCR assay. In order to perform a qPCR assay using plasmids or any other standard for virus enumeration, it is important to ensure that the most sensitive and reliable gDNA extraction method is utilised. Furthermore, this method of enumeration requires that the virus being enumerated contains a single genome per OB. The virus of interest in this study belongs to the betabaculovirus genus with a single virion, and therefore a single genome is occluded in each granule (Lange and Jehle 2003; Rohrmann, 2019). A single OB in a virus sample releases one genome when the gDNA is extracted. However, no DNA extraction technique reliably ensures that each genome is released from each OB in the sample; one that yields the highest gDNA from viral samples is desirable. All three genes of interest are present as a single copy within the virus genome; therefore, the number of virus particles present can be accurately quantified as each plasmid also consists of a single target gene region.

A few studies have evaluated different extraction methods in terms of the viral gDNA concentration produced and have found that different methods have different reproducibility (De Moraes *et al*., 1999; Dhladhla, 2012). In this chapter, methods of gDNA extraction from CrleGV OBs were compared, one being the commonly used CTAB method (Opoku-Debrah *et al*., 2013). Several studies have found this method to be satisfactory for extracting genomic DNA from baculoviruses (Aspinall *et al*., 2002; Parnell *et al*., 2002; Van der Merwe *et al*., 2017; Dhladhla *et al.*, 2018; Jukes, 2018). Unlike other viruses, baculoviruses consist of an occluded virion that is encapsulated in a thick protein matrix which forms the common OB morphology (Rohrmann, 2019). The CTAB method has been a successful method for gDNA extraction of baculoviruses because of the step at which the OBs are completely dissolved by incubation with an alkaline solution, Na_2CO_3. However, there are potential issues related to this extraction method, including the duration of the extraction method as it is a two-day process, and the technique uses hazardous reagents.

The second extraction method used for comparison was the Quick-DNA Miniprep Plus Kit (Zymo Research, CA, USA), known for being an inexpensive kit with a short processing time. To date, there is no published literature whereby the kit is utilised to extract the gDNA of baculoviruses. The studies that have used the kit show that the Quick-DNA Miniprep Plus kit efficiently extracts the gDNA, resulting in high DNA yield in a short processing time (Zhang *et al*., 2018; Thamamongood *et al*., 2020). This commercial DNA extraction kit was preferred for this study as it provides superior reproducibility and produces high quality DNA that is ready for downstream applications such as qPCR. Furthermore, the kit can recover gDNA sized fragments greater than 50 kb. The limitations of extraction kits, in general, are associated with considerable variability in terms of column binding capacity and contaminant removal. Although this kit is designed to extract DNA from various samples, including viruses, it could be inefficient for baculovirus gDNA extraction as unlike the CTAB method; it does not have a pre-treatment step whereby an alkaline solution dissolves OBs. To overcome this, samples could be pre-treated with the alkaline solution (Na_2CO_3 and Tris-HCl) prior to using the kit.

This chapter aims to compare two different methods of CrleGV-SA gDNA extraction to determine which method has the best yields in terms of concentration and purity. The first objective was to extract gDNA from CrleGV-SA OBs using the Quick-DNA Miniprep Plus kit according to manufacturer's instructions (Method 1a). Secondly, CrleGV-SA OBs were pre-treated with Na_2CO_3 prior to using the Quick-DNA Miniprep Plus kit (Method 1b). Thirdly, the CrleGV-SA OBs sample was pre-treated with Na_2CO_3 and neutralised with Tris-HCl prior to gDNA extraction using the Quick-DNA Miniprep Plus kit (Method 1c). Lastly, gDNA was extracted from CrleGV-SA OBs using the CTAB method (Method 2). The gDNA concentration and purity for all samples were determined using a Nanodrop spectrophotometer.

4.2 Materials and methods

4.2.1 Extraction methods

Genomic DNA was extracted from a sample of CrleGV-SA OBs (6.78×10^9 OBs/ml) (extracted from infected *T. leucotreta* larvae) using the methods listed in Table 4.1. A 1:10 dilution was performed on the OBs sample, and each extraction was done in triplicate to determine the most suitable DNA extraction method.

Table 4.1: The compared methods of gDNA extraction.

Method	Description
1a	Quick-DNA Miniprep Plus kit
1b	Na_2CO_3 pre-treatment + Quick-DNA Miniprep Plus kit
1c	Na_2CO_3 and Tris-HCl pre-treatment + Quick-DNA Miniprep Plus kit
2	CTAB

4.2.1.1 Method 1a

A 200 µl volume of CrleGV-SA OB sample was treated with 200 µl BioFluid and Cell Buffer (Red) and 20 µl Proteinase K, vortexed 10-15 seconds and incubated at 55ºC for 10 minutes. One volume of Genomic Binding Buffer was added to the digested sample and vortexed for 10-15 seconds. The mixture was transferred to a Zymo-Spin™ IIC-XLR Column in a collection tube and centrifuged at ≥ 12,000× g for 1 minute. The collection tube was discarded with the flow-through. A volume of 400 µl of DNA Pre-Wash Buffer was added to the spin column in a new Collection Tube and centrifuged at ≥ 12,000× g for 1 minute. The collection tube was emptied. A volume of 700 µl of gDNA Wash Buffer was added to the spin column and centrifuged at ≥ 12,000× g for 1 minute. The flow-through was discarded, and a volume of 200 µl gDNA Wash Buffer was then added to the spin column and centrifuged at ≥ 12,000× g for 1 minute. The collection tube was discarded with the flow-through. The spin column was transferred to a clean microcentrifuge tube. A preheated (70ºC) 30 µl DNA Elution Buffer was added directly on the matrix and incubated for 5 minutes at room temperature and then centrifuged at maximum speed for 1 minute to elute the DNA. The eluted DNA sample was added directly to the column membrane and incubated for 3 minutes at room temperature for the second time. The sample was then centrifuged at maximum speed for 1 minute to elute the DNA and stored at -20ºC.

4.2.1.2 Method 1b

A volume of 200 µl of CrleGV-SA OBs sample was pre-treated with 90 µl of 1 M Na_2CO_3 and incubated at 37 °C for 30 minutes. Subsequently, the Quick-DNA Miniprep Plus kit (method described in Section 4.2.1.1) was used to extract gDNA from the pre-treated sample, with a starting volume of 290 µl.

4.2.1.3 Method 1c

A 200 µl volume of CrleGV-SA OBs sample was pre-treated with 90 µl of 1 M Na_2CO_3 and was incubated at 37 °C for 30 minutes. Thereafter, the pH of the pre-treated sample was neutralised by adding 120 µl of 1 M Tris-HCl with a pH of 6.8. The Quick-DNA Miniprep Plus kit (method described in Section 4.2.1.1) was utilised with a starting volume of 410 µl.

4.2.1.4 Method 2

A 200 µl volume of CrleGV OB sample was mixed with 90 µl of 1 M Na_2CO_3 and incubated at 37 °C for 30 minutes. The sample was then treated with 120 µl of 1 M Tris-HCl with pH of 6.8, 90 µl of 10% SDS and 20 µl of Proteinase K (25 mg/ml), and further incubated at 37 °C for 30 minutes. A 10 µl volume of RNase A (10 mg/ml) was added to the sample, following a final incubation at 37 °C for 30 minutes. Samples were centrifuged at a speed of 12,100× g for 3 min, the supernatants were collected, and 400 µl of preheated (70 °C) CTAB buffer (54 mM CTAB, 0.1 M Tris-HCl pH 8, 20 mM Na_2EDTA, 1.4 M NaCl) was added prior to incubation at 70 °C for 45 minutes. A volume of 400 µl of chloroform that was pre-cooled to 4 °C was added to the CTAB mixture and inverted several times before centrifugation at 6700× g for 10 minutes. The upper aqueous phase was collected, and 400 µl of ice-cold isopropanol was added to the samples in order to precipitate the DNA overnight at −20 °C. The DNA was centrifuged at 12,100× g for 20 minutes and washed with ice-cold ethanol (70% v/v, −20 °C) before the final centrifugation at 12,100× g for 5 minutes. The pellet was dried, thoroughly removing the ethanol before re-suspending the samples in 30 µl of ddH_2O and storing them at −20 °C until use.

4.2.2 Agarose gel electrophoresis

A volume of 5 µl gDNA was analysed by 1% agarose gel electrophoresis (AGE) stained with ethidium bromide. Electrophoresis was performed using 1 × TAE buffer (40 mM Tris-acetate, 20 mM acetic acid, 1 mM EDTA) and a constant voltage of 80 V for 30 minutes. Additionally, a GeneRuler 1 kb DNA Ladder (Thermo Scientific, USA) was used as a molecular weight marker, and the DNA bands were visualised, and images were acquired using ChemiDoc™ XRS+ (Bio-Rad, USA).

4.2.3 Concentration and purity measurement

The concentration and purity (A260/A280 ratio) were measured in triplicate with a Nanodrop 2000 spectrophotometer (Thermo Scientific, USA) using 1 µl of each sample.

4.2.4 Statistical analysis

Statistical analyses were done using the GraphPad Prism version 9.2.0 (GraphPad Holdings, LLC, USA). The two-choice test was analysed using a t-test, with a significance level set to P = 0.05.

4.3 Results

4.3.1 Comparison of CrleGV-SA extraction methods

The CrleGV-SA gDNA was extracted using the methods listed in Table 4.1 above. A comparison of these extraction methods was conducted to determine which method yields higher DNA purity and quantity.

4.3.1.1 Visualizing DNA by agarose gel electrophoresis

The extracted gDNA was resolved by 1% AGE with an image of these samples captured (Figure 4.1). No bands were observed on the gel image of the gDNA samples extracted using the kit (Method 1a). Single faint bands were visible in lanes 1, 2, and 3 of the Na_2CO_3 pre-treated samples in Method 1b. In method 1c, bright single gDNA bands running above the 10000 bp ladder band were observed in lanes 1, 2, and 3. Single faint bands larger than the 10000 bp ladder band were observed for replicate 2 and 3 samples extracted using the CTAB method in lanes 2 and 3 of method 2.

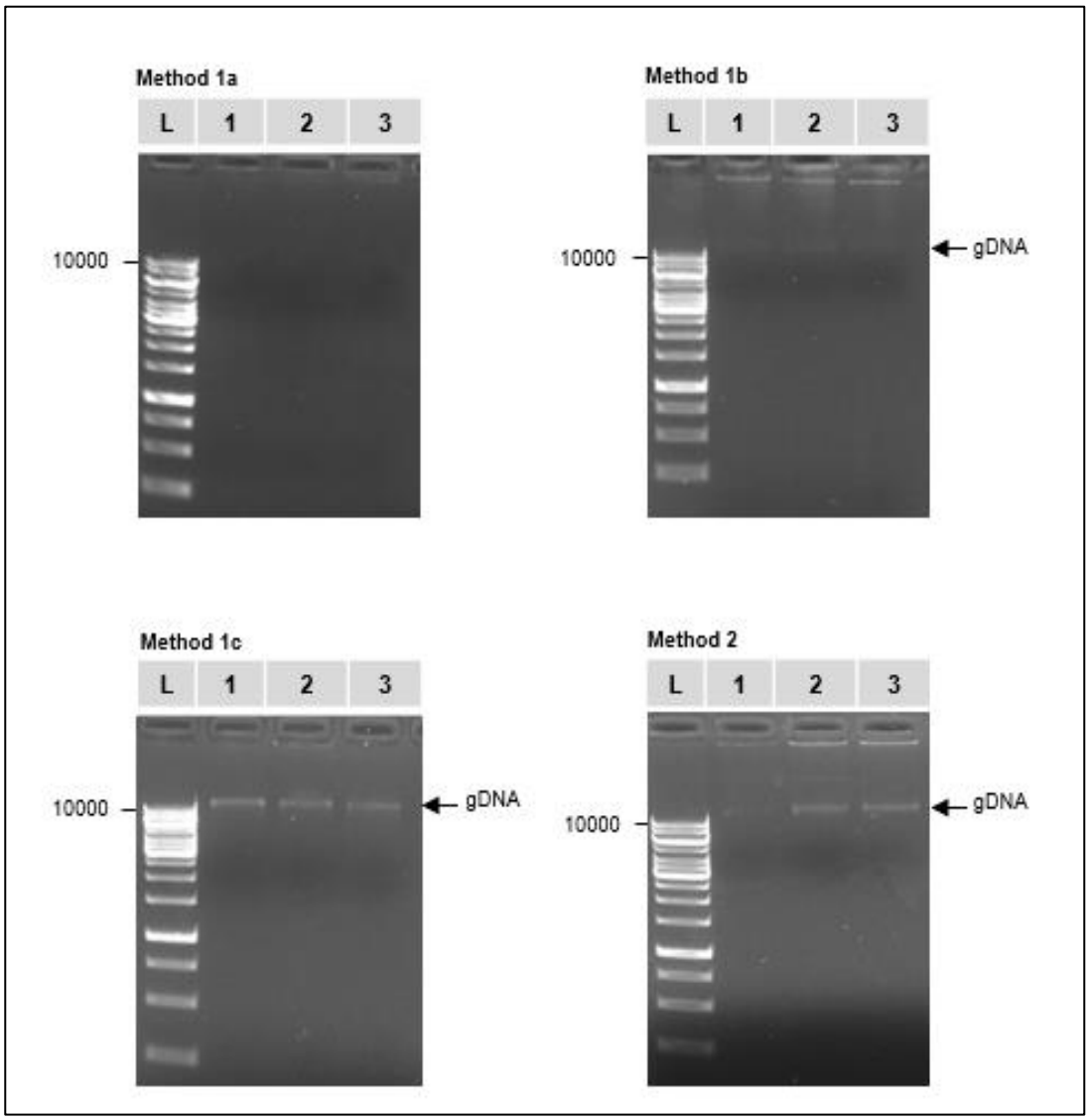

Figure 4.1: Agarose gel electrophoresis image of genomic DNA extraction. With Method 1a (standard kit), Method 1b (Na_2CO_3 Pre-treated + kit), Method 1c (Na_2CO_3 and Tris-HCl Pre-treated + kit), and Method 2 (CTAB). For each gel; Lane L – GeneRuler 1kb DNA ladder; Lane 1 - extracted gDNA (replica 1); Lane 2 - extracted gDNA (replica 2); Lane 3 - extracted gDNA (replica 3).

4.3.1.2 DNA quality and quantity assessment

The concentration and purity (A260/280) of the extracted gDNA samples were measured in triplicate using a Nanodrop 2000 (Table 4.2). Table 4.2 summarises the DNA yield and purity range obtained for all sample extracts using the two extraction methods.

Table 4.2: Concentrations of the extracted gDNA for each extraction method.

		Concentration		Purity	
	Treatment	**ng/µl**	**Standard Deviation**	**$A_{260/280}$**	**Standard Deviation**
Method 1a	standard	3.63	0.287	1.94	0.042
Method 1b	Na2CO3	7.63	0.967	1.87	0.034
Method 1c	Na2CO3 & Tris-HCl	17.73	0.834	1.93	0.024
Method 2	CTAB	6.8	1.867	1.49	0.127

The concentration data that was obtained was analysed using GraphPad Prism, significant differences were recorded between methods 1a and 1b (P = 0.0050), methods 1a and 1c (P <0.0001), methods 1b and 1c (P = 0.0004), and method 1c and 4 (P = 0,0016) (Figure 4.2A). The gDNA concentration yielded with Methods 1b and 2 had no significant difference (P = 0.6051). Similarly, Methods 1a and 2 had no significant difference with a P-value of 0.0768.

Similarly, the purity obtained data were analysed using GraphPad Prism. There was no significant difference between methods 1a and 1b (P = 0.1722), methods 1a and 1c (P = 0.8554), and methods 1b and 1c with a P-value of 0.1284. Meanwhile, significant differences were recorded between methods 1a and 2 (P = 0.0089), methods 1b and 2 (P = 0.0142), and methods 1c and 2 with a P-value of 0.0084 (Figure 4.2B). Overall, method 1c performed best, as it had the highest gDNA concentration and high quality (purity) characterised by a 260/280 absorbance ratio of approximately 1.9.

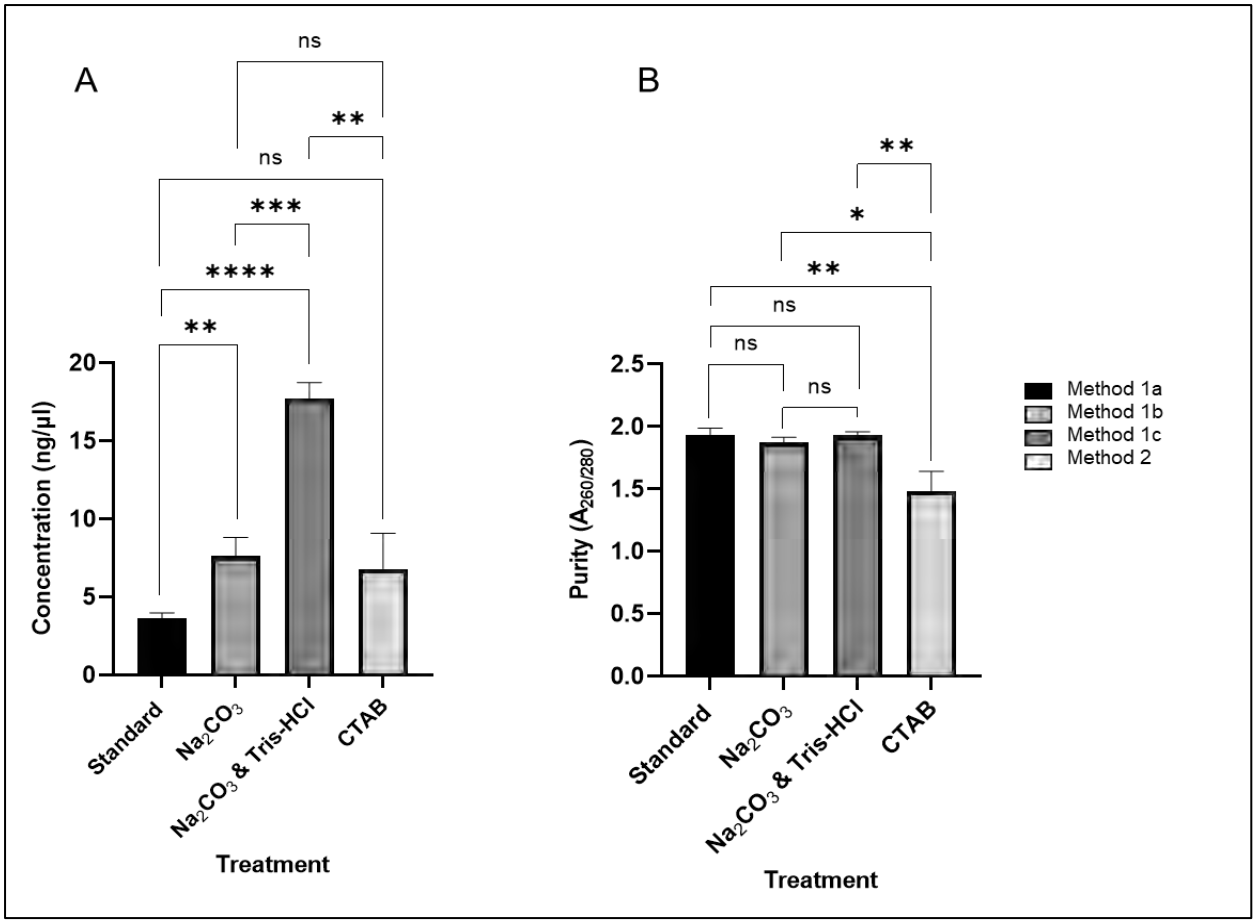

Figure 4.2: Genomic DNA concentration and purity measurement. A- comparison of gDNA concentration between the two methods. B- comparison of gDNA purity. *, **, ***and **** indicate significant differences between two Methods (treatments) according to an unpaired t-test ($P < 0.05$ and $P < 0.01$, respectively), ns indicates that differences were not significant.

4.4 Discussion

The overall aim of this chapter was to compare two different gDNA extraction methods to determine which of the methods provides the highest yield. Firstly, the Quick-DNA Miniprep Plus Kit (Method 1a) was utilised to extract gDNA from CrleGV-SA OBs as per the manufacturer's instructions. Secondly, CrleGV-SA OBs were pre-treated with Na_2CO_3 prior to using the kit (Method 1b). Subsequently, method 1c was used whereby CrleGV-SA OBs were pre-treated with Na_2CO_3 and Tris-HCl before using the kit. Lastly, gDNA was extracted from purified CrleGV-SA OBs using the CTAB DNA extraction method (Method 2) described by Opoku-Debrah *et al*., (2013).

As previously mentioned, the gene of interest is present as a single copy within the virus genome; thus, one genome is released by a single OB in a virus sample during DNA extraction.

Nevertheless, no DNA extraction technique reliably ensures that gDNA is completely extracted from all OBs in a viral sample. Thus, a DNA extraction method that yields the highest gDNA quantity from viral samples is necessary for qPCR assay.

Dhladhla, (2012) investigated CrleGV-SA gDNA extraction using viral DNA extraction kits (ZR Viral DNA kit™ and the ZR Insect/Tissue DNA kit-5™ (Zymo Research, USA)) and the commonly used CTAB DNA extraction method. Their study aimed to use commercial viral gDNA extraction kits for DNA extraction and avoid using hazardous reagents. The CTAB method yielded the best results. Though this DNA extraction method has demonstrated effectiveness in isolating DNA, it consists of multiple precipitation steps and ethanol washes to produce RNA-free gDNA of high purity. These become a limitation in the qPCR assay, as they reduce overall yield and may fail to produce large amounts of high-quality DNA while also having poor reproducibility.

In this chapter, gDNA was then extracted using Method 1a (standard Quick-DNA Miniprep Plus Kit). The NanoDrop absorbance profile is useful for detecting contaminants such as protein and polysaccharides (Abdel-Latif and Osman, 2017). Although the gDNA had a 260/280 nm ratio of 1.94, indicating high purity, this method failed to obtain good DNA yields, as the obtained gDNA concentration was too low and no gDNA bands were visible on the AGE image. This result possibly relates to a failure of the kit to efficiently degrade the OB granulin matrix during the initial lysis steps, preventing subsequent binding of the DNA to the purification column. Therefore, the extraction of gDNA using the Quick-DNA Miniprep Plus Kit method was slightly modified to improve DNA yield.

Firstly, the OB sample was pre-treated with Na_2CO_3 prior to utilising the standard method of the kit (Method 1b). The method yielded low quantities of DNA as the DNA bands visible on the AGE image were very faint. The DNA concentration was not significantly higher than the concentration obtained from using the CTAB method and the standard kit; thus, an additional modification was needed. The result was possibly related to the increased pH of the sample, which may have interfered with the subsequent extraction step. Therefore, before using the kit, the sample was pre-treated with Na_2CO_3, and the pH was neutralised by adding Tris-HCl (Method 1c). This method was found to be the most efficient in extracting high DNA quantity as bright DNA bands were visible on the AGE, and the obtained DNA concentration was significantly higher compared to the other three extraction methods. Furthermore, methods 1a, 1b, and 1c, in which the kit was utilised yielded good quality DNA with an insignificant

260/280 nm ratio difference ranging from 1.87 - 1.94, indicating that the extracted DNA had high purity with the absence of protein contaminants.

Lastly, the CTAB DNA extraction protocol (method 2) produced low gDNA concentration and inconsistent gDNA quantity between replicate experiments, indicating poor reproducibility. The 260/280 nm ratio of 1.49 indicated that the extracted DNA had low purity with possible protein contamination, being significantly lower than all other methods tested.

Overall, Method 1c (Na_2CO_3 and Tris-HCl pre-treated plus Quick-DNA Miniprep Plus kit) was the most efficient at extracting genomic DNA compared with the other methods, resulting in the highest DNA yield and purity in the short processing time. Therefore, Na_2CO_3 and Tris-HCl were used for further experiments to pre-treat the OBs prior to gDNA extraction. The next chapter describes the development and optimisation of a qPCR assay for the enumeration of CrleGV OBs using the plasmids previously constructed as standards and the selected DNA extraction method described in this chapter.

Chapter 5

Evaluation of plasmid standards for the qPCR assay

5.1 Introduction

In the previous chapter, methods of CrleGV-SA gDNA extraction were compared to determine which method has the best yield in terms of concentration and purity in preparation for the development of a qPCR assay. To perform a qPCR assay, it is important to ensure that the technique can accurately quantify the unknown samples in relation to predefined standards. The qPCR technique allows for the accurate quantification of a sample based on the rate at which a target region amplifies in relation to a known set of standards (Dhladhla *et al.*, 2018; Jukes, 2018). Thus, a set of standards with a known concentration from which the values for the unknown targets can be extrapolated are required.

The qPCR technique is based on specific amplification of a gene region of interest using oligonucleotides, dNTPs (deoxyribonucleotide triphosphates), and the *Taq* polymerase enzyme (Pfaffl and Berg, 2010). The template DNA amplification is monitored by a camera or detector using SYBR Green fluorescent dyes that intercalate with double-stranded DNA (dsDNA) during each cycle of the PCR reaction. Each PCR cycle consists of three steps namely, denaturation, annealing, and extension. These steps are temperature-dependent, and a temperature change initiates each step. The temperature changes control the separation of the DNA strands, the *Taq* polymerase enzyme activity, and the binding of two oligonucleotides that flank the DNA fragment to be amplified. In each cycle, the amount of DNA is doubled; thus, the level of fluorescence increases exponentially (Yang and Rothman, 2004). The double-stranded DNA is measured to give information on the progression of the amplification of the DNA fragment. Ultimately, the exponential DNA amplification is reduced as the reaction reagents become rate-limiting (Wong and Medrano, 2005). Therefore, to quantify the starting DNA template concentration, a threshold cycle (Cq), the least number of PCR cycles required to generate enough fluorescent signal to be detected above the background fluorescence, is determined early in the exponential amplification stage of PCR reaction. By determining the Cq values from a range of samples for which the starting quantity of template DNA is known (predefined standards), a regression curve can be generated to which samples with unknown quantities of starting DNA can be compared. Quantitative PCR does however have some challenges which require consideration, such as the ability of SYBR Green to bind non-

specifically to dsDNA; the dye can also bind to oligonucleotide-dimers that may be generated during the qPCR reaction, thus, giving incorrect fluorescent signals. To overcome this, a melt curve is generated by the thermocycler, in which a single sharp peak indicates the presence of one product sequence and confirms high specificity of the oligonucleotides (Yang and Rothman, 2004). Furthermore, multiple peaks indicate that the oligonucleotides have bound to other DNA template sequences within the PCR reaction, which may be DNA that cross-hybridises with the oligonucleotides or a result of oligonucleotide-dimers generated during the PCR reaction. Moreover, no template controls containing all the PCR components except the DNA template are run parallel to the DNA samples analysed to detect contamination or non-specific amplification in the PCR reaction (Real-Time PCR Applications Guide, 2006).

Previous research has utilised qPCR to quantify *Spodoptera exempta* NPV (SpexNPV) in agricultural pests to understand further covert infections (Graham *et al*., 2015). Also, Garnier *et al*., (2009) conducted a study on CpGV using qPCR assays and showed that the technique could be used as a quantitative method in the production of GVs as biopesticides. Recently, Kaletta *et al*., (2020) conducted a similar study comparing viral quantification techniques for an accurate and precise enumeration of pure viral strains and environmental water samples of unknown viral composition. They compared five different quantification methods [plaque-based assay (PA), qPCR, Epifluorescence microscopy (EPI), flow cytometry (FC), and nanoparticle tracking analysis (NT)] on four viral strains (with different genome types) as well as on four environmental water samples. From the methods tested in the study, it was questionable to what extent small viral particles are captured. They concluded that each method has its requirements for minimal particle concentrations and particle sizes which must be met to ensure reliable results. Wennmann and Jehle (2014) also conducted a study whereby an identification and quantitation method based on quantitative polymerase chain reaction (PCR) for AgseNPV-A, AgseNPV-B, AgipNPV and AgseGV was established. The established method was based on highly specific oligonucleotides for multiplex polymerase chain reaction (PCR) that led to the amplification of discriminating fragments of the *polyhedrin* and *granulin* gene of AgseNPV-A, AgseNPV-B, AgipNPV and AgseGV. Furthermore, the AgseNPV-B and AgseGV specific pairs of primers were applied in qPCR for AgseNPV-B/AgseGV ratio determination in samples of mixed infections. It was demonstrated further that for quantifying NPVs and GVs in mixed infections, the method of occlusion body isolation is most crucial and significantly influences the results. As mentioned previously, Dhladhla *et al.*, (2018) investigated and compared methods of enumeration on GVs and qPCR was one of the methods

used. Their results showed that qPCR technique offered the most significant potential as an accurate enumeration method as it was not affected by contamination with non-biological contaminating debris.

This chapter describes the evaluation of plasmid standards, and a qPCR assay is developed. The evaluation of the plasmid standards for the qPCR technique, was necessary for this study as it is important to consider the efficacy of the oligonucleotides. This includes the ability of the oligonucleotides to anneal to the appropriate segment of DNA without extensive formation of oligonucleotides dimers, non-specific annealing, or formation of secondary structure. Furthermore, it is important to ensure that highly accurate standard curves are generated. As mentioned previously, the quantification of samples depends on a standard curve produced from serial dilutions of a standard sample of known concentration. These standard dilutions are analysed in parallel with known samples to verify the accuracy of the standard curve (Ginzinger, 2002). The standard curve is then used to determine the concentration or quantity (copy number) in unknown samples by interpolation, reading from the values within the standard curve.

The overall aim of this chapter was to conduct a qPCR assay using the internal oligonucleotides, SYBR Green Taq, and plasmid standards as a template. The internal oligonucleotides designed in Chapter 2 were optimised for KAPA SYBR green ReadyMix (KAPA Biosystems, USA). However, the SsoAdvanced Universal SYBR Green Supermix was selected for this study as it is inexpensive, easily available and has increased resistance to PCR inhibitors, ensuring maximum efficiency, sensitivity, and reproducibility. Therefore, new sets of internal oligonucleotides were designed to meet specific criteria for the SsoAdvanced Universal SYBR Green Supermix manufacturer (Bio-Rad Lab, CA). The first objective was to design new sets of qPCR oligonucleotides which can bind to the target regions in the recombinant plasmids pJET1.2-gran, pJET1.2-lef-9, and pJET1.2-lef-8. Secondly, the designed oligonucleotides were tested by conventional PCR, using the plasmid DNA as template. Finally, a qPCR assay was performed to evaluate whether thepJET1.2-gran, pJET1.2-lef-9, and pJET1.2-lef-8 plasmids could be successfully used as the predefined standards for downstream experiments.

5.2 Materials and methods

5.2.1 Quantitative PCR oligonucleotide design

A set of internal oligonucleotides was designed using the Primer3 (v4.0.0) online tool for qPCR assays. Oligonucleotides were designed to meet the SsoAdvanced Universal SYBR Green

Supermix specific criteria, such that the length is 18-20 bp and the amplicon size is 70-150 bp. Additionally, a melting temperature (T_m) of 58 °C - 62 °C, one GC clamp, and a GC percentage ranging between 40 and 60 was targeted, enabling them to be further utilised in the qPCR analysis. The designed oligonucleotides were tested *in silico* and were synthesised by Inqaba Biotech (Pretoria, South Africa).

5.2.2 Oligonucleotide test by conventional PCR

The target regions of the pJET1.2-gran, pJET1.2-lef-9, and pJET1.2-lef-8 plasmids were amplified using the newly designed internal oligonucleotides. The PCR reactions were assembled according to the manufacturer's protocol for the SsoAdvanced Universal SYBR Green Supermix.

Each 10 µl PCR reaction contained 5 µl SsoAdvanced Universal SYBR Green Supermix, 1 µl of 10 µM forward oligonucleotide, 1 µl of 10 µM reverse oligonucleotide, 1 µl of plasmid template DNA and 2 µl of distilled water. The control reactions were set up the same as described above for each reaction but with no template DNA. The PCR master mix reactions were transferred to individual PCR tubes, and the individual reactions were mixed by brief centrifugation.

The PCR cycle parameters had an initial denaturation step of 95 °C for 30 seconds and 30 cycles of 95 °C for 15 seconds, 60 °C for 30 seconds, and a final extension step 60 °C for 15 seconds. A volume of 2 µl for each amplicon was visualised alongside Quick-Load 50 bp DNA Ladder (Ampliqon, Denmark) by 3% AGE stained with ethidium bromide and separated at 80 V for 30 minutes in 1 × TAE buffer (40 mM Tris-acetate, 20 mM acetic acid, 1 mM EDTA).

5.2.3 Quantitative PCR development

A qPCR assay was developed to evaluate the pJET1.2-gran, pJET1.2-lef-9, and pJET1.2-lef-8 plasmid standards. Each qPCR test reaction consists of four standards and an NTC reaction. The concentration of the plasmid standards was measured using a NanoDrop® 2000 Spectrophotometer (NanoDrop products, Wilmington, DE, USA). The concentration measured was converted to copy number using Equation 5.1.

$$Copy\ number = (\ amount\ (ng)\ \times\ 6.022 \times 10\text{^}23)\ \div\ (legnth\ \times\ 1 \times 10\text{^}9 \times 650)$$

Where, *ng* = the amount of DNA, 6.022 x 10^{23} is Avogadro's number, *Length* = the length of your DNA fragment in base pairs, and 1 x 10^9 is to convert answer to nanograms

Equation 5.1: Formula used to convert ng to copy number. (http://cels.uri.edu/gsc/cndna.html)

The standard curves were developed using 10-fold dilutions of plasmid DNA of known concentration using nuclease-free qPCR grade H_2O. These dilutions were labelled Std1 to Std4, with Std1 representing the standard with the highest plasmid DNA concentration and Std4 the lowest (Table 5.1).

Table 5.1: Concentrations for the plasmid standards.

Standard	Concentration (copy number)		
	pJET1.2-gran	**pJET1.2-lef-8**	**pJET1.2-lef-9**
Std1	1.29×10^9	1.22×10^9	9.43×10^8
Std2	1.29×10^8	1.22×10^8	9.43×10^7
Std3	1.29×10^7	1.22×10^7	9.43×10^6
Std4	1.29×10^6	1.22×10^6	9.43×10^5

Each 10 µl qPCR reaction contained 5 µl SsoAdvanced Universal SYBR Green Supermix, 1 µl of 10 µM forward oligonucleotide, 1 µl of 10 µM reverse oligonucleotide, 1 µl of plasmid template DNA, 0.2 µl carboxy-X-rhodamine (ROX) (KAPA Biosystems, USA), and 1.8 µl of distilled water. The control reactions were set up the same as described above for each reaction but with no template DNA. The PCR master mix reactions were transferred to qPCR strip tubes, and the reactions were mixed by brief centrifugation.

Reactions were run using the QuantStudio™ 3 Real-Time PCR System (Thermo Scientific, USA) with the cycle parameters as follows: an initial denaturation cycle of 95 °C for 30 seconds followed by 35 cycles of 95 °C for 15 seconds, and 60 °C for 30 seconds, with fluorescence measured after each cycle. A final denaturation cycle at 95 °C for 15 seconds was performed, followed by generating the melt curve starting at 60 °C increasing to 95 °C at 0.15 °C intervals each of 1 second. Fluorescence levels were captured after each interval of 0.15 °C. Data was analysed to generate the amplification curves for each reaction, the melt peak for all amplicons generated, and the standard curves using the QuantStudio™ 3 Design and Analysis tool.

5.3 Results

5.3.1 Oligonucleotide design

Oligonucleotides were designed and tested using the Primer3 (v4.0.0) online tool and Geneious R11 software based on the target regions of pJET1.2-gran, pJET1.2-lef-9, and pJET1.2-lef-8 plasmids. Primer3 (v4.0.0) was set to select regions that did not form hairpin/secondary structures and primer dimers while having an optimal melting temperature of 58 °C - 62 °C (Table 5.2).

Table 5.2: Internal oligonucleotide design against cloned regions of pJET1.2-gran, pJET1.2-lef-9, and pJET1.2-lef-8 plasmids.

New internal oligonucleotide name	Oligonucleotide sequence (5' – 3')	Melting temperature °C	Length bp	Hairpin	GC %	PCR product size bp
Gran-int R	TAGGGTGCATCGGTCGTAGC	61.7	20	0	60	101
Gran-int F	GCGAGACTTGGACCCGTTTC	61.3	20	0	55	
Lef-8-int R	TGTGGATCAGAGCGGAGGAG	61	20	0	50	102
Lef-8-int F	CGCCTTTTTGTCCATGTATTCC	58	22	0	55	
Lef-9-int R	CACCATCACAATCCCTGTTGG	59.2	21	0	55	107
Lef-9-int F	TCAGCTGTCCACCCAATTTTC	58.8	21	0		

5.3.2 Oligonucleotide testing by PCR

The pJET1.2-gran, pJET1.2-lef-9, and pJET1.2-lef-8 target regions were successfully amplified using the newly designed internal oligonucleotides. Figure 5.1 below shows the amplicons obtained using the new internal oligonucleotides designed for each target internal plasmid region. In lanes 1, 3 and 5, single bands with the expected sizes of approximately 100 bp are visible for pJET1.2-gran, pJET1.2-lef-9, and pJET1.2-lef-8, respectively. For all three target regions of pJET1.2-gran, pJET1.2-lef-9, and pJET1.2-lef-8, no bands were visible in lanes 2, 4 and 6, respectively, representing the negative controls as no gDNA template was added to these PCR reactions.

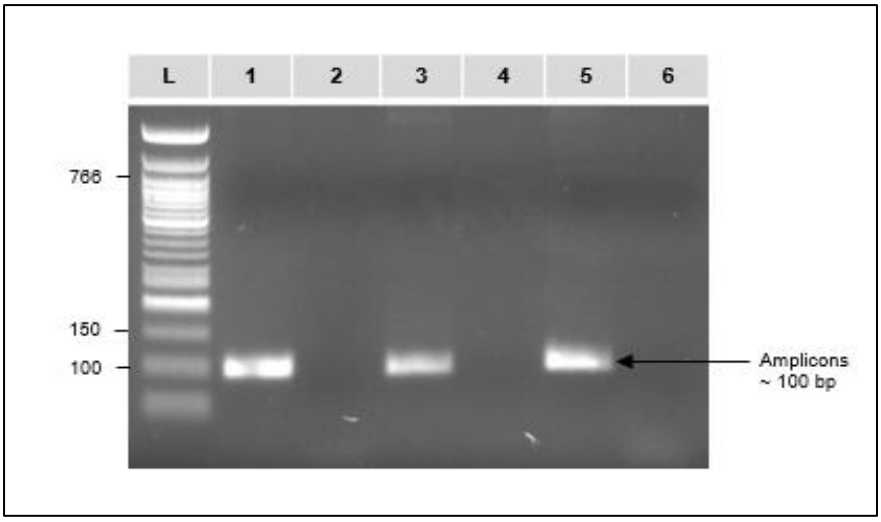

Figure 5.1: PCR amplification of pJET1.2-gran, pJET1.2-lef-9, and pJET1.2-lef-8 plasmid target regions. L– Quick-Load 50 bp DNA Ladder, 1 - pJET1.2-gran amplicon, 2 - pJET1.2-gran no template control, 3 - pJET1.2-lef-9 amplicon, 4 - pJET1.2-lef-9 no template control, 5 - pJET1.2-lef-8 amplicon, 6 - pJET1.2-lef-8 no template control.

5.3.3 Development of a quantitative PCR analysis

The development of the predefined standards for the quantitative PCR technique was evaluated using the pJET1.2-gran, pJET1.2-lef-9, and pJET1.2-lef-8 plasmids. This technique would enable the quantification of CrleGV-SA test samples in downstream experiments. Each plasmid was evaluated using the newly designed oligonucleotides reported in Table 5.2. For each plasmid standard, qPCR amplification curves, melt peaks, and standard curves are shown in Figures 5.2, 5.3, and 5.4 for the *granulin*, *lef-8* and *lef-9* target regions respectively.

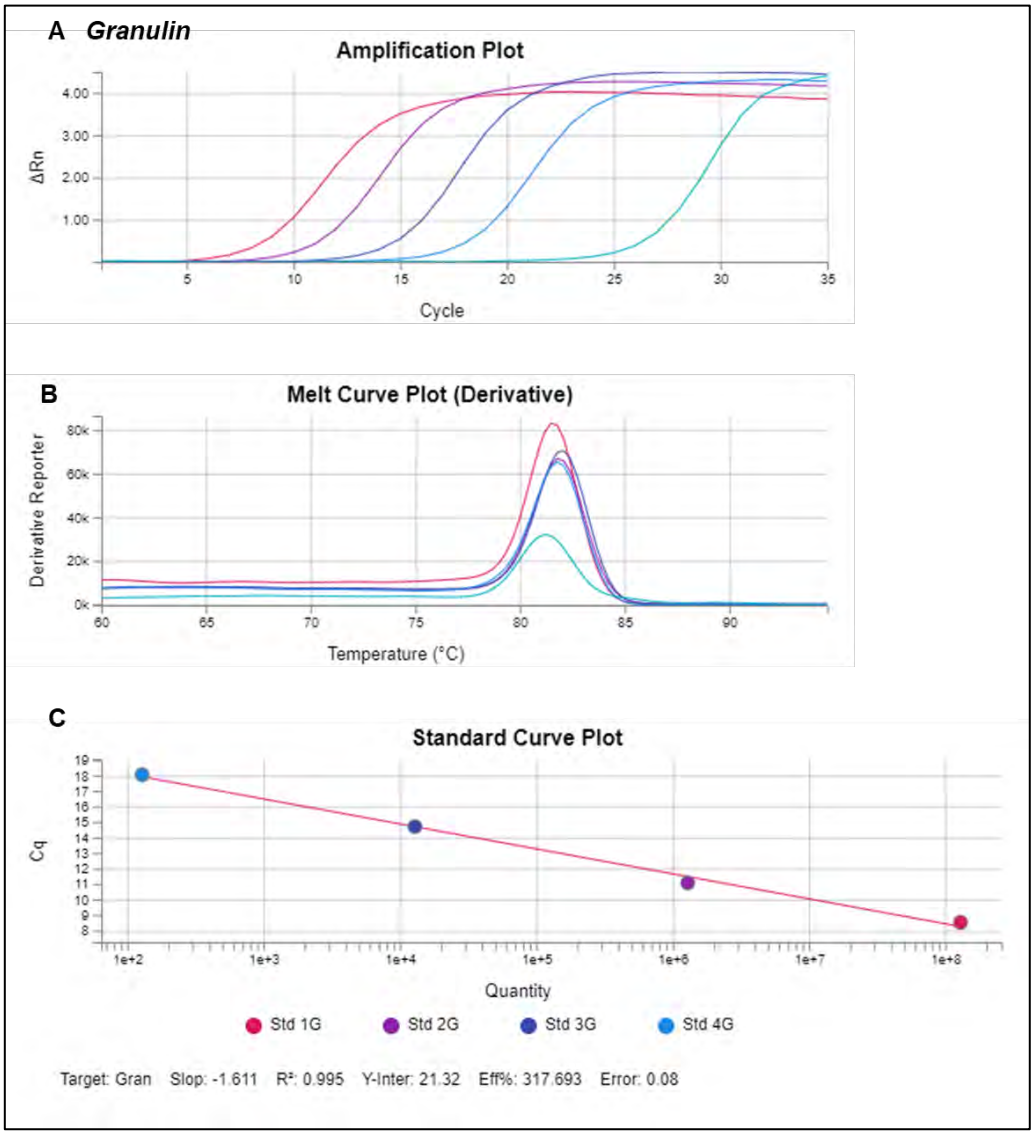

Figure 5.2: Evaluation of a qPCR analysis technique using the pJET1.2-gran plasmid standards with the A) Amplification curve B) Melt peak and C) standard curves shown.

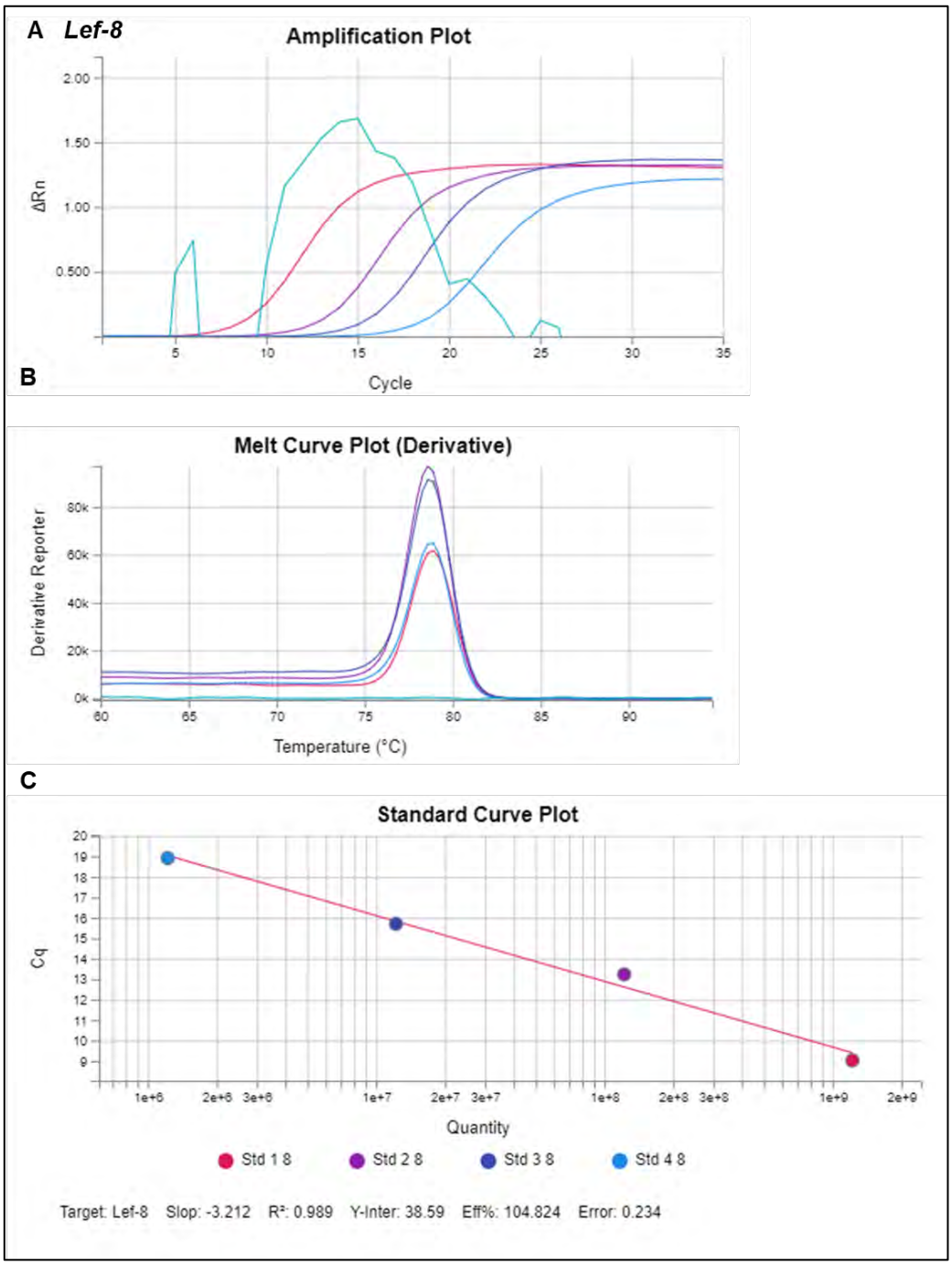

Figure 5.3: Evaluation of a qPCR analysis technique using the pJET1.2-lef-8 plasmid standards with the A) Amplification curve B) Melt peak and C) standard curves shown.

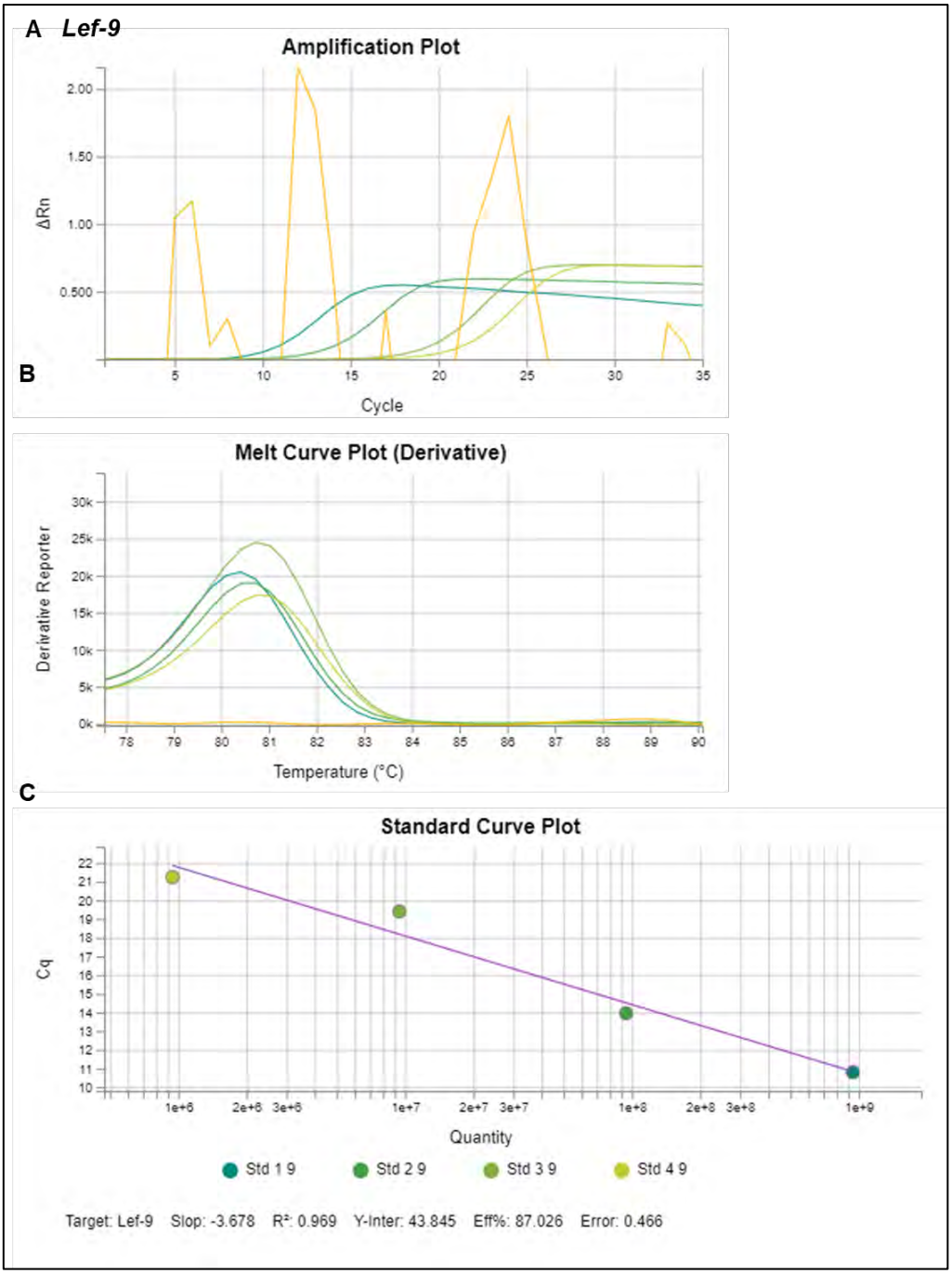

Figure 5.4: Evaluation of a qPCR analysis technique using the pJET1.2-lef-9 plasmid standards with the A) Amplification curve B) Melt peak and C) standard curves shown.

For each plasmid in Figures 5.2, 5.3, and 5.4, the amplification curves for each reaction are shown in graph A, with the standards prepared from Std 1 to Std 4 each shown to peak after an increasing number of cycles. Similarly, a single melt peak was observed for each (Figure 5.2B, 5.3B, and 5.4B), with 81.9 °C, 78.8 °C and 80.5 °C T_m, respectively, indicating that a single amplicon was produced for each reaction. Figures 5.2, 5.3, and 5.4C show the standard curves

produced from the plasmid standards. The pJET1.2-gran plasmid standards produced an R^2 value of 0.995. The pJET1.2-lef-8 standards had an R^2 value of 0.989, and the pJET1.2-lef-9 had an R^2 value of 0.969 reported. There was amplification observed in the no template control of the *granulin* amplification curve, which indicates potential contamination. However, the no template control of the *lef-8* and *lef-9* amplification curves deviated from the normal, although no amplification occurred as it shown in the melt curves.

5.4 Discussion

The overall aim of this chapter was to develop a qPCR analysis technique that can be used to enumerate CrleGV-SA test samples in the downstream experiment. Firstly, new internal oligonucleotides were designed to meet the SsoAdvanced Universal SYBR Green Supermix manufacturer's specific criteria, such that the length is 18-20 bp and the amplicon size is 70-150 bp, a melting temperature (T_m) of 58 °C - 62 °C, and one GC clamp. Secondly, newly designed oligonucleotides were tested by conventional PCR using plasmid DNA as the template. Lastly, the predefined standards which will be applied in downstream qPCR assays were evaluated to determine whether they could be successfully utilised to quantify the amount CrleGV-SA OBs in unknown sample.

The first objective was to design new oligonucleotides targeting the internal insert regions of the pJET1.2-gran, pJET1.2-lef-9, and pJET1.2-lef-8 plasmids. They were designed to meet specific criteria, such as the length and melting temperature, enabling them to be further utilised directly in the qPCR analysis using the SsoAdvanced Universal SYBR Green Supermix. The Gran-int oligonucleotides were designed to produce amplicons with a size of 101 bp, the Lef-9-int oligonucleotides produced amplicons with a size of 107 bp, and the Lef-8-int oligonucleotides produced amplicons with a size of 102 bp. As previously mentioned in Chapter 2, reliable qPCR demands good oligonucleotides; therefore, no hairpin structures or cross-dimerisation potential were present, and an optimal GC % content was targeted.

The second objective was to amplify the target internal insert regions of the pJET1.2-gran, pJET1.2-lef-9, and pJET1.2-lef-8 plasmids using the respective internal oligonucleotides via conventional end-point PCR. When complementary plasmid DNA was present, the new internal oligonucleotides targeted regions in the pJET1.2-gran, pJET1.2-lef-9, and pJET1.2-lef-8 plasmids producing the expected amplicons with each having an approximate size of 100 bp.

The last objective was to conduct a qPCR analysis using the newly designed oligonucleotides to test the plasmid standards. As mentioned in the previous chapters, using plasmid DNA as standards in qPCR is advantageous due to its high stability (i.e., little degradation during storage) and ease in preparation (Wong and Medrano, 2005). Absolute quantification in qPCR depends entirely on the accuracy of the standards. Therefore, the amplification of the insert internal target regions was not problematic as good amplification curves, melt curves, and standards curves were produced. Although, there was amplification observed in the no template control of the *granulin* amplification curve, which indicates potential contamination. Single melt peaks were observed for all three plasmid standards qPCR assays, indicating one product sequence, and confirming high specificity of the oligonucleotides (BioRad Real-Time PCR brochure, 2009; Maddocks and Jenkins, 2016). A standard curve with an R^2 value greater than 0.90 is desirable for qPCR, whereas standard curves that have further low R^2 values from this are discarded (BioRad Real-Time PCR brochure, 2009; Maddocks and Jenkins, 2016). Therefore, the preliminary results showed that these plasmid standards could be utilised to accurately quantify the test samples in the downstream qPCR.

In conclusion, a qPCR technique was successfully developed and can be used to quantify test samples of CrleGV-SA OBs. This technique will be applied in the downstream experiments of Chapter 6. In the next chapter, different methods of enumeration, darkfield microscopy and qPCR will be compared using CrleGV-SA test samples with unknown concentrations.

Chapter 6

Evaluation of the test samples using darkfield microscopy and qPCR enumeration methods

6.1 Introduction

The previous chapter described the evaluation and application of plasmids to determine whether they could be used as predefined standards in a qPCR assay for the enumeration of betabaculovirus particles. As previously mentioned, CrleGV-SA has been formulated as a registered biopesticide, namely Cryptogran, to control *T. leucotreta*, and has been successfully used in the field for over 15 years (Moore *et al.*, 2015). The production of insect viruses for use as biopesticides requires accurate quantitative methods for determining the concentration of virus particles in the formulations. Quantifying CrleGV OBs is a sophisticated task that remains challenging. Presently, darkfield light microscopy is the traditional method to quantify OBs (Grzywacz and Moore, 2017). This method uses a specially designed counting chamber, onto which a small volume of viral suspension is placed, then viewed under dark-field illumination, and the virus particles (OBs) are counted directly.

Nevertheless, this technique is a tedious and somewhat inaccurate part of the production, as it requires significant sample preparation prior to use that can have an impact on what is visualised. The technique cannot distinguish viral particles positioned within the different focal planes of the counting chamber. So high concentrations of particles can "run together" to create the appearance of larger particles. Additionally, the technique is time-consuming and can yield inconsistent results (Grzywacz and Moore, 2017). This technique requires an experienced technician, and the accuracy of the method is questionable. This highlights the importance of continuing research into developing an accurate enumeration method for these viral particles.

In this chapter darkfield microscopy and the qPCR enumeration methods are compared to establish their accuracy and suitability for use in standardisation and quality control in the commercial production of CrleGV-SA. As mentioned before, a few studies have compared enumeration methods for baculoviruses. Several techniques have been utilised to quantify baculoviruses, such as scanning electron microscopy (SEM), light microscopy, spectrophotometry, qPCR, enzyme-linked immunosorbent assays (ELISA), flow cytometry (FCM), and high-performance liquid chromatography (HPLC). Some of these methods were

investigated and compared by Dhladhla *et al.*, (2018). Quantitative PCR was one of the methods used; this technique offered the most significant potential as an accurate enumeration method as it was not affected by contamination with non-biological contaminating debris or by other biological material due to the specificity of oligonucleotides. Standard curves with 100% efficiency were generated as shown by the coefficient of determination (R^2) of the slope of the line, indicating that qPCR could be used as an alternative enumeration method for baculoviruses. However, further work was required to fully develop the qPCR technique as an enumeration method for baculoviruses. Ferris *et al*., (2011) conducted a comparison of baculovirus quantitation results from the Virus Counter, relative to plaque assay, which is one of the most important procedures used to measure the virus titre. The Virus Counter is a specialised flow cytometer designed to provide rapid virus quantitation for liquid samples. The Virus Counter results were evaluated relative to plaque assay results. The results showed that the Virus Counter can provide rapid baculovirus quantitation with results that significantly correlate with plaque assay titter values. Another comparison of baculovirus enumeration methods was done by Roberts *et al*., (2012). Their study demonstrated the first use of Scanning ion occlusion sensing (SIOS) for the accurate, direct, rapid, in-sample measurement of quantitative nanoparticle concentrations, synthetic and biological particles. The SIOS was applied to measure concentrations in two biological samples, first for baculovirus occlusion bodies (OBs) and then for the marine cyanobacterium *Prochlorococcus*. In both cases, the concentration determined by SIOS agreed very closely with values obtained using conventional techniques such as counting by microscopy in the case of baculovirus OBs and flow cytometry for *Prochlorococcus*.

This chapter aims to quantify purified, crude-purified, and viral formulated suspensions using the darkfield microscopy and qPCR methods of enumeration to verify their accuracy and determine the most consistent and comparable method. The first objective was to enumerate purified CrleGV-SA test samples using darkfield microscopy. The second objective was to extract CrleGV-SA gDNA from the enumerated test samples. Thirdly, the concentration of the CrleGV-SA test samples was determined utilising the qPCR assay. Lastly, a statistical analysis was conducted to compare the results produced by the two enumeration methods.

6.2 Materials and methods

6.2.1 Enumeration of purified CrleGV-SA OBs

The CrleGV-SA test samples listed in Table 6.1 were enumerated using a counting chamber and dark field microscopy to determine the virus concentration. For each sample, a 1:5 dilution

of the purified OB suspension was prepared by mixing 20 µl of the virus with 80 µl of ddH_2O and homogenised by vortexing for 15 seconds. A further 1:5 dilution of this suspension was made by mixing 400 µl of 0.07 % SDS (w/v) with 100 µl of the virus suspension resulting in a 1:25 dilution. The virus suspension was then sonicated at 60 Hz for 4 × 15 second intervals. A final 1:2000 dilution was prepared by adding 10 µl of the sonicated virus suspension to 790 µl of ddH_2O and mixed by vortexing for 15 seconds. A Helber counting chamber with a depth of 0.02 mm was used to count the virus samples. The counting chamber was cleaned with 70 % ethanol solution (v/v) between uses. A volume of 5 µl of the 1:2000 virus suspension was loaded onto the counting chamber through capillary action. Occlusion bodies were allowed to settle for 3 - 5 minutes prior to counting. The counting chamber was viewed under darkfield illumination on a light microscope at 400× magnification. In triplicate, the number of OBs were counted from five central square quadrants: the top left, bottom left, top right, bottom right, and a random centre square, each consisting of 16 smaller squares. The OB concentration was then determined using Equation 6.1.

$$OBs\ per\ ml = (D \times x) \div (N \times V)$$

Where D = *dilution factor*, x = *Average No. of OBs counted*, N = *Number of small squares* and V = *Volume*.

Equation 6.1: Formula used to determine the number of OBs per ml using a counting chamber.

Table 6.1: CrleGV-SA test samples with unknown concentration. (Provided by: *T. Bennet, **Dr M. Jukes, ***Dr M. van der Merwe)

Test Sample Number	Description	Purification Method
1	CrleGV-SA	Glycerol gradient purification
2	CrleGV-SA	Crude purification
3	CrleGV-SA	Crude purification
4	CrleGV-SA*	Glycerol gradient purification
5	Cryptogran sample**	Crude purification
6	Cryptogran sample***	Crude purification
7	CrleGV-SA	Crude purification

6.2.2 CrleGV-SA gDNA extraction from test samples

Genomic DNA was extracted from the test samples listed in Table 6.1 using the gDNA extraction method described previously in Chapter 4.

A volume of 5 µl gDNA was analysed by 1% agarose gel electrophoresis (AGE) stained with ethidium bromide. Electrophoresis was performed using 1 × TAE buffer (40 mM Tris-acetate, 20 mM acetic acid, 1 mM EDTA) and a constant voltage of 80 V for 30 minutes. Additionally, a GeneRuler 1 kb DNA Ladder (Thermo Scientific, USA) was used as a molecular weight marker, and the DNA bands were visualised, and imaged using a ChemiDoc™ XRS+ (Bio-Rad, USA).

6.2.3 Evaluation of the test samples using the qPCR assay

Quantitative PCR was performed to evaluate the concentration of the test samples listed in Table 6.1. This was done using the method developed in Chapter 5, section 5.2.3. All reactions were prepared in three sterile VA 4002P Uni-directional flow bench (Vivid Air, South Africa). This was done by tripling the contents of each reaction to 30 µl during reaction preparation. These master mixes were then split into three qPCR tubes, each receiving 10 µl of the mixture. The reagents were prepared as master mixes in nuclease-free 1.5 ml tubes, then aliquoted out when necessary. Pipetting was done using sterile DNase/RNase free filter pipette tips in nuclease-free 1.5 ml tubes and nuclease-free optically clear PCR tube strips. Nuclease-free qPCR grade H_2O was utilised for all reactions. Reactions were run using the QuantStudio™ 3 Real-Time PCR System (Thermo Scientific, USA) with the same cycle parameters described in Chapter 5, section 5.2.3. Data was analysed using QuantStudio Design and Analysis (Thermo Scientific, USA) to generate the amplification curves for each reaction, the melt peak for all amplicons generated, and the standard curves.

6.2.4 Statistical analysis

Prior to conducting a statistical analysis, the qPCR values obtained from absolute qPCR assays were converted to determine the OBs concentration in copies/ml. The equation below constructed based upon the copy number, elution volume, and the volume used per reaction was utilised for these calculations. The copy number is determined by the Thermo cloud software based on the standards, elution ratio is the elution volume over the utilised volume used per reaction; and the sample ratio is the number of OBs used (to get back to 1 ml).

$$Concentration\ (copies\ per\ ml) = (qPCR\ value\ \times Elution\ Ratio\ \times\ Sample\ Ratio)$$

Where *qPCR value = copy number obtained, Elution Ratio* = 30 and *Sample ratio = 50.*

To analyse and compare the quantification results obtained using darkfield miscopy and the qPCR assay, statistical analyses were done using the GraphPad Prism version 9.2.0 (GraphPad Holdings, LLC, USA). Data were log-transformed and statistical evaluation of differences between darkfield microscopy and qPCR assay results were performed by analysis of variance (ANOVA), with a significance level set to P = 0.05.

6.3 Results

6.3.1 Enumeration of purified CrleGV-SA OBs using darkfield microscopy

The CrleGV-SA test samples were enumerated using a haemocytometer and darkfield microscopy to determine the virus concentration.

6.3.2 *Granulin*, *lef-8* and *lef-9* amplification curves, melt peaks and standard curves

Quantitative PCR was performed on gDNA extracted from the test samples of unknown concentration (gel not shown). The *granulin*, *lef-8* and *lef-9* target region amplification curves, melt peaks, and standard curves for all samples are shown below in Figure 6.1, 6.2, and 6.3, respectively. All experimental reactions are coloured per treatment, with replicates of each treatment sharing the same colour.

Quantitative PCR for the *granulin*, *lef-8* and *lef-9* target regions was performed on all 7 samples with unknown concentrations in triplicate. Figure 6.1A, B, and C show the *granulin* target region analysis results. Consistent amplification of each sample was observed in Figure 6.1A. The sample reactions produced a single amplicon as identical melt peaks were formed, except for test samples 2, 5, and 6, where multiple melt peaks were observed, indicating the production of multiple amplicons. The standard curve generated from the *granulin* target region qPCR analysis is shown in Figure 6.1C. These are plotted along the regression line generated from the *granulin* plasmid standards. Samples 2, 5, and 6 fell outside the standard curve, meaning the quantity of these samples could not be determined. The R^2 value was 0.996, indicating a good fit for the regression line. The amplification efficiency for the qPCR reactions was 105%, falling within the recommended range of 90-105 %.

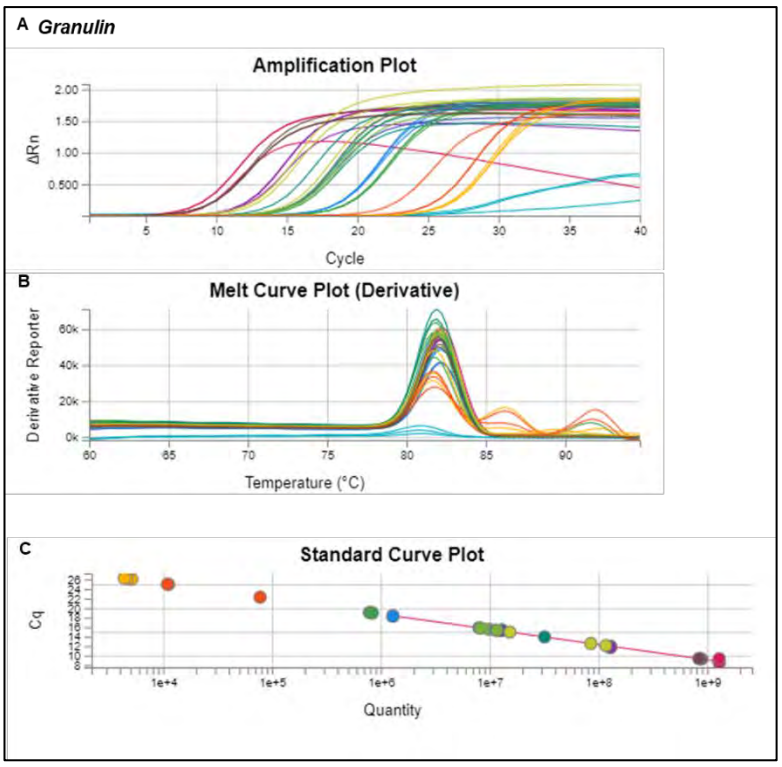

Figure 6.1: Quantitative PCR analysis results of the *granulin*. A) amplification curve, B) melt peak, C) standard curve.

Figure 6.2A, B, and C show the *lef-8* target region qPCR analysis results of the 7 samples with unknown concentrations. All the reactions produced ideal amplification curves as shown in Figure 6.2A, with the standards, NTCs, and the test samples coloured by sample. The melt peak for the *lef-8* reactions is shown in Figure 6.2B, with a single peak observed for all samples. The standard curve shown in Figure 6.2C was generated for the *lef-8* target region qPCR analysis. One sample fell outside the standard curve, namely, sample 6. The amplification efficiency was 102 %, signifying an ideal rate of product generation. The R^2 value obtained for the regression line generated from the *lef-8* plasmid standards was 0.981, indicating an ideal fit to the experimental data.

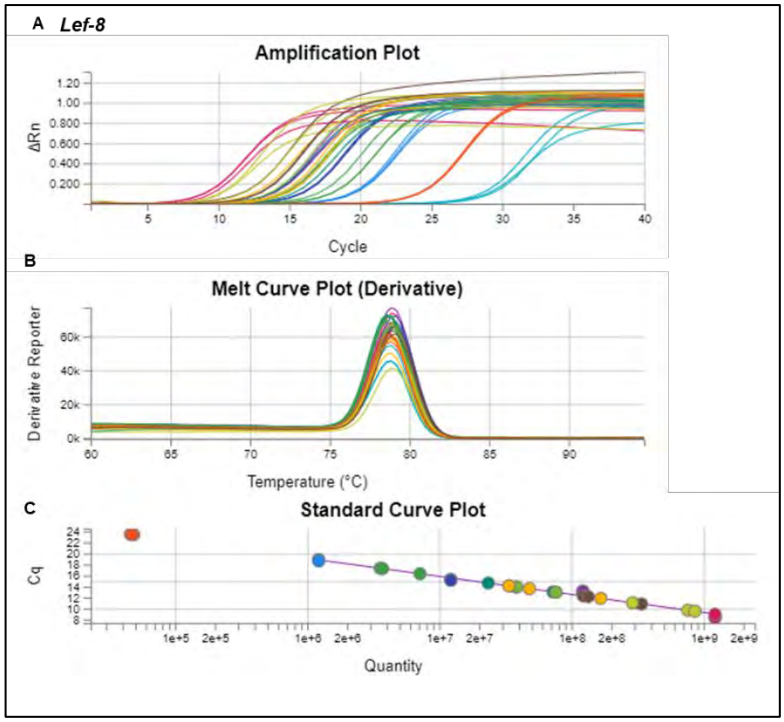

Figure 6.2: Quantitative PCR analysis results of the *lef-8*, with A) showing the amplification curve, B) melt peak, and C) standard curve.

Figure 6.3A, B, and C show the *lef-9* target region analysis results. Similarly, the reactions produced ideal amplification curves (Figure 6.3A). All reactions were found to form an identical melt peak, as shown in Figure 6.3B, indicating the production of a single amplicon. Similar to the *lef-8* target region qPCR analysis results, only sample 6 fell outside the standard curve. The R^2 value was 0.98, indicating a good fit for the regression line with an amplification efficiency of 91%.

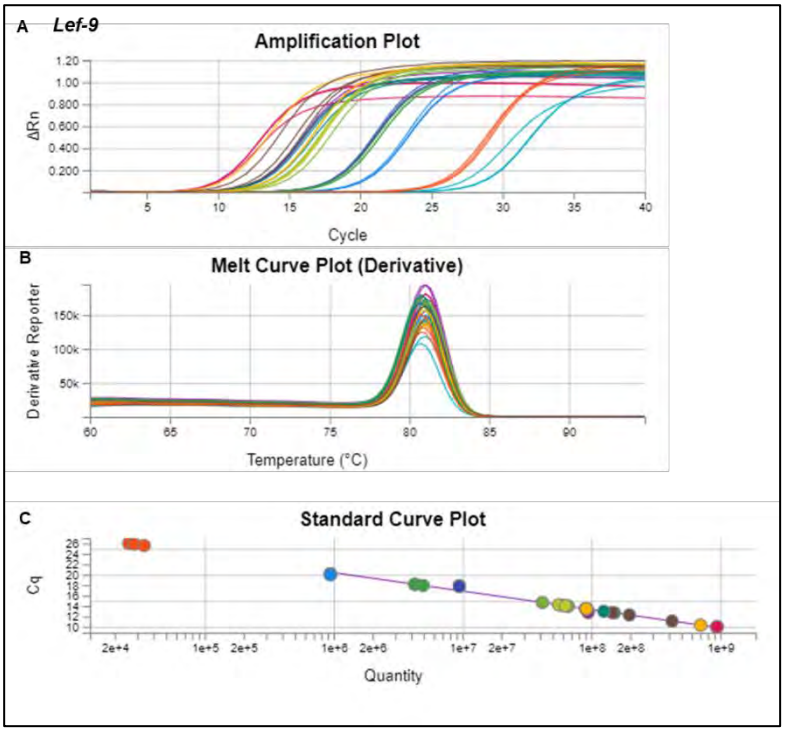

Figure 6.3: Quantitative PCR analysis results of the *lef-9*, with A) showing the amplification curve, B) melt peak, and C) standard curve.

6.3.3 Comparison of the methods dark field and qPCR enumeration

CrleGV-SA OBs were enumerated using a darkfield microscope under phase contrast with the Helber counting chamber. Subsequently, the *granulin, lef-8,* and *lef-9* target regions of the test samples were analysed by qPCR to determine the concentration of the samples. An ANOVA test was conducted to compare the concentration values determined for each test sample to determine whether the data obtained from these methods differed significantly (Figure 6.4). However, sample 5 *granulin* qPCR results were not included on the ANOVA test as the quantity value fell outside the standard curve. Similarly, sample 6 qPCR data results were not analysed as the quantity values obtained fell outside the standard curve. Figure 6.4A shows the comparison of enumeration methods for sample 1. There was no significant difference recorded between sample 1 concentration results obtained using the *granulin* and *lef-8* qPCR (P = 0.4229), *granulin* qPCR and darkfield microscopy (P = 0.8895), and the *lef-8* qPCR and darkfield microscopy (P = 0.1675). However, the results show that the concentration obtained by *granulin* qPCR significantly differed from the *lef-9* qPCR concentration (P = 0.0012). Similarly, *lef-8* qPCR (P = 0.0083) and the darkfield microscopy count (P = 0.006) were significantly lower than the *lef-9* qPCR.

Figure 6.4B shows the enumeration results for sample 2; the *granulin* qPCR results were not included as the quantity value fell outside the standard curve. The ANOVA test showed no significant differences between *lef-8* qPCR and *lef-9* qPCR (P = 0.9814), *lef-8* qPCR and darkfield microscopy (P = 0.3599), and *lef-9* qPCR and darkfield microscopy (P = 0.5427).

Similar results were obtained for sample 3 (Figure 6.4C), there were no significant statistical differences between *granulin* qPCR and darkfield microscopy (P = 0.1015), *lef-8* qPCR and *lef-9* qPCR (P = 0.8917), *lef-8* qPCR and darkfield microscopy (P = 0.8190), and *lef-9* qPCR and darkfield microscopy (P = 0.4403). The *granulin* qPCR concentration results were lower than *lef-8* qPCR (P = 0.0298) and the *lef-9* qPCR (P = 0.0115).

Figure 6.4D shows the enumeration comparison for sample 4; the *granulin* qPCR results did not significantly differ from the *lef-9* qPCR (P = 0.9995) and darkfield microscopy (P = 0.9635). The *lef-8* qPCR results obtained were significantly greater than the *granulin* qPCR results (P = 0.0089), *lef-9* qPCR (P = 0.0078), and the darkfield microscopy (P = 0.0050).

Sample 5 ANOVA test results show that there is no significant difference between *lef-8* qPCR and *lef-9* qPCR (P = 0.5075), *lef-8* qPCR and darkfield microscopy (P = 0.9498), and *lef-9* qPCR and darkfield microscopy (P = 0.2725) (Figure 6.4E).

Figure 6.4F shows the comparison of the enumeration methods for sample 7, the *granulin* qPCR results were significantly higher than the *lef-8* qPCR (P =0.0001), *lef-9* qPCR (P = 0.0003), and darkfield microscopy (P < 0.0001). However, there were no significant differences between the *lef-8* qPCR and *lef-9* qPCR (P = 0.8839), *lef-8* qPCR and darkfield microscopy (P = 0.3951), and *lef-9* qPCR and darkfield microscopy (P = 0.1544).

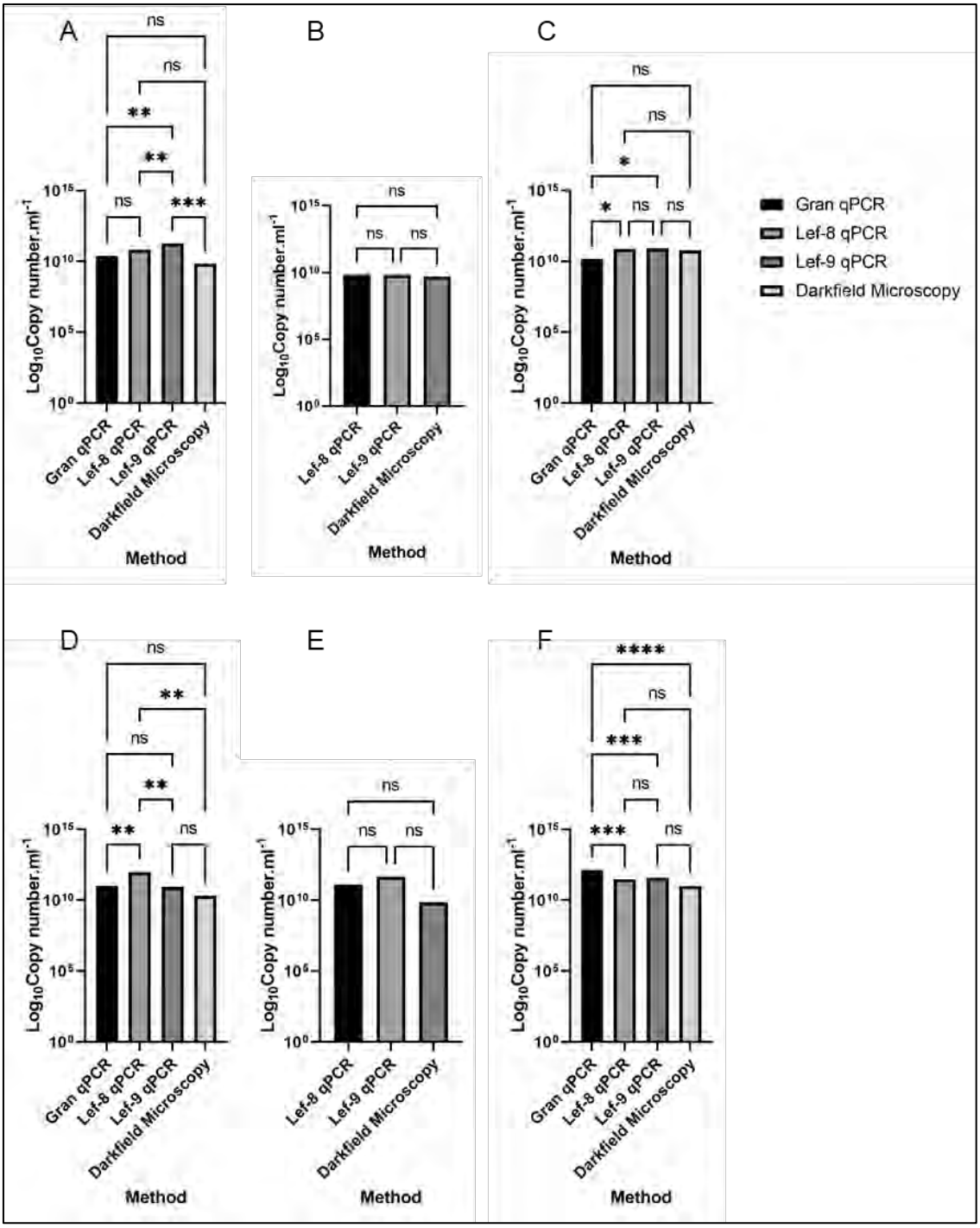

Figure 6.4: Comparison of the concentration values obtained using the different enumeration methods for each unknown sample. Each sample with an unknown concentration was enumerated using *granulin*, *lef-8*, *lef-9* qPCR, and darkfield microscopy. With A- Sample 1, B- Sample 2, C- Sample 3, D- Sample 4, E- Sample 5 and F- Sample 7. *, **, ***and **** indicate significant differences between each method according to

ANOVA test ($P < 0.05$ and $P < 0.01$, respectively), ns indicates that differences were not significant.

In summary, the concentration, P-values and standard deviations of test samples are shown in Table 6.2, with significant P-values highlighted in bold. The *lef-9* and *lef-8* qPCR results showed almost no significant difference to the darkfield counts, with each assay only having a single result that significantly differed from the darkfield count. The *gran* qPCR result differed most from the other two qPCR assays, meanwhile the *lef-9* and *lef-8* qPCR showed general agreement ($P > 0.05$)

Table 6.2: Summary of the concentration values, P- values and standard deviation obtained between the *Granulin*, *Lef-8* and *Lef-9* qPCR results and the darkfield microscopy counts.

Test Samples	Methods								P-Value					
	***Granulin* qPCR**		***Lef-8* qPCR**		***Lef-9* qPCR**		**Darkfield microscopy**		***Granulin* qPCR & *Lef-8* qPCR**	***Granulin* qPCR & *Lef-9* qPCR**	***Granulin* qPCR & Darkfield microscopy**	***Lef-8* qPCR & *Lef-9* qPCR**	***Lef-8* qPCR & Darkfield microscopy**	***Lef-9* qPCR & Darkfield microscopy**
	Concentration (Copy number.ml^{-1})	**Standard Deviation**	**Concentration (Copy number.ml^{-1})**	**Standard Deviation**	**Concentration (Copy number.ml^{-1})**	**Standard Deviation**	**Concentration (Copy number.ml^{-1})**	**Standard Deviation**						
1	2.25×10^{10}	1.95×10^{10}	6.7×10^{10}	3.78×10^{10}	1.83×10^{11}	4.61×10^{10}	7.0×10^{9}	8.1×10^{9}	0.4229	**0.0012**	0.8835	**0.0083**	0.1672	**0.0006**
2	-	-	7.21×10^{9}	3.03×10^{9}	6.74×10^{9}	5.91×10^{8}	5.0×10^{9}	5.8×10^{9}	-	-	-	0.9814	0.3599	0.5427
3	1.49×10^{10}	2.55×10^{9}	7.45×10^{10}	3.50×10^{10}	8.64×10^{10}	2.07×10^{10}	6.21×10^{10}	7.17×10^{10}	**0.0298**	**0.0115**	0.1015	0.8917	0.8190	0.4403
4	1.09×10^{11}	7.82×10^{10}	9.55×10^{11}	4.57×10^{11}	8.87×10^{10}	5.41×10^{9}	1.55×10^{10}	1.78×10^{10}	**0.0089**	0.9995	0.9635	**0.0078**	**0.0050**	0.9824
5	-	-	1.24×10^{11}	1.10×10^{11}	4.44×10^{11}	5.30×10^{11}	7.0×10^{9}	8.1×10^{9}	-	-	-	0.5075	0.9498	0.2725
6	-	-	-	-	-	-	8.0×10^{8}	9.23×10^{8}	-	-	-	-	-	-
7	1.30×10^{12}	3.51×10^{10}	2.97×10^{11}	1.82×10^{11}	3.83×10^{11}	2.22×10^{11}	1.198×10^{11}	1.38×10^{11}	**0.0001**	**0.0003**	< **0.0001**	0.8839	0.3951	0.1544

6.4 Discussion

The aim of this chapter was to compare the traditional method of enumeration, which is darkfield microscopy, with the qPCR assay method developed in this study to determine if the two methods are consistent. This was achieved by first counting CrleGV-SA OBs samples using a darkfield microscope under phase contrast with the Helber counting chamber. Subsequently, gDNA was extracted from the counted OBs utilising the method developed in Chapter 4. A quantitative PCR assay was utilised to quantify the CrleGV-SA OBs samples using the extracted gDNA as template. Lastly, the obtained quantity data for both enumeration methods were statistically analysed to compare and determine whether the methods yield similar CrleGV-SA OB quantities.

As previously mentioned, CrleGV-SA is a naturally occurring endemic virus isolate formulated into a biological control agent Cryptogran (Moore 2002). It has also been mentioned that darkfield microscopy is the traditional enumeration method. However, as GVs are very small, counting the OBs is challenging, strenuous to the eye, and time-consuming. Thus, developing a highly accurate, effective, and time-efficient alternative quantitative technique is essential. A technique that will be compared with the current enumeration method to establish their accuracy for use in quality control in the commercial production of CrleGV-SA.

In this chapter, a qPCR assay was utilised to enumerate test samples of unknown concentration and was compared with the traditional darkfield microscopy technique. As mentioned in the previous chapters, the target regions chosen for qPCR amplification in the CrleGV-SA genome were of the *granulin*, *lef-8* and *lef-9* genes, which are present as a single copy in baculovirus genomes. Therefore, if the gene is present as a single copy within the virus genome, then the concentration of virus particles can be accurately quantified from the gene copy number within the sample as each plasmid also consists of a single target gene region. The absolute quantification method using a standard curve was used to quantify the amount of DNA in unknown samples, whereby their Cq values are compared to a standard curve (Yu *et al*., 2005). All reactions produced ideal amplification curves for the *granulin*, *lef-8* and *lef-9* qPCR assays, such that qPCR efficiency could be determined from the slope of the exponential phase. Importantly, no amplification curve was observed in the no template control for *granulin* qPCR; although, for *lef-8* and *lef-9* qPCR assays, amplification curves were observed at the late cycles. Nonetheless, if the no template control crosses the threshold, their Cq should be at least five cycles, and preferably more than ten cycles, from the Cq of the least concentrated sample (Stratagene, 2010). The least concentrated test sample was sample 2, as sample 6 data

was disregarded because it fell outside the standard curve. For the *lef-8* qPCR, test sample 2 reached the Cq value at cycles 16.33, 17.31, and 17.26, while the NTC reached this threshold at cycles 28.29, 28.58, and 27.82, respectively. Similarly, for the *lef-9* qPCR, sample 2 reached the Cq value at cycles 18.19, 18.18, and 17.95, while the NTC reached this threshold at cycles 28.60, 28.68, and 27.21, respectively. It is safe to presume that the results are accurate as the no template Cq values are more than five cycles, from the Cq of the least concentrated sample.

The plotted melt curves had single peaks for the *lef-8* and *lef-9* qPCR assays, which indicated the presence of a single amplicon and confirmed the high specificity of the oligonucleotides. However, a surprising result was observed on the *granulin* qPCR; samples 2, 5, and 6 deviated from the typical melt curve, with multiple melt peaks observed. As previously discussed, multiple peaks indicate that the oligonucleotides have bound to other DNA template sequences within the PCR reaction, which may be DNA that cross-hybridises with the oligonucleotides or a result of oligonucleotide-dimers generated during the PCR reaction (Real-Time PCR Applications Guide, 2006).

Standard curves were produced from the *granulin*, *lef-8,* and *lef-9* plasmid standards, each of which had a known range of concentrations. The standard curves were then utilised to determine the concentration of the test samples. The *granulin*, *lef-8* and *lef-9* qPCR standard curves were ideal for the experimental data with R^2 values of 0.996, 0.981, and 0.980 for the generated regression line, respectively. As previously discussed, the efficiency of a standard curve is determined by the value of its slope, and an R^2 value greater than 0.90 is desirable for qPCR (Dhladhla *et al.*, 2018).

The quantity values obtained were statistically analysed, and the enumeration methods were compared. The *granulin* qPCR results for samples 2 and 5 were excluded from the analysis as their quantity values fell outside the standard curve. Similarly, sample 6 *granulin*, *lef-8* and *lef-9* qPCR results were discarded as they were also outliers. Unexpectedly, test sample 5 Cq value was significantly lower than the Cq value of sample 6 in the *granulin* qPCR assay; this was possibly due to pipetting error as this was not the case for the other qPCR assays. The qPCR quantity values of these excluded samples were below the plasmid standard with the lowest concentration.

Contrary to expectation, the qPCR results significantly differed for some samples; the *granulin* qPCR quantity values differed significantly from the *lef-8* and *lef-9* qPCR values for unknown samples 3, 4, and 7. Similarly, in samples 1 and 4, the *lef-8* and *lef-9* qPCR values obtained

differed significantly. Test sample 1, the *granulin* qPCR quantity value did not differ significantly from that of the *lef-8* qPCR but significantly differed from that of *lef-9* qPCR. Considering that these qPCR assays were not conducted the same day, gDNA samples kept for prolonged periods at -20 ˚C or repeated freeze/thaw cycles result in poor amplification efficiency as they become susceptible to degradation (Burns *et al*., 2006). However, the *granulin* qPCR assay was conducted a week prior to performing the other two qPCR assays for this study. Additionally, the *granulin* qPCR values for all the test samples except for sample 7 are significantly lower than those of *lef-8* and *lef-9* qPCR assays. Thus, these differences are not due to repeated freeze/thaw cycles. One of the potential causes for such a deviating trend could be pipetting error. To avoid pipetting error, which would affect the observed Cq values, and the PCR efficiency derived from a dilution series, pipettes used for qPCR analysis should be regularly calibrated (Ruijter et *al*., 2021).

There were no significant differences in *lef-8* and *lef-9* qPCR values of test samples 2, 3, 5, and 7. These results were expected as the same samples were quantified by qPCR, targeting different genes. Additionally, the ANOVA test of the previously mentioned samples for the *lef-8* and *lef-9* qPCR showed that the quantity values obtained did not differ significantly from the enumeration values obtained by darkfield microscopy. Similarly, for samples 1, 3, and 4, the comparison of *granulin* qPCR with darkfield microscopy results did not significantly differ. It was only for test sample 7, where the *granulin* qPCR results differed significantly from the darkfield microscopy results. Nonetheless, these results confirm that darkfield microscopy can be used as an accurate enumeration method for baculoviruses, although it has numerous drawbacks. Similarly, application of the *lef-8* and *lef-9* qPCR assays were demonstrated to produce comparable results as darkfield and could be used as a viable alternative, offering several important advantages which are discussed at length in the final chapter. Additionally, darkfield microscopy and the developed qPCR were investigated using raw, purified, and crude (semi-purified) CrleGV-SA and Cryptogran stocks. The results showed that both methods were reliable in counting virus particles (OBs) in all three preparations.

In conclusion, a qPCR assay was developed and successfully utilised to quantify CrleGV-SA test samples. This chapter showed that the qPCR assay developed has great potential as an alternative enumeration method for CrleGV OBs compared to microscopy, although things like pipetting error need to be carefully considered. Alternatively, multichannel pipettes could also be used to avoid pipetting error. The qPCR method is more convenient as the method saves time and is more sensitive for detecting and quantifying CrleGV samples. Furthermore, this

method allows for the enumeration of more than one sample in a single run, making it rapid and more cost-effective compared to traditional microscopy.

Chapter 7

General discussion

7.1 Study overview

In South Africa, *T. leucotreta* is a significant pest to the citrus industry. The betabaculovirus, CrleGV-SA has been formulated and registered into the biopesticides Cryptogran and Cryptex for the control of *T. leucotreta* and has been successfully used commercially for more than 15 years in South Africa (Moore *et al*., 2015). In order to use it as a biopesticide, OBs have to be quantified to perform laboratory bioassays, field trials and for formulation, among other applications. Traditionally, darkfield microscopy is used to quantify these viruses; however, the technique consists of numerous drawbacks. These drawbacks create a necessity for the development of an alternative enumeration technique. In this study, a qPCR assay was developed to enumerate CrleGV-SA using plasmids as standards. The first objective of this study was to determine the degree of nucleotide conservation between CrleGV-SA and CrleGV-CV3 *granulin*, *lef-8*, and *lef-9* gene sequences available on GenBank to design two sets of oligonucleotides (internal and external oligonucleotides) on highly conserved regions as described in Chapter 2. The successfully designed oligonucleotides (external oligonucleotides) were used to amplify the target regions of the three selected genes. After that, recombinant plasmids were constructed by cloning each amplified region into a pJET1.2/blunt cloning vector for use as standards in the qPCR assay (Chapter 3). Subsequently, two different methods of gDNA extraction were compared to determine which of the methods provides the highest gDNA yield (Chapter 4). A qPCR assay was developed for use in the enumeration of CrleGV-SA test samples (Chapter 5). The final objective was to compare the traditional method of enumeration, which is darkfield microscopy, with the qPCR assay method developed in this study to determine if the two methods were consistent (Chapter 6).

7.2 The construction and validation of plasmid standards

In this study, a qPCR assay was developed; a few studies have successfully utilised the qPCR technique to quantify CrleGV as an alternative to darkfield microscopy (Dhladhla *et al.*, 2018; Jukes, 2018). However, the standards used in these studies were CrleGV gDNA. The use of gDNA as standards consists of numerous drawbacks for example, gDNA kept for prolonged periods at -20 ˚C or repeated freeze/thaw cycles results in poor amplification efficiency because they become susceptible to degradation (Burns *et al*., 2006). Additionally, in the study by Jukes (2018) the relative concentrations for the gDNA standards were determined by first

enumerating CrleGV OBs by darkfield microscopy, from which gDNA was subsequently extracted using the ZR Viral DNA extraction kit (Zymo Research, USA). This introduced at least two potential limitations. First, the enumeration of the baculovirus OBs by darkfield microscopy only provides an estimation of the concentration, with some degree of variability inevitable introduced during this process. Second, the extraction kit used had a maximum cut-off of 50 kb, decreasing the proportion of gDNA which was successfully extracted from the OBs, as the CrleGV has a much larger genome size of 111,334 bp (Van Der Merwe *et al.*, 2017). It should be noted that the same gDNA extraction kit was used on all test samples, which may mitigate this limitation by maintaining similar proportions when applied to different OB samples. However, a process which avoids these limitations would be ideal.

The reliability of standards for qPCR is a crucial issue, therefore, choosing the appropriate standards is essential. Among the various types of standard DNA available, plasmid DNA is most commonly chosen due to its high stability and reproducibility (Lo and Chao, 2004; Zwart *et al*., 2008; Lin *et al*., 2011; George *et al*., 2012). The use of plasmids as standards in qPCR assays is important for accuracy when enumerating baculoviruses. Plasmids are highly stable molecules even after prolonged storage times at room temperature; they generate extremely reproducible standard curves with reliable efficacy and sensitivity (Formisano-Tréziny *et al*., 2012). They are easy to construct and can be produced in large quantities; plasmids have independent means of quantification, as the count is based on the concentration and purity of the DNA, both of which are measured after plasmid DNA extraction. Several studies have demonstrated that plasmids could be used as standards to produce a calibration curve for quantifying unknown samples. This is done by introducing the sequence of interest from the target gene into the plasmid and producing a linear dilution series (Burns *et al*., 2006). In the study by Burns *et al*., (2006), which compared the use of plasmid and genomic DNA as standards, for all the test samples assessed, the plasmid standard curves gave a better estimation of the expected percentage of the test samples. Moreover, compared to gDNA standards, plasmid standards are easier and cheaper to sequence, and because of their stability, they are easy to distribute worldwide (Burns *et al*., 2006).

A few studies have constructed plasmid standards for the qPCR enumeration of baculoviruses. George *et al*., (2012) constructed and prepared plasmid standards for use in the qPCR assay to quantify baculoviruses. Another study was done by Lo and Chao (2004), whereby plasmid standards were constructed and utilised in a qPCR assay to develop a simple and rapid method

for titre determination of baculovirus OBs. Both these studies demonstrated that plasmids can be used for accurate quantification of baculoviruses.

Nonetheless, there is no published study whereby plasmid standards are constructed to enumerate CrleGV using a qPCR assay. Although plasmid construction may be time-consuming, using plasmids as qPCR standards has many advantages compared with other strategies. In the current study, the plasmids of interest (pJET1.2-Gran, pJET1.2-lef-9, and pJET1.2-lef-8) containing partial regions of the *granulin*, *lef-8*, and *lef-9* genes were constructed for use as standards in the qPCR assay. The *granulin*, *lef-9* and *lef-8* genes were selected for this study as they have been identified in all fully sequenced *betabaculovirus* genomes and have previously been shown to be suitable for studying baculovirus phylogeny (Herniou *et al.*, 2001; Herniou *et al.*, 2003; Lange *et al.*, 2004). The purpose of using three genome regions to construct three different plasmid standards was to validate the accuracy and consistency of the developed qPCR assay. The recombinant plasmids were confirmed by colony PCR, restriction digestion, and Sanger Sequencing. The success of constructing plasmid standards demonstrated that these plasmids have potential for use in the enumeration of CrleGV in both research and commercial settings.

7.3 Comparison of the gDNA extraction methods

When conducting a qPCR assay for virus enumeration, ensuring that the most sensitive and reliable gDNA extraction method is utilised is important. For gDNA extraction on baculoviruses, most studies utilise the CTAB extraction method (Opoku-Debrah *et al*., 2013) and have found this method to be satisfactory for extracting gDNA (Aspinall *et al*., 2002; Parnell *et al*., 2002; Van der Merwe *et al*., 2017; Dhladhla *et al.*, 2018; Jukes, 2018). However, traditional methods such as phenol/chloroform extraction have been reported to yield inconsistent DNA recovery from baculovirus samples (Lo and Chao, 2004). Additionally, other drawbacks that are associated with phenol/chloroform-based extraction techniques include, working with hazardous chemicals in sometimes many repetitive steps often result in phenol contamination of the extract and (partial) inhibition of subsequent PCR, as well as poor extraction efficiency when working with small sample volumes (Lebuhn *et al*., 2016).

Dhladhla, (2012) compared CrleGV gDNA extraction methods to avoid using hazardous reagents. The kits used in their study were the ZR Viral DNA kit™ and the ZR Insect/Tissue DNA kit-5™ (Zymo Research, USA). The efficiency of two viral DNA extraction kits was determined; however, low concentrations of gDNA were obtained from the CrleGV-SA stock

compared to the typically used CTAB DNA extraction method, possibly due to the limitations discussed above. Another study comparing baculovirus gDNA extraction methods was published by De Moraes *et al*. (1999). They developed two DNA isolation procedures, which were phenol-ether and magnetic capture-hybridization (MCH), to directly extract baculovirus gDNA from the soil. The MCH procedure was more effective in removing the humic acids that are usually coextracted with DNA from soil and are inhibitory to PCR amplification and other enzymatic procedures.

The current study compared two different gDNA extraction methods to determine which of the methods provides the highest gDNA yield. One is the Quick-DNA Miniprep Plus Kit (Zymo Research, USA) (method 1a) as per the manufacturer's instructions. For the second method, CrleGV-SA OBs were pre-treated with Na_2CO_3 prior to using the kit (method 1b). Similarly, for method 1c, CrleGV-SA OBs were pre-treated with Na_2CO_3 and Tris-HCl before using the kit. For the last method, which is method 2, gDNA was extracted from purified CrleGV-SA OBs using the CTAB DNA extraction method described by Opoku-Debrah *et al*., (2013). The slight modifications of the kit in methods 1b and 1c were done to improve DNA yield. The CTAB DNA extraction protocol (method 2) had a lower gDNA concentration than method 1c. Additionally, the CTAB gDNA quantity was inconsistent between replicates, thus indicating poor reproducibility. Method 1c was identified as the ideal extraction method when compared with the other methods, producing the highest concentration and purity within a short processing time.

The gDNA extraction method developed in this study (Method 1c) is simple, and unlike the commonly used CTAB extraction method, it reduces assay times from two days to less than an hour. The method consistently produced the highest yield and best-quality gDNA, while also being affordable. This technique produces reliable results and could be used routinely in laboratories for the extraction of gDNA from baculoviruses. As with all extraction protocols, losses are unavoidable, and extraction efficiencies are subject to fluctuations given the makeup of the samples (George *et al*., 2012). Additionally, no DNA extraction technique reliably ensures that each genome is released from each OB in the sample; one that yields the highest gDNA concentration from viral samples, in this case Method 1c, is desirable.

The virus from which the gDNA extractions are conducted must also be considered, which in this study was one belonging to the genus Betabaculovirus. Viruses within this genus contain a single virion within each OB, and therefore a single genome is occluded in each granule

(Lange and Jehle 2003; Rohrmann, 2019). Additionally, the three genes of interest are only present as single copies within the virus genome. Put differently, a single OB in a virus sample releases one genome during gDNA extraction. This enables a direct correlation between the number of genomes (and therefore the genes of interest) and the number of OBs, enabling quantification of OBs via the number of genome copies present in a sample.

7.4 Comparison of darkfield and qPCR methods for enumeration of CrleGV test samples

Quantitation of betabaculoviruses is vital to establish a highly reliable and reproducible production process (George *et al*., 2012). This study aimed to quantify glycerol gradient purified, crude-purified, and viral formulated suspensions using darkfield microscopy and qPCR methods of enumeration to verify their accuracy and determine consistency and comparability. As previously discussed, the traditionally used darkfield microscopy method consists of numerous drawbacks such as being tedious, subjective, and time-consuming. Quantitative PCR protocols are the quickest method for quantitation (Roldao *et al*., 2009) and have been based on the amplification of sections of genes that are common in baculoviruses genomes, which vary from study to study. Many studies have demonstrated the qPCR technique to be a valid and accurate method for determining baculovirus concentrations when compared to other methods (Hitchman *et al*., 2007; George *et al*., 2012; Dhladhla *et al*., 2018; Jukes, 2018). An additional advantage of this technique is the ease of implementation and the ability to process a large number of samples simultaneously, which is impossible with the other commonly used methods. The listed advantages encourage the use of qPCR over other techniques for baculoviruses and further investigations to improve the method.

In this work, a qPCR enumeration method was developed and compared with the traditional counting method, which is darkfield microscopy. This comparison was done to determine the accuracy and suitability of the newly developed technique for use in quality control in the commercial production of CrleGV-SA. As previously discussed, three sets of plasmid standards containing the *granulin*, *lef-8*, and *lef-9* gene target regions were constructed for use in the qPCR assay. Using more than one plasmid as standard in the qPCR assay is important to verify or validate empirical data or the observed results. Thus, the relative differences of data from the three sets of plasmids can be measured and compared.

The overall results showed that the *granulin*, *lef-8* and *lef-9* qPCR values did not significantly differ from the darkfield microscopy results. However, the *granulin* qPCR values for most of the test samples were significantly lower than those of *lef-8* and *lef-9* qPCR assays. These

findings were contrary to the expected results, as one would expect all three qPCR assays of the same test samples to yield similar results. The main reason for the difference of the *granulin* qPCR values from the *lef-8* and *lef-9* qPCR values can possibly be explained. For instance, in many qPCR assays, standard curves are typically generated by using a single plasmid or gDNA standard and the quantification is not validated by other standards. Considering that possible factors such as quality of reagents, pipette calibration, and nonspecific binding can introduce uncertainty into data interpretation (Sivaganesan *et al*., 2008), using more than one standard for qPCR assays is important to validate the data obtained. Additionally, the use of multichannel pipets to avoid pipetting error or human error which could result in uncertainties should be implemented. Recently, a newly available and affordable open-source liquid handling multichannel pipette, namely Opentron-2 (OT-2), has been developed by Opentrons (USA), which could be utilised to overcome these drawbacks while improving the rate of sample preparation and repeatability, further increasing the advantages of using qPCR-based quantification methods.

Samples that contained low gDNA concentrations could not be accurately quantified by the qPCR assay, as their qPCR values fell outside the range of the standard curve. An example of this was sample 6, where the gDNA quantity was too low to be incorporated within the range of the standard curves for any of the three plasmids used in the qPCR assay. Similarly, the concentration of samples 2 and 5 were too low, such that they fell outside the range of the *granulin* qPCR standard curve. Further dilution of the standards may overcome this limitation, by increasing the quantitative range of the assay, potentially incorporating these outliers within the respective standard curves.

Studies also use melt curve analysis to assess whether single or multiple amplicons are generated during a qPCR assay. In this study, an unexpected result was the presence of multiple peaks observed in the *granulin* qPCR data for the above-mentioned samples 2, 5, and 6. As discussed before, multiple peaks indicate that the oligonucleotides may have bound to non-target regions of the gDNA template producing non-specific amplicons or this may be a result of oligonucleotide-dimers generated during the PCR reaction (Mackay *et al*., 2004). It is unclear what caused the generation of multiple peaks during the *granulin* qPCR assay of samples 2, 5, and 6, warranting further investigation and evaluation.

7.5 Conclusion and future perspectives

In conclusion, the primary aim of this study was to construct plasmid standards, develop a more efficient gDNA extraction method and develop a qPCR assay for the enumeration of the CrleGV-SA OBs. The plasmid standards were successfully constructed for application in the qPCR assay. Similarly, the gDNA extraction method was successfully optimised, producing the highest CrleGV-SA gDNA concentration and purity compared to other methods. The qPCR assay was also successfully developed and was found to be comparable with the traditional darkfield microscopy counting technique. This is the first study to reveal that the two qPCR assays, the *lef-8* and *lef-9* assays, are robust, sensitive, and can accurately enumerate CrleGV-SA OBs using plasmid standards. Additionally, these results prove that this method can be applied for accurate measurement of the occurrence of CrleGV in commercial settings. Additionally, the developed gDNA extraction method is simple and rapid, producing results in under two hours. These features provide an advantageous application of the enhanced (Na_2CO_3 and Tris-HCl pre-treated plus Quick-DNA Miniprep Plus kit) extraction protocol for laboratories that may have limited resources.

In future research, diluting standard samples further before conducting the qPCR assay could enable the incorporation of test samples with low gDNA concentrations, increasing the likelihood of these falling within the quantitative range of the standard curve. Additionally, test samples with high concentrations which would similarly fall outside the quantitative range of the standard curve could be diluted. To reduce uncertainties that could be caused by pipetting error, in the future, multichannel pipettes should be utilised.

The qPCR assay developed in this study has a great potential to be utilised as an alternative to the darkfield microscopy method, using the constructed plasmids as standards. In addition, an important benefit of the qPCR method developed in this study is that it is a reliable, rapid, and cost-effective technique for the enumeration of CrleGV-SA that can be applied in laboratory and commercial settings.

References

Abdel-Latif, A. and Osman, G. 2017. Comparison of three genomic DNA extraction methods to obtain high DNA quality from maize. *Plant Methods*. 13(1):1-9.

Ahmad, I., Ahmad, F. & Pichtel, J. 2011. Microbes and microbial technology. *Agricultural and Environmental Applications*. 29–57.

Arthurs, S.P., Lacey, L.A & De La Rosa, F. 2008. Evaluation of a granulovirus (PoGV) and *Bacillus thuringiensis* subsp. kurstaki for control of the potato tuberworm (Lepidoptera: Gelechiidae) in stored tubers. *Journal of Economic Entomology*. 101:1540-1546.

Aspinall, T., Marlee, D., Hyde, J & Sims, P. 2002. Prevalence of *Toxoplasma gondii* in commercial meat products as monitored by polymerase chain reaction - food for thought? *International Journal of Parasitology*. 32:1193-1199.

Asser-Kaiser, S., Fritsch, E., Undorf-Spahn, K., Kienzle, J., Eberle, K.E., Gund, N. A, Reineke, A, Zebitz, C.P.W., Heckel, D.G., Huber, J & Jehle, J. a. 2007. Rapid emergence of baculovirus resistance in codling moth due to dominant, sex-linked inheritance. *Science*. 317:1916–1918.

Bajwa, W.I. & Kogan, M. 2002. Compendium of IPM Definitions (CID) What is IPM and how is it defined in the Worldwide Literature? *IPPC Publication*. 998(998):1–14.

Bale, J., van Lenteren, J. and Bigler, F. 2008. Biological control and sustainable food production, Philosophical Transactions of the Royal Society B. *Biological Sciences*. 363(1492):761–776.

Bio-Rad, L. 2006. Real-time PCR applications guide. *Hercules: Bio-Rad Laboratories Inc*. 41

Brunel, S., Suffert, M., Petter, F. & Baker, R. 2013. Interface between pest risk science and policy: the EPPO perspective. *NeoBiota*. 18:9–23.

Burns, M., Corbisier, P., Wiseman, G., Valdivia, H., McDonald, P., Bowler, P., Ohara, K., Schimmel, H., Charels, D., Damant, A. and Harris, N. 2006. Comparison of plasmid and genomic DNA calibrants for the quantification of genetically modified ingredients. *European Food Research and Technology*. 224(2):249-258.

Bustin, S. and Huggett, J. 2017. qPCR primer design revisited. *Biomolecular Detection and Quantification*. 14:19-28.

CGA, 2019. Citrus Growers' Association of Southern Africa Annual Report. [Online], Available: http://c1e39d912d21c91dce811d6da9929ae8.cdn.ilink247.com/ClientFiles/cga/CitrusGowers Association/Company/Documents/CGA%20Annual%20Report%202019%20FINAL.pdf

Clarke, J.F.G., 1955. Catalogue of the types specimens of Microlepidoptera in the British Museum (Natural History) described by Edward Meyrick.

Clem, R.J. & Passarelli, A.L. 2013. Baculoviruses: Sophisticated Pathogens of Insects. *PLoS Pathogens*. 9(11):11–14.

Coombes, C.A., Hill, M.P., Moore, S.D., Dames, J.F. & Fullard, T. 2015. Beauveria and Metarhizium Against False Codling Moth (Lepidoptera: Tortricidae): A Step Towards Selecting Isolates for Potential Development of a Mycoinsecticide. *African Entomology*. 23(1):239–242.

Daiber, C.C., 1979a. A study of the biology of the false codling moth (*Cryptophlebia leucotreta* (Meyr.)): The cocoon. *Phytophylactica*. 11(3):151–157.

Daiber, C.C., 1979b. A study of the biology of the false codling moth ((*Cryptophlebia leucotreta* (Meyer.)): The egg. *Phytophylactica*. 11(4):129–132.

Daiber, C.C., 1979c. A study of the biology of the false codling moth (*Cryptophlebia leucotreta* (Meyr.)): The larva. *Phytophylactica*. 11(4):141–144.

Daiber, C.C., 1980. A study of the biology of the false codling moth *Cryptophlebia leucotreta* (Meyr.): The adult and generations during the year. *Phytophylactica*. 12:182–193.

DALRRD. 2020. A profile of the South African citrus market value chain. *DALRRD*. 1–107. [Online], Available: https://www.dalrrd.gov.za/doaDev/sideMenu/Marketing/Annual%20Publications/Citrus%20 Market%20Value%20Chain%20Profile%202020.pdf

De Moraes, R.R., Maruniak, J.E. and Funderburk, J.E. 1999. Methods for detection of Anticarsia gemmatalis nucleopolyhedrovirus DNA in soil. *Applied and Environmental Microbiology*. 65(6):2307-2311.

Dhladhla, B.I. 2012. Enumeration of Insect Viruses Using Microscopic and Molecular Analyses: South African Isolate of *Cryotophlebia Leucotreta* Granulovirus as a Case Study (Doctoral dissertation, Nelson Mandela Metropolitan University).

Dhladhla, B.I.R., Mwanza, P., Lee, M.E., Moore, S. & Dealtry, G.B. 2018. Comparison of microscopic and molecular enumeration methods for insect viruses: Cryptophlebia leucotreta granulovirus as a case study. *Journal of Virological Methods*. 256:107–110.

Elyazghi, Z., El Yazouli, L., Sadki, K. and Radouani, F. 2017. ABI Base Recall: Automatic Correction and Ends Trimming of DNA Sequences. *IEEE Transactions on NanoBioscience*. 16(8):682-686.

EPPO, 2019. Pest risk analysis for *Thaumatotibia leucotreta*. [Online], Available: https://onlinelibrary.wiley.com/doi/epdf/10.1111/epp.12580

Erlandson, M. 2008. Insect Pest Control by Viruses. *Encyclopedia of Virology*. 125–133.

Ferris, M.M., Stepp, P.C., Ranno, K.A., Mahmoud, W., Ibbitson, E., Jarvis, J., Cox, M.M., Christensen, K., Votaw, H., Edwards, D.P. and Rowlen, K.L. 2011. Evaluation of the Virus Counter® for rapid baculovirus quantitation. *Journal of Virological Methods*. 171(1):111-116.

Formisano-Tréziny, C., de San Feliciano, M. and Gabert, J. 2012. Development of plasmid calibrators for absolute quantification of miRNAs by using real-time qPCR. *The Journal of Molecular Diagnostics*. 14:314-321.

Fritsch, E., Undorf-Spahn, K., Kienzle, J., Zebitz, C.P. and Huber, J. 2007. Codling moth granulovirus: First indication of variations in the susceptibility of local codling moth populations. *Iobc Wprs Bulletin*. 30(1):181.

Garavaglia, M.J., Miele, S.A.B., Iserte, J.A., Belaich, M.N. & Ghiringhelli, P.D. 2012. The ac53, ac78, ac101, and ac103 Genes Are Newly Discovered Core Genes in the Family Baculoviridae. *Journal of Virology*. 86(22):12069–12079.

Garnier, L., Gaudin, J.C., Bensadoun, P., Rebillat, I. and Morel, Y. 2009. Real-time PCR assay for detection of a new simulant for poxvirus biothreat agents. *Applied and Environmental Microbiology*. 75(6):1614-1620.

George, S., Sokolenko, S. and Aucoin, M.G. 2012. Rapid and cost-effective baculovirus sample preparation method as a viable alternative to conventional preparation for quantitative real-time PCR. *Journal of Virological Methods*. 182(1-2):27-36.

Ginzinger D.G. 2002. Gene quantification using real-time quantitative PCR: An emerging technology hits the mainstream. *Experimental Hematology*. 30:503-512

Graham, R.I., Tummala, Y., Rhodes, G., Cory, J.S., Shirras, A., Grzywacz, D. & Wilson, K. 2015. Development of a real-time qPCR assay for quantification of covert baculovirus infections in a major African crop pest. *Insects*. 6(3):746–759.

Grzywacz, D. and Moore, S. 2017. Production, formulation, and bioassay of baculoviruses for pest control. *Microbial Control of Insect and Mite Pests*. 109-124.

Guarino, L.A., Xu,f B., Jin, J. & Dong, W. 1998. A virus-encoded RNA polymerase purified from baculovirus-infected cells. *Journal of Virology*. 72(10):7985–91.

Harrison, R.L., Rowley, D.L., Mowery, J.D., Bauchan, G.R. & Burand, J.P. 2017. The operophtera brumata nucleopolyhedrovirus (OpbuNPV) represents an early, divergent lineage within genus Alphabaculovirus. *Viruses*. 9(10).

Hatting, J. L., Moore, S. D. and Malan, A. P. 2019. Microbial control of phytophagous invertebrate pests in South Africa: Current status and future prospects. *Journal of Invertebrate Pathology*. 165:1–13.

Hattingh, V. 1994. IPM on citrus in southern Africa. *Citrus Journal*. 4(3):21-24

Hattingh, V., Moore, S., Kirkman, W., Goddard, M., Thackeray, S., Peyper, M., Pringle, K. 2020. An Improved Systems Approach as a phytosanitary measure for *Thaumatotibia leucotreta* (lepidoptera: tortricidae) in export citrus fruit from South Africa. *Journal of Economic Entomology*. 1-12.

Herniou, E.A., Luque, T., Chen, X., Vlak, J.M., Winstanley, D., Cory, J.S. & O'Reilly, D.R. 2001. Use of whole genome sequence data to infer baculovirus phylogeny. *Journal of Virology*. 75(17):8117–8126.

Herniou, E.A., Olszewski, J.A., Cory, J.S. and O'Reilly, D.R. 2003. The genome sequence and evolution of baculoviruses. *Annual Review of Entomology*. 48(1):211-234.

Hitchman, R.B., Siaterli, E.A., Nixon, C.P. & King, L.A. 2007. Quantitative real-time PCR for rapid and accurate titration of recombinant baculovirus particles. *Biotechnology and Bioengineering*. 96(4):810–814.

Hofmeyr, J.H., Hofmeyr, M., Hattingh, V., Slabbert, J.P. 2016. Postharvest Phytosanitary Disinfestation of *Thaumatotibia leucotreta* (Lepidoptera: Tortricidae) in Citrus Fruit: Determination of Ionising Radiation and Cold Treatment Conditions for Inclusion in a Combination Treatment. *African Entomology*. 24:208–216.

Hoseini, S.S. and Sauer, M.G. 2015. Molecular cloning using polymerase chain reaction, an educational guide for cellular engineering. *Journal of Biological Engineering*. 9(1):1-13.

Jehle, J.A., and Baekhaus H. 1994. Genome organization of the DNA-binding protein gene region of Cryptophlebia leucotreta granulosis virus is closely related to that of nuclear polyhedrosis viruses. *Journal of General Virology*. 75:1815-182.

Jehle, J.A., 2008. The future of Cydia pomonella granulovirus in biological control of codling moth. *Ecofruit-13th International Conference on Cultivation Technique and Phytopathological Problems in Organic Fruit-Growing: Proceedings to the Conference from 18thFebruary to 20th February 2008 at Weinsberg/Germany*. 265-270.

Jehle, J.A., Blissard, G.W., Bonning, B.C., Cory, J.S., Herniou, E.A., Rohrmann, G.F., Theilmann, D.A., Thiem, S.M. and Vlak, J.M. 2006. On the classification and nomenclature of baculoviruses: a proposal for revision. *Archives of Virology*. 151(7):1257-1266.

Jehle, J.A., Schulze-Bopp, S., Undorf-Spahn, K. and Fritsch, E. 2017. Evidence for a second type of resistance against *Cydia pomonella* granulovirus in field populations of codling moths. *Applied and Environmental Microbiology*. 83(2):2330-16.

Jehle, J.A., Wahl-Ermel, B. 2006. What do we (need to) know about low-susceptibility of codling moth against *Cydia pomonella* granulovirus (CpGV). *Journal of General Virology*. 14-18.

Jukes, M.D. 2018. Baculovirus Synergism: Investigating Mixed Alphabaculovirus and Betabaculovirus Infections in the False Codling Moth, *Thaumatotibia leucotreta*, for Improved Pest Control (Rhodes University).

Kaletta, J., Pickl, C., Griebler, C., Klingl, A., Kurmayer, R. and Deng, L. 2020. A rigorous assessment and comparison of enumeration methods for environmental viruses. *Scientific Reports*. 10(1):1-12.

Kirkman, W. & Moore, S. 2007. A study of alternative hosts for the false codling moth, *Thaumatotibia* (*Cryptophlebia*) *leucotreta* in the Eastern Cape. *SA Fruit Journal*. 6(2):33–38.

Knox, C., Moore, S., Luke, G., & Hill, M. P. 2015. Baculovirus-based strategies for the management of insect pests: a focus on development and application in South Africa. *Biocontrol Science and Technology*. 25:1-20.

Komai, F. 1999. A taxonomic review of the genus Grapholita and allied genera (Lepidoptera: Tortricidae) in the Palaearctic region. *Entomologica scand*. 55:1–226.

Krejmer-Rabalska, M., Rabalski, L., Jukes, M., Lobo de Souza, M., Moore, S., Szewczyk, B. 2019. New Method for Differentiation of Granuloviruses (Betabaculoviruses) Based on Real-Time Polymerase Chain Reaction (Real-Time PCR). *Viruses*. 11: 115.

Kroemer, J. A., Bonning, B. C., & Harrison, R. L. 2015. Expression, Delivery and Function of Insecticidal Proteins Expressed by Recombinant Baculoviruses. *Viruses*. 7: 422-455.

Krokene, P., Heldal, I. & Fossdal, C.G. 2013. Quantifying Neodiprion sertifer nucleopolyhedrovirus DNA from insects, foliage and forest litter using the quantitative real-time polymerase chain reaction. *Agricultural and Forest Entomology*. 15(2):120–125.

Lange, M. and Jehle, J.A. 2003. The genome of the Cryptophlebia leucotreta granulovirus. *Virology*. 317(2):220-236.

Lange, M., Wang, H., Zhihong, H. & Jehle, J.A. 2004. Towards a molecular identification and classification system of lepidopteran-specific baculoviruses. *Virology*. 325(1):36–47.

Lebuhn, M., Derenkó, J., Rademacher, A., Helbig, S., Munk, B., Pechtl, A., Stolze, Y., Prowe, S., Schwarz, W.H., Schlüter, A. and Liebl, W. 2016. DNA and RNA extraction and quantitative real-time PCR-based assays for biogas biocenoses in an interlaboratory comparison. *Bioengineering*. 3(1):7.

Lin, C.H., Chen, Y.C. and Pan, T.M. 2011. Quantification bias caused by plasmid DNA conformation in quantitative real-time PCR assay. *PloS one*. 6(12):29101.

Lo, H.R. and Chao, Y.C. 2004. Rapid titer determination of baculovirus by quantitative real-time polymerase chain reaction. *Biotechnology Progress*. 20(1):354-360.

Mackay, I.M., Arden, K.E. and Nitsche, A. 2004. Real-time fluorescent PCR techniques to study microbial–host interactions. *Methods in Microbiology*. 34:255-330.

Maddocks, S. and Jenkins, R. 2016. Understanding PCR: A practical bench-top guide.

Malan, A. P., von Diest, J. I., Moore, S. D., & Addison, P. 2018. Control options for false codling moth, *Thaumatotibia leucotreta* (Lepidoptera: Tortricidae), in South Africa, with emphasis on the potential use of entomopathogenic nematodes and fungi. *African Entomology*. 26:14-29.

Malan, A.P., Knoetze, R. & Moore, S.D. 2011. Isolation and identification of entomopathogenic nematodes from citrus orchards in South Africa and their biocontrol potential against false codling moth. *Journal of Invertebrate Pathology*. 108(2):115–125.

Miele, S.A.B., Garavaglia, M.J., Belaich, M.N. & Ghiringhelli, P.D. 2011. Baculovirus: Molecular insights on their diversity and conservation. *International Journal of Evolutionary Biology*. 2011:1–15.

Mkiga, A.M., Mohamed, S.A., Du Plessis, H., Khamis, F.M. & Ekesi, S. 2019. Field and laboratory performance of false codling moth, *Thaumatotibia leucotreta* (Lepidoptera: Torticidae) on orange and selected vegetables. *Insects*. 10(3).

Moore, S. D. 2019. False codling moth (*Thaumatotibia leucotreta* Meyr.). *Integrated Pest and Disease Management*. 3:1-10.

Moore, S. D. 2021. Biological Control of a Phytosanitary Pest (*Thaumatotibia leucotreta*): A Case Study. *International Journal of Environmental Research and Public Health*. 18:1198.

Moore, S., & Hattingh, V. 2012. A Review of Current Pre-harvest Control Options for False Codling Moth in Citrus in southern Africa. *SA Fruit Journal*. 11:82-85.

Moore, S., & Jukes, M. 2020. Advances in microbial control in IPM: entomopathogenic viruses. In M. Kogan, & E. Heinrichs, Integrated management of insect pests: Current and future developments. *Burleigh Dodds Science Publishing Limited*. 593-648.

Moore, S., Kirkman, W. and Stephen, P. 2004. Cryptogran. A virus for the biological control of false codling moth. *SA Fruit Journal* (South Africa).

Moore, S., Kirkman, W., Richards, G., Stephen, P. 2015. The Cryptophlebia leucotreta Granulovirus—10 Years of Commercial Field Use. *Viruses* 7:1284–1312.

Moore, S.D. 2002. The development and evaluation of Cryptophlebia leucotreta granulovirus (CrleGV) as a biological control agent for the management of false codling moth, *Cryptophlebia leucotreta*, on citrus (Doctoral dissertation, Rhodes University).

Moore, S.D. 2017. Moths and Butterflies: False Codling Moth. *Integrated Production Guidelines*. 1–9.

Moore, S.D. and Hattingh, V. 2016. A review of control measures and risk mitigation options for false codling moth (FCM), *Thaumatotibia leucotreta*, and their efficacy. *Citrus Research International*.

Moore, S.D., Hendry and D.A., Richards, G.I. 2011. Virulence of a South African isolate of the Cryptophlebia leucotreta granulovirus to *Thaumatotibia leucotreta* neonate larvae. *BioControl*. 56:341–352.

Moore, S.D., Kirkman, W., Stephen, P.R., Albertyn, S., Love, C.N., Grout, T.G. & Hattingh, V. 2017. Development of an improved postharvest cold treatment for *Thaumatotibia leucotreta* (Meyrick) (Lepidoptera: Tortricidae). *Postharvest Biology and Technology*. 125:188–195.

Moscardi, F. 1999. Assessment of the Application of Baculoviruses for Control of Lepidoptera. *Annual Review of Entomology*. 44(1):257–289.

Motsoeneng, B., Jukes, M.D., Knox, C.M., Hill, M.P. & Moore, S.D. 2019. Genome analysis of a novel south african *Cydia Pomonella* granulovirus (CpGV-SA) with resistance-breaking potential. *Viruses*. 11(7):658.

Newton, P.J. 1989. The influence of citrus fruit condition on egg laying by the false codling moth, Cryptophlebia leucotreta. *Entomologia Experimentalis et Applicata*. 52:113–117.

Nusse, M., Recknagel, S. and Beisker, W. 1992. Micronuclei induced by 2-chlorobenzylidene malonitrile contain single chromosomes as demonstrated by the combined use of flow cytometry and immunofluorescent staining with anti-kinetochore antibodies. *Mutagenesis*. *7*(1):57-57.

Okano, K., Vanarsdall, A.L., Mikhailov, V.S. & Rohrmann, G.F. 2006. Conserved molecular systems of the Baculoviridae. *Virology*. 344(1):77–87.

Opoku-Debrah, J.K., Hill, M.P., Knox, C., Moore, S.D. 2013. Overcrowding of false codling moth, *Thaumatotibia leucotreta* (Meyrick) leads to the isolation of five new Cryptophlebia leucotreta granulovirus (CrleGV-SA) isolates. *Journal of Invertebrate Pathology*. 112:219-228.

Parnell, M., Grzywacz, D., Jones, K. A., Brown, M., Odour, G. & Ong'garo, J. 2002. The strain variation and virulence of granulovirus of diamond back moth, Plutella xylostella (Linnaeus) (Lepidoptera: Nomeutidae) isolated in Kenya. *Journal of Invertebrate Pathology*. 79:192-196.

Pfaffl, M.W. and Berg, W. 2010. Guest editor's introduction: the ongoing evolution of qPCR. *Methods*. 50(4):215-336.

PPECB, 2017. Cape Town The Perishables Products Export Control Board, Annual Report 2016/17.

Roberts, G.S., Yu, S., Zeng, Q., Chan, L.C., Anderson, W., Colby, A.H., Grinstaff, M.W., Reid, S. and Vogel, R. 2012. Tunable pores for measuring concentrations of synthetic and biological nanoparticle dispersions. *Biosensors and Bioelectronics*. 31(1):17-25.

Rodriguez, V.A., Belaich, M.N. and Ghiringhelli, P.D. 2012. Baculoviruses: Members of integrated pest management strategies. *Integrated Pest Management and Pest Control-Current and Future Tactics*. 463-480.

Rohrmann, G.F., 2019. Baculovirus molecular biology. 4th ed. *National Center for Biotechnology Information (US)*. Bethesda (MD).

Ruijter, J.M., Barnewall, R.J., Marsh, I.B., Szentirmay, A.N., Quinn, J.C., van Houdt, R., Gunst, Q.D. and van den Hoff, M.J. 2021. Efficiency correction Is required for accurate quantitative PCR analysis and reporting. *Clinical Chemistry*. 67(6):829-842.

Shen, C.F., Meghrous, J. & Kamen, A. 2002. Quantitation of baculovirus particles by flow cytometry. *Journal of Virological Methods*. 105(2):321–330.

Singh S. (2001). The Characterisation of a South African isolate of Cryptophlebia leucotreta granulovirus (CleGV) (Masters Thesis, Rhodes University).

Singh, S., Moore, S., Spillings, B. & Hendry, D. 2003. South African isolate of Cryptophlebia leucotreta granulovirus. *Journal of Invertebrate Pathology*. 83(3):249–252.

Sivaganesan, M., Seifring, S., Varma, M., Haugland, R.A. and Shanks, O.C. 2008. A Bayesian method for calculating real-time quantitative PCR calibration curves using absolute plasmid DNA standards. *BMC bioinformatics*. *9*(1):1-12.

Stibick, J. 2007. New pest response guidelines: False codling moth *Thaumatotibia leucotreta*. USDA–APHIS–PPQ–Emergency and Domestic Programs, Riverdale, Maryland.

Stratagene. 2010. Introduction to Quantitative PCR. *Methods and Applications Guide*.

Szewczyk, B., Hoyos-Carvajal, L., Paluszek, M., Skrzecz, I. & Lobo De Souza, M. 2006. Baculoviruses - Re-emerging biopesticides. *Biotechnology Advances*. 24(2):143–160.

Thamamongood, T., Aebischer, A., Wagner, V., Chang, M.W., Elling, R., Benner, C., García-Sastre, A., Kochs, G., Beer, M. and Schwemmle, M. 2020. A genome-wide CRISPR-Cas9 screen reveals the requirement of host cell sulfation for Schmallenberg virus infection. *Journal of Virology*. 94(17):752-20.

Thieme, F., Engler, C., Kandzia, R. and Marillonnet, S. 2011. Quick and clean cloning: a ligation-independent cloning strategy for selective cloning of specific PCR products from non-specific mixes. *PLoS One*. 6(6):20556.

van den Berg, M.A. 1995. Pests Attacking Macadamia in South Africa. Sixth Conference of the Australasian Council on Tree and Nut Crops. *Lismore, NSW, Australia*. 11-15

Van der Merwe, M., Jukes, M.D., Rabalski, L., Knox, C., Opoku-Debrah, J.K., Moore, S.D., Krejmer-Rabalska, M., Szewczyk, B. and Hill, M.P. 2017. Genome analysis and genetic stability of the Cryptophlebia leucotreta granulovirus (CrleGV-SA) after 15 Years of commercial use as a biopesticide. *International Journal of Molecular Sciences*. 18(11):2327.

Venette, R.C., Davis, E.E., DaCosta, M., Heisler, H. & Larson, M. 2003. Mini Risk Assessment False codling moth, (*Thaumatotibia Cryptophlebia*) *leucotreta* (Meyrick) [Lepidoptera: Tortricidae]. *University of Minnesota*, *Department of Entomology*. 1–30.

Wennmann, J.T. and Jehle, J.A. 2014. Detection and quantitation of Agrotis baculoviruses in mixed infections. *Journal of Virological Methods*. 197:39-46.

Wennmann, J.T., Keilwagen, J. and Jehle, J.A. 2018. Baculovirus Kimura two-parameter species demarcation criterion is confirmed by the distances of 38 core gene nucleotide sequences. *Journal of General Virology*. 99:1307-1320.

Wong, M.L. & Medrano, J.F. 2005. Real-time PCR for mRNA quantitation. *Biotechniques*. 39(1):75-85.

Yang, S. and Rothman, R.E. 2004. PCR-based diagnostics for infectious diseases: uses, limitations, and future applications in acute-care settings. *The Lancet infectious diseases*. 4(6):337-348.

Zhang, C., Lee, H.J., Shrivastava, A., Wang, R., McQuiston, T.J., Challberg, S.S., Pollok, B.A. and Wang, T. 2018. Long-term in vitro expansion of epithelial stem cells enabled by pharmacological inhibition of PAK1-ROCK-Myosin II and TGF-β signalling. *Cell Reports*. 25(3):598-610.

Zwart, M.P., van Oers, M.M., Cory, J.S., van Lent, J.W., van der Werf, W. and Vlak, J.M. 2008. Development of a quantitative real-time PCR for determination of genotype frequencies for studies in baculovirus population biology. *Journal of Virological Methods*. 148(1-2):146-154.